

Interface Correlators in Symmetric Product Orbifolds

Sebastian Harris,^{a,b} Volker Schomerus,^{a,b,c} and Takashi Tsuda^d

^a*Deutsches Elektronen-Synchrotron DESY, Notkestr. 85, D-22607 Hamburg, Germany*

^b*Zentrum für Mathematische Physik, Bundesstrasse 55, D-20146 Hamburg, Germany*

^c*II. Institut für Theoretische Physik, Universität Hamburg, Luruper Chaussee 149, D-22761 Hamburg, Germany*

^d*Center for Gravitational Physics and Quantum Information, Yukawa Institute for Theoretical Physics, Kyoto University, Kitashirakawa Oiwakecho, Sakyo-ku, Kyoto 606-8502, Japan*

E-mail: sebastian.harris@desy.de, volker.schomerus@desy.de,
takashi.tsuda@yukawa.kyoto-u.ac.jp

ABSTRACT: Symmetric product orbifolds provide a controlled environment to explore generic features of gauge theory and holography. The tractability of these theories lies in the complete characterisation of their gauge structure through holomorphic covering maps. In this paper, we introduce a novel class of generalised covering maps, which define a universal family of interfaces between symmetric product orbifolds. These interfaces coincide with the holographic interfaces that were recently proposed as duals to AdS_2 branes in pure NSNS AdS_3 backgrounds. The new covering-map description enables efficient evaluation of interface correlators via a generalisation of the Lunin–Mathur method. To organise these computations, we derive a generalised Riemann–Hurwitz formula for interface coverings and introduce novel diagrammatic rules that systematically classify these maps. The new framework allows us to define a concrete grand-canonical ensemble that has the correct properties to compute correlation functions dual to open string scattering amplitudes. Using the generalised Riemann–Hurwitz formula, we explicitly show that the correlators of the ensemble structurally match string perturbation theory to all orders in the string coupling.

Contents

1	Introduction	2
2	Interfaces in symmetric product orbifolds	5
2.1	Branched coverings	5
2.2	Symmetric product orbifolds	7
2.3	Interface covering maps	11
2.4	Holographic interfaces	13
3	Generalised Pakman-Rastelli-Razamat diagrammatics	20
3.1	Pakman-Rastelli-Razamat diagrams	20
3.2	Interface PRR diagrams	24
3.3	Symmetry group of interface PRR diagrams	31
3.4	Gauge fixing of interface PRR diagrams	32
3.5	The large N expansion	35
4	Generalised Lunin-Mathur construction	38
4.1	Review of the bulk method	38
4.2	The interface generalisation	41
5	String theory and the interface grand-canonical ensemble	45
5.1	Holographic motivation	45
5.2	The bulk grand-canonical ensemble	46
5.3	The grand-canonical ensemble for interfaces	49
6	Conclusion	52
A	Symmetric product orbifolds as discrete gauge theories	54
B	Wilson and 't Hooft lines in symmetric orbifolds	57
C	Comments on the normalisation of the interfaces	60
D	Generalised Lunin-Mathur construction – computational details	61
D.1	Details on the regularisation procedure	61
D.2	Regularisation for the upper half plane	64
D.3	Computing covering maps	65
E	Proving the diagrammatic rules	66

1 Introduction

In many respects, symmetric product orbifolds are close cousins of higher dimensional weakly coupled gauge theories and can serve as a very controlled laboratory to study features of perturbative expansions and most importantly of holography. In particular, correlation functions of symmetric product orbifolds $\text{Sym}^N(\mathcal{M})$ of some seed CFT \mathcal{M} are known to possess a Feynman-like expansion. The role of the Feynman diagrams is played by covering maps Γ of the 2-dimensional surface X the symmetric product orbifold is defined on. These covering maps even possess a diagrammatic description that is quite reminiscent of the usual double line networks that are used in gauge theory [1]. More importantly, the large N expansion is similar to the 't Hooft expansion in gauge theory, suggesting a holographic description through some dual string theory in AdS_3 . And indeed, an exact dual string theory for the symmetric product orbifold of a supersymmetric 4-torus has been established in [2, 3]. It involves strings on an $AdS_3 \times S^3 \times T^4$ geometry with one unit of NSNS- and no RR-flux turned on. This correspondence is quite remarkable. Tensionless strings are deeply quantum and hence dual to a weakly coupled theory. Finding similar dual pairs between weakly coupled gauge theories in higher dimensions and (non-geometric) dual string theories is an important challenge that has seen limited progress, see however [4] for some recent proposal and further references. On the other hand, many aspects of holography are actually still better understood in higher dimensional setups and in particular for the paradigmatic example of the duality between $\mathcal{N} = 4$ SYM theory and string theory in $AdS_5 \times S^5$. This applies in particular to the emergence of a geometric supergravity regime which is well established in some higher dimensional versions of the correspondence. In addition, the higher dimensional theories have been probed by a wide range of different observable, including non-local ones such as line and surface defects and interfaces. These have received much less attention in the context of symmetric product orbifolds. Karch-Randal like interfaces that connect two symmetric product orbifolds with different degree of the orbifold group, for instance, have only been constructed a few months ago in [5]. In this paper, we continue our analysis of these interfaces by providing the necessary tools to efficiently compute their local correlation functions, especially with the aim to establish universal holographic features.

The interfaces under consideration connect symmetric product orbifolds with orbifold groups $S_{N_{\pm}}$ of degrees N_{\pm} . Two essential pieces of data enter their construction: A pair of boundary states $|a_{\pm}\rangle$ of the seed theory \mathcal{M} and an integer $P \leq \min(N_{\pm})$. While the former controls the precise way in which bulk excitations in the symmetric product orbifold are reflected off the interface, the integer P determines the *degree of transmissivity*, with large values of P corresponding to a maximally transparent setup. Note that, for $N_+ \neq N_-$, reflection processes are unavoidable. It is conjectured that these interfaces provide a holographic dual for AdS_2 -branes in minimal pure NSNS flux limits of string theory on AdS_3 backgrounds. Concretely, this proposal was brought forward in [5] for strings on $AdS_3 \times S^3 \times T^4$, and recently also extended to $AdS_3 \times S^3 \times S^3 \times S^1$ [6]. Using the boundary states of the folding trick description of the interfaces, Reference [5] computed the torus partition function for a pair of interfaces. This CFT partition function was then compared

with the annulus partition function of open strings on the relevant AdS_2 branes and both quantities were found to agree. In this sense, the interfaces defined in [5] appear as natural low-dimensional analogues of Wilson lines in four-dimensional gauge theories. They can also be viewed as two-dimensional counterparts of Karch-Randall interfaces [7].

As convincing as the agreement of partition functions may seem, a complete derivation of the holographic correspondence does require to also match CFT correlation functions of bulk and interface operator with scattering amplitudes of tensionless closed and open strings on AdS_2 -branes in AdS_3 . In order to approach such a comparison, we need to be able to compute the relevant CFT correlators. This is the problem we address in the current work. In order to achieve this goal, we extend the Lunin-Mathur covering space techniques to interface CFT. This involves two steps. In a first step, the correlation functions in the interface symmetric product orbifold CFT are represented as a sum over an appropriate set of interface branched coverings Γ , see Subsection 2.3 and eq. (2.33). The summands involve correlation functions in the seed CFT \mathcal{M} on surfaces with boundaries. These are weighted with some coefficients $\alpha[\Gamma]$ that do not depend on the seed CFT. Following the ideas of Lunin-Mathur [8], the correlation functions in the seed CFT can then be calculated with the help of (boundary) Liouville field theory. For pure twist field insertions, the dependence on the seed CFT is restricted to the bulk and boundary entropies, i.e. the central charge c and the g -factors g_{\pm} of the two boundary conditions a_{\pm} , see for example eq. (4.23).

In order to construct the sum over coverings Γ and compute the weight factors $\alpha[\Gamma]$, we develop a diagrammatic approach that extends the Feynman-like diagrams that were introduced for bulk symmetric product orbifolds by Pakman, Rastelli and Razamat in [1]. In our case, the diagrams are built from five different types of propagator-lines. Three of them are represented by double lines. We shall refer to them as *aligned* and *misaligned* $_{\pm}$. In addition there are two single lines of opposite orientation. Bulk twist fields of order w are represented by vertices with w misaligned double lines, see Figure 3a. Interface twist field of order ω , on the other hand, are represented by vertices with two single lines and $\omega - 1$ aligned double lines, see Subfigure a, b, c and d of Figure 7. In addition to these vertices that represent field insertions there are also two classes of trivalent vertices that are not associated with any field insertions. These additional trivalent vertices allow to split a misaligned double line into either a pair of aligned double lines, see Figure 3b, or into a pair of single lines, see Subfigure e and f of Figure 7. In order to describe a valid interface covering map Γ , a diagram built out of these basic ingredients needs to satisfy some simple rules, see Section 3.2. Given a valid diagram it is then easy to read off the degrees N_{\pm} of the associated covering map, the degree of transmissivity P of the interface and the symmetry factor $\alpha[\Gamma]$.

If the diagram has no single lines, it actually describes an ordinary bulk covering map. In the corresponding diagrams, it is possible to eliminate all the misaligned double lines by splitting them into pairs of aligned ones. Hence, these diagrams can be drawn with a single type of double line which agrees with the pictorial descriptions proposed by Pakman-Rastelli-Razamat (PRR). After we split the misaligned lines, bulk twist field of order w are represented by a vertex with $2w$ aligned double lines rather than w misaligned ones, see Figure 4b. Thereby, we recover the graphical rules for PRR diagrams. Let us note that

our representation of the aligned double lines looks a bit different from the one in the work of Pakman et al. who used double lines with one dashed and one solid edge.

Another central result that we obtain from our new understanding of interface covering maps concerns the structure of the large N_{\pm} and large P expansion that is shown to match the string genus expansion for scattering amplitudes of closed and open strings to all orders in the string coupling. In the bulk case it has been well understood that the comparison of the two expansions requires passing to a grand-canonical ensemble in which the parameter N is controlled by a dual fugacity μ . The latter scales with the string coupling g_s as $\mu \sim g_s^{2G-2}$ where G denotes the genus of the holographic boundary X . In the grand-canonical ensemble, N is not a number but one can check that the expectation value of N scales as $N \sim g_s^{-2}$. We extend these insights to the interface setup. In particular, we introduce a new grand-canonical ensemble in which N_{\pm} and the degree of transmissivity P are controlled by dual fugacities, see eq. (5.21). With some appropriate scaling behaviour of these three fugacities, see eq. (5.22), the expectation values of N_{\pm} and P scale as g_s^{-2} while the expectation value of $N_{\pm} - P$ turns out to scale as g_s^{-1} .

The plan for this work is as follows. The next section is devoted to covering maps and their role in computing correlation functions in symmetric product orbifolds. We begin by reviewing the well known notion of branched coverings in Section 2.1 before we recall, in Section 2.2, how correlation functions on symmetric product orbifolds on a closed surface X can be expressed as a sum over branched coverings of X . The individual summands involve correlation functions of the seed theory on the covering surface Σ . We then extend this discussion to the case of interfaces. In Subsection 2.3, we introduce the relevant notion of generalised covering maps before we spell out how to compute correlation functions involving interfaces as a sum over these covering maps, see Subsection 2.4 and in particular eq. (2.33). We evaluate the right hand side of this equation for some special setup in which we just insert two parallel interfaces along some cycle of the torus, without any further local insertions of either bulk or interface fields. The resulting formula coincides with the interface partition functions we calculated in [5] from an algebraic construction that involves the folding trick and explicit boundary states. This justifies a posteriori the rather natural notion of generalised covering maps we propose in Subsection 2.3.

Section 3 is devoted to the diagrammatic representation of interface covering maps that we summarised above. After a short review of the PRR diagrams for correlation functions in symmetric product orbifolds in Section 3.1, we describe the corresponding interface diagrams in Section 3.2. This is followed by a brief discussion of the symmetries of interface PRR diagrams in Sections 3.3 and 3.4. These symmetries allow to read off the group of deck transformations of the associated branched covering. Finally, we determine the large N behaviour of the expansion in Section 3.5.

With all this control over the interface PRR expansion of correlation functions in symmetric product orbifolds with holographic interface insertions, it remains to evaluate its individual diagrams, i.e. the relevant correlation functions of the seed theory on the covering surfaces Σ . This is addressed in Section 4 where we extend the ideas proposed by Lunin and Mathur for symmetric product orbifolds on a closed surface to the interface setup. Once

again, we start with a short review of the bulk analysis before we discuss its extension to interfaces and several concrete examples. Section 5 is about grand-canonical partition functions. After a brief review of the bulk case in Section 5.2, we introduce grand-canonical interface partition functions in Section 5.3 and show that these indeed have the same structure as partition functions of closed and open strings with the scalings we described above. In Section 6, we conclude by listing a number of interesting open problems and directions for future research. Some more technical explanations and additional material are collected in five appendices.

2 Interfaces in symmetric product orbifolds

In this section, we discuss a family of universal interfaces of symmetric product orbifolds that were introduced in Reference [5]. Using the folding trick, Section 2 of that work gave a fully explicit construction of these interfaces in terms of boundary states, from which in particular a closed formula for the grand-canonical torus partition function with two interface insertions was computed. Some very special cases of the interfaces had been considered previously, for instance in References [9, 10].

However, all these previous discussions, including Reference [5], took a fairly algebraic perspective on symmetric product orbifolds. In this section, we would like to complement the existing literature on the topic by an analytic perspective that focuses on an interpretation of objects in symmetric product orbifolds in terms of branched covering maps, i.e. we represent interface correlation functions in symmetric product orbifolds through a sum over appropriately defined “interface covering maps”.

In order to set the stage, we first review the corresponding description for correlation functions of local fields in symmetric product orbifolds, see Section 2.2. To make this work self-contained, the relevant mathematical notions concerning branched coverings of Riemann surfaces are collected in Section 2.1. Analogously, our discussion of interface correlators starts by introducing a class of generalised covering maps in Section 2.3 and proving that they satisfy a modified Riemann-Hurwitz formula. Equipped with this mathematical background, the final Section 2.4 provides a new description of the interfaces whose correlation functions are explored in the rest of this work. As a first application of the definition in terms of a sum over generalised covering maps, we re-calculate the interface partition functions that were first computed in [5]. Crucially, the new calculation turns out to be considerably easier than the original one, which allows us to study much more general partition functions and correlators in this paper, than those accessible with the methods of Reference [5].

2.1 Branched coverings

To prepare for our discussion of correlations of local fields in symmetric product orbifolds, we start with a lightning review of branched coverings. The definition of unramified and branched coverings is stated in the next two paragraphs. This is followed by three paragraphs in which we introduce the notation of monodromy and deck transformations of

branched coverings. The final paragraph reviews a classical result of the theory of covering maps: The Riemann-Hurwitz formula.

Unramified coverings. Throughout this section, let Σ and X be Riemann surfaces. Unless stated otherwise, neither Σ nor X are assumed to be closed. Furthermore, let $\Gamma : \Sigma \rightarrow X$ be a holomorphic surjection. If Γ is locally invertible and if every point $x \in X$ has $|\Gamma^{-1}(x)| = N$ preimages, then Γ is called a degree N *unramified covering* of X by Σ .

Branched coverings. Let B be a finite subset of X and $R := \Gamma^{-1}(B)$. If R is a finite set and the restriction of Γ to $\Sigma \setminus R$ is a holomorphic covering of $X \setminus B$ then Γ is a *branched covering* of X . In this case, we refer to elements of B and R as *branch points* and *ramification points* respectively. At each ramification point $z \in \Sigma$, the covering map Γ locally takes the form

$$\Gamma(z + \delta z) = \Gamma(z) + O(\delta z^w). \quad (2.1)$$

The integer w is the *ramification index* of Γ in z . For $z \notin R$, the index is one.

Monodromy. For a connected surface X , consider a closed curve $\gamma : [0, 1] \rightarrow X \setminus B$ based in the point $x \in X$, i.e. a curve satisfying $\gamma(0) = \gamma(1) = x$ that does not pass through any of the branch points of the covering map Γ . For each element z of the set $\Gamma^{-1}(x)$ there is a unique lift $\Gamma^* \gamma_z$ of γ to Σ such that

$$\Gamma \circ \Gamma^* \gamma_z = \gamma \quad \text{and} \quad \Gamma^* \gamma_z(0) = z. \quad (2.2)$$

The map $z \mapsto \Gamma^* \gamma_z(1)$ is a bijection of the set $\Gamma^{-1}(x)$ onto itself i.e. an element of $\text{Aut}[\Gamma^{-1}(x)]$. It only depends on the homotopy class $[\gamma]$ of the curve γ and therefore defines a group homomorphism

$$M_\Gamma : \pi_1(X, x) \rightarrow \text{Aut}[\Gamma^{-1}(x)] \quad (2.3)$$

which sends γ to an automorphism α_γ of the set $\Gamma^{-1}(x) \subseteq \Sigma$. The map M_Γ is the *monodromy action* of the covering map Γ . Its image is the *monodromy group* of Γ .

Deck transformations. A *Deck transformation* of the covering Γ is an automorphism D of Σ with the property $\Gamma \circ D = \Gamma$. If Σ is connected, then the image $D(z)$ of an arbitrary unramified point $z \in \Sigma$ already fixes D completely. In this sense, the group $\text{Deck}[\Gamma]$ of deck transformations can be identified with a subgroup of $\text{Aut}[\Gamma^{-1}(x)]$ for a generic $x \in X$ in this case. Since deck transformations are precisely the maps that preserve Γ , this subgroup is the stabiliser of the monodromy group of Γ under the conjugation of $\text{Aut}[\Gamma^{-1}(x)]$.

Local gauge choice. Given a point $x \in X$ and a set C of degree N coverings of X , for which x is not a branch point, we refer to a choice of labelling the N points in the preimage $\Gamma^{-1}(x)$ of x w.r.t. every covering map $\Gamma \in C$ by the numbers $1, \dots, N$ as a *local*

*gauge choice*¹ for C at $x \in X$. In particular, a local gauge choice for $C = \{\Gamma\}$ is a bijection

$$\psi : \underline{N} := \{1, 2, \dots, N\} \rightarrow \Gamma^{-1}(x), \quad (2.4)$$

that allows to identify elements α of $\text{Aut}[\Gamma^{-1}(x)]$ with elements $\alpha^\psi := \psi^{-1} \circ \alpha \circ \psi$ of the symmetric group S_N . Thus, local gauge choices lead to an identification of the monodromy group and deck transformations with subgroups of S_N . As an application, we can for example use a local gauge choice to define a map

$$M_\Gamma^R : \pi_1(X, x) \rightarrow \mathbb{C}, \quad [\gamma] \mapsto \chi_R(M_\Gamma[\gamma]) := \chi_R(M_\Gamma^\psi[\gamma]), \quad (2.5)$$

given a representation R of S_N with character χ_R . Since characters are invariant under the inner automorphisms of S_N , the value of $\chi_R(M_\Gamma[\gamma])$ is independent of the choice of ψ .

Riemann-Hurwitz formula. In this paragraph, we assume that Σ and X are closed. If Γ is unramified, sufficiently fine triangulations of X lift along Γ to triangulations of Σ with $N = \deg[\Gamma]$ times as many vertices, edges and faces. Thus, the Euler characteristics of Σ and X are related by $\chi(\Sigma) = N\chi(X)$. More generally, consider a triangulation of X whose vertices include all branch points of Γ . Then the lifted triangulation still has the expected number of edges and faces. However, $w - 1$ vertices on Σ are lost for each ramification point with index w . Therefore, the Euler characteristic $\chi(\Sigma)$ of Σ is given by

$$\chi(\Sigma) = N\chi(X) - \sum_{i=1}^n (w_i - 1), \quad (2.6)$$

where w_1, \dots, w_n are the ramification indices of Γ . This is the *Riemann-Hurwitz formula*.

2.2 Symmetric product orbifolds

This section introduces symmetric product orbifolds as two-dimensional CFTs defined by lifting correlation functions of a seed theory \mathcal{M} on a closed Riemann surface X to various covering spaces. It is divided into several paragraphs, each devoted to one aspect of the lift. The first of these provides a definition. The definition is then applied to the computation of vacuum partition functions. These allow us to determine the spectrum of the symmetric orbifold and its local correlation functions.

Covering space lift. Let us denote by $\mathcal{A}_X[\mathcal{T}]$ the set of observables \mathcal{O} of a CFT \mathcal{T} on the surface X , i.e. the set of all objects that can be inserted in its correlation functions. The most basic elements of $\mathcal{A}_X[\mathcal{T}]$ are products $\mathcal{O}_S = \mathcal{O}_1(x_1)\mathcal{O}_2(x_2)\cdots\mathcal{O}_n(x_n)$ of local operators \mathcal{O}_i that are inserted at some finite set of points $x_i \in S \subseteq X$. Beyond those, \mathcal{A}_X also includes non local observables such as line operators.

We define the symmetric product orbifold $\text{Sym}^N(\mathcal{M})$ of the seed theory \mathcal{M} by a prescription that expresses the correlation functions of its observables in terms of correlators

¹This terminology is justified in Appendix A, where symmetric product orbifolds are discussed in the language of gauge theory, and the local gauge choices we define here are shown to correspond to local trivialisations of the gauge bundle.

of \mathcal{M} . This is achieved through the following two steps. First, we associate a set $C_N[\mathcal{O}]$ of N -sheeted branched coverings² of X with each observable $\mathcal{O} \in \mathcal{A}_X[\text{Sym}^N(\mathcal{M})]$.

Second, we associate an observable \mathcal{O}^Γ of the seed theory to any pair (\mathcal{O}, Γ) of an observable \mathcal{O} of the symmetric product orbifold and a covering map $\Gamma \in C_N[\mathcal{O}]$. For the multipoint observables \mathcal{O}_S we described above, for example, the associated observable in the seed theory is essentially given by some $\mathcal{O}_{\Gamma^{-1}(S)}$. Given these two ingredients, i.e. the space $C_N[\mathcal{O}]$ of covering maps associated with \mathcal{O} and the map

$$\mathcal{O} \mapsto \mathcal{O}^\Gamma \in \mathcal{A}_\Sigma[\mathcal{M}], \quad (2.7)$$

that sends $\mathcal{O} \in \mathcal{A}_X[\text{Sym}^N(\mathcal{M})]$ to the observable $\mathcal{O}^\Gamma \in \mathcal{A}_\Sigma[\mathcal{M}]$, we lift expectation values in the symmetric product orbifolds to expectation values in the seed theory as,

$$\langle \mathcal{O} \rangle_{\text{Sym}^N(\mathcal{M})}^{\text{unnormalised}} = \frac{1}{N!} \sum_{\Gamma \in C_N[\mathcal{O}]} \langle \mathcal{O}^\Gamma \rangle_{\mathcal{M}}, \quad (2.8)$$

where $\langle \mathcal{O}^\Gamma \rangle_{\mathcal{M}}$ is a correlator of \mathcal{M} on Σ with a metric that is obtained by pulling back the metric of X along Γ . We have placed a subscript ‘unnormalised’ on this correlator since it does not necessarily yield 1 for the one-point functions of the identity operator $\mathbb{1}$. We define its normalised analogue as the quotient

$$\langle \mathcal{O} \rangle_{\text{Sym}^N(\mathcal{M})} = \frac{\langle \mathcal{O} \rangle_{\text{Sym}^N(\mathcal{M})}^{\text{unnormalised}}}{\langle \mathbb{1} \rangle_{\text{Sym}^N(\mathcal{M})}^{\text{unnormalised}}}. \quad (2.9)$$

The vacuum. As a first example, let us discuss the concrete realisation of the general equation (2.8) for the case $\mathcal{O} = \mathbb{1}$ of the identity, or vacuum operator. The set $C_N[\mathbb{1}]$ is

$$C_N[\mathbb{1}] := \{N \text{ sheeted unramified coverings of } X\}. \quad (2.10)$$

Given some $\Gamma \in C_N[\mathbb{1}]$, the observable $\mathbb{1}^\Gamma$ of the seed theory on the covering surface Σ is the identity operator, up to some normalising prefactor $\alpha[\Gamma]$, i.e.

$$\mathbb{1}^\Gamma = \alpha[\Gamma] \cdot \mathbb{1} \quad \text{where} \quad \alpha[\Gamma] := \frac{\deg[\Gamma]!}{|\text{Deck}[\Gamma]|}. \quad (2.11)$$

By definition, the vacuum partition function Z_N^X of $\text{Sym}^N(\mathcal{M})$ on the surface X is

$$Z_N^X := \langle \mathbb{1} \rangle_{\text{Sym}^N(\mathcal{M})}^{\text{unnormalised}}. \quad (2.12)$$

Let us compute Z_N^X in the simplest case $X = \mathbb{S}^2$, where the set $C_N[\mathbb{1}]$ has only a single element Γ , which covers the sphere by N disconnected spheres. The group $\text{Deck}[\Gamma]$ consists of the $N!$ permutations of these spheres. Therefore, we obtain $Z_N^{\mathbb{S}^2} = 1/N!$ in a normalisation where the sphere partition function of the seed theory is set to one. A much greater amount of information is encoded in the partition function of higher genus surfaces X . In particular, the torus partition function contains the entire spectral data of local operators and the genus two partition function yields all structure constants.

²We consider coverings that are related by an isomorphism that identifies their covering spaces as identical. A more precise statement would be that $C_N[\mathcal{O}]$ is a set of equivalence classes of covering maps.

Torus partition function. Let us compute the torus partition function from def. (2.10). Using the Riemann-Hurwitz formula, one can easily conclude that the covering space of an unramified covering of \mathbb{T}^2 must be a disjoint union of tori. More precisely, all connected unramified coverings $\Gamma_{w,\ell}^k$ of the torus $\mathbb{C}/(\mathbb{Z} + \tau\mathbb{Z})$ arise from linear maps

$$\Gamma : \mathbb{C} \rightarrow \mathbb{C}, \quad z \mapsto (m\tau + w)z \quad \text{with} \quad m, w \in \mathbb{Z} \quad (2.13)$$

by quotienting out the lattices $\mathbb{Z} + t\mathbb{Z}$ and $\mathbb{Z} + \tau\mathbb{Z}$ of the domain and image of Γ respectively. The modular parameter t of the covering space takes the form $t = \frac{\ell\tau + k}{m\tau + w}$ with $\ell, k \in \mathbb{Z}$ and modular transformations allow us to fix $m = 0$, $w, \ell > 0$ and $1 \leq k \leq w$. As anticipated, the coverings are thus labelled by three integers. Since $\text{Deg}[\Gamma_{w,\ell}^k] = w\ell$, we find

$$Z_N^{\mathbb{T}^2} = \frac{1}{N!} \sum_{\Gamma \in C_N[\mathbb{1}]} \alpha[\Gamma] \langle \mathbb{1} \rangle_{\mathcal{M}} = \sum_{\sum w_i \ell_i n_i = N} \sum_{k_i=1}^{w_i} \prod_i \frac{1}{n_i!} \left(\frac{Z(\frac{\ell_i \tau + k_i}{w_i})}{|\text{Deck}[\Gamma_{w_i, \ell_i}^{k_i}]|} \right)^{n_i}. \quad (2.14)$$

$\text{Deck}[\Gamma_{w,\ell}^k]$ is the group of translations $z \mapsto z + \frac{a\tau + b}{w}$ with integer a and b , which has size $|\text{Deck}[\Gamma_{w,\ell}^k]| = w\ell$. In the grand-canonical ensemble, the constraint $\sum w_i \ell_i n_i = N$ is lifted and we obtain the simple formula

$$\sum_{N=0}^{\infty} Z_N^{\mathbb{T}^2} \mu^N = \exp \left(\sum_{w,\ell=0}^{\infty} \sum_{k=1}^w \frac{\mu^{w\ell}}{w\ell} Z \left(\frac{\ell\tau + k}{w} \right) \right), \quad (2.15)$$

from which the spectrum of the orbifold can be read off. This completes our short computation of the torus partition function in symmetric product orbifolds.

Correlation functions of twist fields. A universal (i.e. seed theory independent) feature of all symmetric product orbifolds is the existence of twist fields – local operators $\sigma_{\mathbf{w}}$ labelled by integer partitions $\mathbf{w} = [w_1, \dots, w_\ell]$ whose conformal weights are

$$h_{\mathbf{w}} = \bar{h}_{\mathbf{w}} = \frac{c_{\mathcal{M}}}{24} \sum_{i=1}^{\ell} \left(w_i - \frac{1}{w_i} \right). \quad (2.16)$$

The state corresponding to $\sigma_{\mathbf{w}}$ contributes to the torus partition function (2.14) through a particular set of covering maps. These are the maps that, upon cutting the torus along the real cycle, yield coverings of a cylinder X by ℓ disconnected cylinders Σ_i , such that Σ_i winds X exactly w_i times. Therefore,

$$C \left[\prod_{i=1}^n \sigma_{\mathbf{w}_i}(x_i) \right] = \left\{ \begin{array}{l} N \text{ sheeted coverings of } X \text{ with branchpts. at } x_i \text{ lifting to} \\ \ell_i \text{ ramification pts. with ramification indices } w_1, \dots, w_{\ell_i}. \end{array} \right\}. \quad (2.17)$$

Observables made up of pure twist fields $\sigma_{\mathbf{w}}$ in the symmetric product orbifolds are mapped to identity fields in the seed theory. More precisely, the prescription is

$$\left[\prod_{i=1}^n \sigma_{\mathbf{w}_i}(z_i) \right]^{\Gamma} = \alpha[\Gamma] \mathbb{1} \quad \text{where} \quad \alpha[\Gamma] = \frac{\text{deg}[\Gamma]!}{|\text{Deck}[\Gamma]|}, \quad (2.18)$$

as for the identity field. Partitions $\mathbf{w} = [w, 1, 1, \dots, 1]$ with only a single $w > 1$ play a special role. They are referred to as single cycle twist fields and we denote them simply as σ_w , labelled by the single integer w .

Connected sphere correlators. As an important example, let us discuss correlators of twist fields on the sphere $X = \mathbb{S}^2$ in more detail. Concretely, let us focus on contributions to these correlators that stem from covering maps

$$\Gamma : \Sigma \sqcup [\mathbb{S}^2]^{\sqcup(N-n_c)} \rightarrow X, \quad (2.19)$$

where Σ is *connected*, $\Gamma|_{\Sigma}$ has degree n_c and Γ is the identity map when restricted to the sphere factors. We denote this subset of covering maps by $C_{n_c}^{\text{conn}}[\mathcal{O}]$. The resulting partial sum of expectation values in the seed theory is referred to as the *connected part* of the correlator. For general observables \mathcal{O} , the connected expectation value is defined as

$$\langle \mathcal{O} \rangle_{\text{Sym}^N(\mathcal{M})}^{\text{conn, unnormalised}} = \frac{1}{N!} \sum_{n_c=1}^N \sum_{\Gamma \in C_{n_c}^{\text{conn}}[\mathcal{O}]} \langle \mathcal{O}^{\Gamma} \rangle_{\mathcal{M}}. \quad (2.20)$$

In order to compute a connected correlator

$$\langle \sigma_{w_1}(x_1) \dots \sigma_{w_n}(x_n) \rangle_{\text{Sym}^N(\mathcal{M})}^{\text{conn, unnormalised}} \quad (2.21)$$

of a product of single cycle twist fields, one has to determine the factor $\alpha[\Gamma]$ of connected covering maps. In order to do so, pick some unramified point $z \in \Sigma$ and choose n closed curves γ_i based in z such that γ_i winds around the ramification point z_i associated with x_i exactly once and has vanishing winding number with respect to all the other ramification points. Furthermore, let $x := \Gamma(z)$. The monodromy action M_{Γ} then associates a cyclic permutation $g_i := M_{\Gamma}[\gamma_i] \in \text{Aut}[\Gamma^{-1}(x)]$ of order $|g_i| = w_i$ to each of the twist fields.

From the collection g_1, \dots, g_n of permutations, we can calculate the symmetry factor $\alpha[\Gamma]$ that appears in the prescription (2.18) as

$$\alpha[\Gamma] = |[g_1, \dots, g_n]| \quad \text{with} \quad [g_1, \dots, g_n] = \{(gg_1g^{-1}, \dots, gg_ng^{-1}) | g \in \text{Aut}[\Gamma^{-1}(x)]\} \quad (2.22)$$

because $\text{Deck}[\Gamma]$ is precisely the stabiliser of (g_1, \dots, g_n) under conjugation. Let us stress that this formula for $\alpha[\Gamma]$ only holds for connected covering maps Γ .

Wilson loops. Let us now introduce a first family of line operators, namely the *Wilson loop* $\mathcal{W}_R[\gamma] \in \mathcal{A}_X[\text{Sym}^N(\mathcal{M})]$. Here, γ is a closed curve on X that starts and ends at some point $x \in X$ and R labels a representation of the symmetric group S_N . Inserting a Wilson loop $\mathcal{W}_R[\gamma]$ into a correlator does not alter the set $C_N[\mathcal{O}]$ of coverings we sum over, i.e.

$$C_N[\mathcal{O}\mathcal{W}_R[\gamma]] = C_N[\mathcal{O}]. \quad (2.23)$$

What changes is only the sum on the right hand side of our defining relation (2.8). After insertion of the Wilson line $\mathcal{W}_R[\gamma]$ the formulas reads

$$\langle \mathcal{O}\mathcal{W}_R[\gamma] \rangle_{\text{Sym}^N(\mathcal{M})}^{\text{unnormalised}} = \frac{1}{N!} \sum_{\Gamma \in C_N[\mathcal{O}]} M_{\Gamma}^R[\gamma] \langle \mathcal{O}^{\Gamma} \rangle_{\mathcal{M}}. \quad (2.24)$$

Here, we have used the map M_{Γ}^R defined in eq. (2.5) as the evaluation of the character of R on the monodromy action of Γ . The only effect of a the Wilson loop insertion into the expectation value of some observable \mathcal{O} of the N -fold symmetric product orbifold is therefore to multiply the individual summands in (2.8) by some complex numbers. For a discussion of open Wilson loops i.e. Wilson lines as well as dual 't Hooft lines, which change the structure of covering maps contributing to correlation functions, see App. B.

2.3 Interface covering maps

In this section, we generalise the notion of (un)ramified coverings to a broader class of maps, which we call *interface coverings*. As the name suggests, these maps compute correlators in the presence of the interfaces, which we introduce in Sec. 2.4. An important result of this section is the generalised Riemann-Hurwitz formula (2.28) satisfied by interface coverings.

Unramified interface coverings. Let us consider a connected Riemann surface X without boundary and a based loop $\gamma : [0, 1] \mapsto X$ with $\gamma(0) = x = \gamma(1)$ therein. We denote the image $\gamma([0, 1])$ by s_γ and assume that the complement $X \setminus s_\gamma$ of s_γ in X splits into two connected components X_\pm^o . Let us denote their closure in X by $X_\pm = X_\pm^o \cup s_\gamma$. By construction the two sets X_+ and X_- possess the same boundary $\partial X_\pm = s_\gamma$.

An *interface covering map* (for an interface localised along the curve γ) is a surjective holomorphic map $\Gamma : \Sigma \rightarrow X$ whose restrictions Γ_\pm to the subspaces $\Sigma_\pm^o := \Gamma^{-1}(X_\pm^o)$ are covering maps in the sense of Sec. 2.1. The degrees N_\pm of these covering maps may differ, i.e. the size N_+ of the set $\Gamma^{-1}(x)$ for an element x of X_+^o may not be the same as the number N_- of points in $\Gamma^{-1}(x)$ for $x \in X_-^o$.³ We define the *degree of transmissivity* P of Γ on γ as

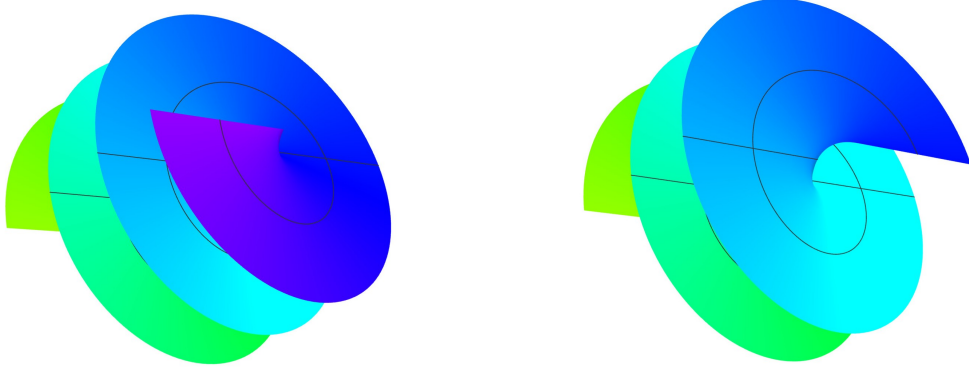
$$P := |\Gamma^{-1}(\gamma(t)) \cap \Sigma^o| \quad (2.25)$$

for any $t \in [0, 1]$. Let us stress that the boundary $\partial \Sigma$ of the covering space is allowed to be non-empty. Since $\Gamma(\partial \Sigma) \subseteq s_\gamma$, our definition of the degree of transmissivity implies that $\partial \Sigma$ has at most $N_+ + N_- - 2P$ connected components. Let us also note that $P \leq \min(N_-, N_+)$. While we, for concreteness and ease of notation, restricted to the specific case of a single curve γ splitting X into two connected components here, the definition given above trivially generalises to an arbitrary number of curves splitting X into arbitrarily many components.

Ramification of interface coverings. Let B be a finite subset of X and $R := \Gamma^{-1}(B)$. If R is a finite set and the restriction of $\Gamma : \Sigma \rightarrow X$ to $\Sigma \setminus R$ is an unramified interface covering of $X \setminus B$ then Γ is a *branched interface covering* of X . We refer to elements of B and R as branch points and ramification points respectively. Branch points that lie on the curve γ are called *interface branch points* below. The other branch points are referred to as *bulk branch points*. The ramification points associated with bulk branch points are simply ramification points of the restrictions Γ_\pm of Γ to X_\pm^o in the sense of Section 2.1.

Ramification points of an interface covering map fall into two different classes: They can either be in the interior of Σ , in which case we speak of *interior ramification points*, or on the boundary $\partial \Sigma$, in which case we speak of *boundary ramification points*. The local behaviour of the covering map near an interior ramification point is captured by eq. (2.1). All ramification points associated with bulk branch points are interior ramification points. However, some interior ramification points may map to interface branch points. We will occasionally find it convenient to associate elements of this subset of interior ramification points with an *interface ramification index* $\omega := 2w$, where w is the index defined through eq. (2.1). If all ramification points of an interface branch point are interior ramification

³Here it is important that $X \setminus s_\gamma$ is not connected. If it was, the degree of Γ could not jump across γ .



(a) Type 6^{LL} ramification point of a $N_{\pm} = 3$ covering. The degree of transmissivity jumps from 2 to 3 at the ramification point.

(b) Type 5^{RL} ramification point of a $N_- = 2$, $N_+ = 3$ covering. The degree of transmissivity is constantly 2.

Figure 1: Visualisation of coverings in a neighbourhood of interface ramification points. The covering map is the vertical projection down the symmetry axis of the spiral. The preimage of the interface is marked by horizontal black lines on the covering space.

points, then the degree of transmissivity P of the interface covering map is the same on both sides of that branch point and bounds the value of the index as $\omega \leq 2P$.

Let us now turn to boundary ramification points, of which we distinguish four different types. To define these types, holomorphically identify a small neighbourhood of the ramification point z with the upper half complex plane, such that z is identified with 0. Let c be the curve in Σ that, through the identification, corresponds to the curve in the upper half plane which maps $\varphi \in [0, \pi]$ to $\varepsilon e^{i\varphi}$. If Γ is unramified in z , then c lies completely within Σ_- or Σ_+ and we say that z has ramification index 1^{LR} or 1^{RL} respectively. If however Γ is ramified in z , there are $\omega - 1 \geq 1$ transitions from Σ_{\pm} to Σ_{\mp} along c . In this case, we say Γ has *interface ramification index* ω in z . We furthermore classify z as

$$\text{type } \omega^{LL} \text{ if } c(0) \in \Sigma_-, c(\pi) \in \Sigma_+, \quad \text{type } \omega^{RR} \text{ if } c(0) \in \Sigma_+, c(\pi) \in \Sigma_-, \quad (2.26)$$

$$\text{type } \omega^{LR} \text{ if } c(0), c(\pi) \in \Sigma_-, \quad \text{type } \omega^{RL} \text{ if } c(0), c(\pi) \in \Sigma_+. \quad (2.27)$$

See Figure 1 for examples. Note that type ω^{LL} and ω^{RR} ramification points force the degree of transmissivity to jump by one unit.

Interface Riemann-Hurwitz formula. In this final paragraph, we prove that interface coverings of closed Riemann surfaces Σ satisfy the modified Riemann-Hurwitz formula

$$\chi(\Sigma) = N_- \chi(X_-) + N_+ \chi(X_+) - \sum_{i=1}^{n_c} (w_i - 1) - \frac{1}{2} \sum_{i=1}^{n_o} (\omega_i - 1), \quad (2.28)$$

where w_1, \dots, w_{n_c} are the indices of the n_c interior ramification points and $\omega_1, \dots, \omega_{n_o}$ are the indices of the n_o boundary ramification points. To simplify the discussion, we

w.l.o.g. assume that all interface branch points correspond to boundary ramification points⁴. To derive eq. (2.28), consider a triangulation of X_- that contains all bulk and boundary branch points as vertices and is fine enough that all edges and faces lift to exactly N_- copies on Σ_- . As discussed in Section 2.1, while generic vertices too lift to N_- copies on Σ_- , we loose $w_i^- - 1$ vertices on Σ_- for each of the n_c^- interior ramification points. The loss of vertices at boundary ramification points of type LL , RR , LR and RL can be determined completely analogously, leading to the formula

$$\chi(\Sigma_-) = N_- \chi(X_-) - \sum_{i=1}^{n_c^-} (w_i^- - 1) - \sum_{i=1}^{n_o^{LR}} \left(\frac{\omega_i^{LR} + 1}{2} - 1 \right) - \sum_{i=1}^{n_o^{RL}} \left(\frac{\omega_i^{RL} - 1}{2} - 1 \right) - \sum_A \sum_{i=1}^{n_o^{AA}} \left(\frac{\omega_i^{AA}}{2} - 1 \right). \quad (2.29)$$

Combining this result with the analogous formula for $\chi(\Sigma_+)$, we obtain

$$\chi(\Sigma_-) + \chi(\Sigma_+) = N_- \chi(X_-) + N_+ \chi(X_+) - \sum_{i=1}^{n_c} (w_i - 1) - \sum_{i=1}^{n_o} (\omega_i - 2). \quad (2.30)$$

Here $n_c = n_c^+ + n_c^-$ and similarly n_o counts the total number of boundary ramification points. We can view $\Sigma_- \cap \Sigma_+$ as a graph whose vertices are the boundary ramification points. The valency of each vertex is $\omega - 1$, where ω is the corresponding ramification index. Therefore,

$$\chi(\Sigma_- \cap \Sigma_+) = n_o - \frac{1}{2} \sum_{i=1}^{n_o} (\omega_i - 1). \quad (2.31)$$

The result (2.28) follows directly from the standard identity

$$\chi(\Sigma) = \chi(\Sigma_-) + \chi(\Sigma_+) - \chi(\Sigma_- \cap \Sigma_+). \quad (2.32)$$

This concludes our proof of the interface Riemann-Hurwitz formula (2.28).

The central role that this result will play in the rest of this work is analogous to the significance that the standard Riemann-Hurwitz formula has for symmetric product orbifolds in the absence of interfaces. It will most prominently be applied to derive topological expansions of interface correlators in Sections 3.5 and 5.3, but is more generally also a useful tool to decide which topologies are allowed to contribute to a given correlation function.

2.4 Holographic interfaces

We now use the interface covering maps introduced in Section 2.3 to define the interfaces of symmetric product orbifolds that are studied in this work. As an application of the new description presented here, we use it to compute a grand-canonical torus partition function with two interface insertions. In the new formalism, the full derivation is rather simple and can conveniently be described in less than a page. Compared to this, the derivation in [5] (which moreover only partially established the result) relied on rather lengthy and complicated combinatorial arguments. This new computational power is one of the key improvements of this paper and ultimately, in Section 5, allows us to compute much more general partition functions that were out of reach with the approach of [5].

⁴Covering maps with interior ramification points that are mapped to interface branch points can be obtained as limits of coverings without such points. Hence eq. (2.28) also directly follows for these maps from the arguments given in this paragraph.

Normalisation of interface correlators. In the setup described in Section 2.3, consider $\text{Sym}^{N_{\pm}}(\mathcal{M})$ on X_{\pm} . To obtain a well defined theory on X , we need to provide CFT glueing data along each of the n connected components $\gamma_1, \dots, \gamma_n$ of ∂X_{\pm} .⁵ In this paper, we only study interfaces that preserve the lifting property that defines symmetric orbifolds. In the presence of such an interface \mathcal{I} , the set $C[\mathcal{IO}]$ of covering maps is no longer restricted to consist of usual branched covers, but generically also includes interface coverings of the type introduced in the previous subsection. With this in mind, the formula for unnormalised interface correlators has exactly the same form (2.9) as in the case of local operator insertions,

$$\langle \mathcal{IO} \rangle_{\text{Sym}^{N_-|N_+}(\mathcal{M})}^{\text{unnormalised}} = \frac{1}{N_-!N_+!} \sum_{\Gamma \in C[\mathcal{IO}]} \langle \mathcal{IO}^{\Gamma} \rangle_{\mathcal{M}} \quad (2.33)$$

Note, however, that we use the convention that the factor $N!$ appearing in eq. (2.9) is replaced by $N_-!N_+!$. As before, we also define normalised interface correlators

$$\langle \mathcal{IO} \rangle_{\text{Sym}^{N_-|N_+}(\mathcal{M})} := \frac{\langle \mathcal{IO} \rangle_{\text{Sym}^{N_-|N_+}(\mathcal{M})}^{\text{unnormalised}}}{\langle \mathcal{I} \rangle_{\text{Sym}^{N_-|N_+}(\mathcal{M})}^{\text{unnormalised}}}. \quad (2.34)$$

In contrast to (2.9), the interface prescription (2.34) is to normalise by an interface partition function that contains the insertion of \mathcal{I} instead of a vacuum bulk partition function.

Definition of the interfaces. Let us define a specific class of interface operators \mathcal{I} that can be inserted along the connected components of ∂X_{\pm} in the setup of the previous paragraph. The definition we give here will later be shown to coincide with the interfaces $\mathcal{I}_{|a_{\pm}\rangle}^{(P)}$ of symmetric product orbifolds that were introduced in [5]. The interfaces are parametrised by a non-negative integer $P \leq \min(N_-, N_+)$, a pair of boundary states $|a_{-}\rangle$ and $|a_{+}\rangle$ of the seed theory \mathcal{M} , as well as characters χ_{\pm} of $S_{N_{\pm}-P}$ and χ_P of S_P .⁶ To simplify notation, we shall denote the collection of these data by $\varpi = (P, |a_{-}\rangle, |a_{+}\rangle; \chi_{-}, \chi_{+}, \chi_P)$. Correlation functions with $\mathcal{I}_{\varpi}[\gamma]$ inserted along some curve γ are computed by summing over all interface coverings Γ whose degrees on X_{\pm} are N_{\pm} and whose degree of transmissivity on γ is P . The relevant correlation functions in the seed theory \mathcal{M} on the covering surfaces Σ depend on the choice of boundary states $|a_{\pm}\rangle$, which describe the boundary condition imposed on the potentially non-trivial boundary $\partial\Sigma$. This boundary splits into disjoint subsets

$$R_{\pm}^{\gamma} := \partial\Sigma_{\pm} \cap \Gamma^{-1}(\gamma) \cap \partial\Sigma. \quad (2.35)$$

The intersection with $\Gamma^{-1}(\gamma)$ is redundant in case where ∂X_{\pm} consists of a single connected component γ . The intersection with $\partial\Sigma$ removes the part of $\Gamma^{-1}(\gamma)$ that runs through the interior of Σ , i.e. the subsets

$$T^{\gamma} := \Gamma^{-1}(\gamma) \cap \Sigma^{\circ}. \quad (2.36)$$

⁵We allow for a straightforward generalisation of the discussion in the previous subsection in which the boundary $\partial X_{+} = \partial X_{-}$ can possess several disconnected components γ_i so that the interface \mathcal{I} is a product $\mathcal{I} = \mathcal{I}_1 \cdots \mathcal{I}_n$.

⁶The dependence on the characters was suppressed in the notation of [5] since we were mostly considering the case in which all three characters are trivial.

By construction, every element of $\Gamma^{-1}(\gamma)$ is either contained in R_{\pm}^{γ} or in T^{γ} , i.e.

$$\Gamma^{-1}(\gamma) = R_{-}^{\gamma} \sqcup T^{\gamma} \sqcup R_{+}^{\gamma}. \quad (2.37)$$

The freedom to choose three characters and two boundary states in the data ϖ that specifies the interface stems from this decomposition of $\Gamma^{-1}(\gamma)$ into three, and its overlap with $\partial\Sigma$ into two, disjoint sets. Concretely, the boundary states $|a_{\pm}\rangle$ describe the boundary conditions of the seed theory that are imposed along the components R_{\pm}^{γ} of $\partial\Sigma$. As for the characters, note that the monodromy of the covering map Γ along the curve γ preserves the decomposition (2.37), i.e.

$$M_{\Gamma}[\gamma] \in \text{Aut}[S \cap R_{-}^{\gamma}] \times \text{Aut}[S \cap T^{\gamma}] \times \text{Aut}[S \cap R_{+}^{\gamma}] \subseteq \text{Aut}[S] \quad (2.38)$$

where $S := \Gamma^{-1}(\gamma(0))$. In other words, the monodromy factorises into a product

$$M_{\Gamma}[\gamma] = M_{\Gamma}^{-}[\gamma] M_{\Gamma}^P[\gamma] M_{\Gamma}^{+}[\gamma]. \quad (2.39)$$

The characters χ_{\pm} and χ_P enter correlations of $\mathcal{I}_{\varpi}[\gamma]$ with $M_{\Gamma}^{\pm}[\gamma]$ and $M_{\Gamma}^P[\gamma]$ as their arguments⁷. More explicitly, correlation functions

$$\left\langle \prod_{i=1}^n \mathcal{I}_{\varpi_i}[\gamma_i] \right\rangle_{\text{Sym}^{N_{-}|N_{+}}(\mathcal{M})}^{\text{unnormalised}} \quad \text{with} \quad \varpi_i := (P^i, |a_{-}^i\rangle, |a_{+}^i\rangle; \chi_{-}^i, \chi_{+}^i, \chi_P^i) \quad (2.40)$$

of products of interfaces are defined through eq. (2.33) with

$$C \left[\prod_{i=1}^n \mathcal{I}_{\varpi_i}[\gamma_i] \right] := \left\{ \begin{array}{l} N_{\pm} \text{ sheeted interface coverings of } X = X_{+} \cup X_{-} \\ \text{with degree of transmissivity } P^i \text{ along } \gamma_i. \end{array} \right\} \quad (2.41)$$

and the characters χ_{\pm}^i and χ_P^i enter through the lift

$$\left[\prod_{i=1}^n \mathcal{I}_{\varpi_i}[\gamma_i] \right]^{\Gamma} := \alpha[\Gamma] \left(\prod_{i=1}^n \chi_{-}^i(M_{\Gamma}^{-}[\gamma_i]) \chi_P^i(M_{\Gamma}^P[\gamma_i]) \chi_{+}^i(M_{\Gamma}^{+}[\gamma_i]) \right) \mathbb{1}, \quad (2.42)$$

where $\mathbb{1}$ is the identity operator of \mathcal{M} on Σ and the coefficient $\alpha[\Gamma]$ is given by

$$\alpha[\Gamma] = \frac{\deg[\Gamma_{-}]! \deg[\Gamma_{+}]!}{|\text{Deck}[\Gamma]|}. \quad (2.43)$$

The only data that do not manifestly appear on the r.h.s. of eq. (2.42) and (2.41) are the boundary states $|a_{\pm}^i\rangle$. These enter in the evaluation of the seed theory expectation value of the r.h.s. of eq. (2.42). As mentioned below eq. (2.37), these boundary states describe the boundary conditions we impose along the component $R_{\pm}^{\gamma_i}$ of the boundary $\partial\Sigma$. The prescription of how to evaluate the vacuum expectation value (2.40) of an arbitrary product of interfaces on an arbitrary Riemann surface X fully defines the interface \mathcal{I}_{ϖ} , just as eqs. (2.10) and (2.11) for arbitrary vacuum partition functions already fully define the bulk theory. Details on the relation of this definition to the one given in Reference [5] are discussed in Appendix C.

⁷As explained in the paragraph “local gauge choice” of Subsection 2.1, the three factors may be identified with elements of the permutation groups $S_{N_{\pm}-P}$ and S_P , respectively, to evaluate the characters without ambiguity i.e. independent of the choice of identification. See in particular eq. (2.5).

Vacuum expectation value. As a first example of an interface correlation function let us consider the simplest setup, namely, a single interface \mathcal{I}_ϖ with $\varpi = (P, |a_\pm\rangle; \chi_\pm, \chi_P)$ inserted along the equator γ of the sphere. The interface splits $X = \mathbb{S}^2$ into two disks $X_\pm = \mathbb{D}_\pm$. The set $C[\mathcal{I}_\varpi]$ consists of a single map Γ , which covers \mathbb{S}^2 by a disjoint union of P spheres and $N_\pm - P$ disks, that are mapped to the upper/lower hemisphere. Every deck transformations is a product of one of the $P!$ permutations of spheres and two permutations of disks chosen from the $(N_\pm - P)!$ possible options. Thus we conclude that

$$Z_{N_\pm, \varpi}^{\mathbb{D}_-, \mathbb{D}_+} := \langle \mathcal{I}_\varpi \rangle_{\text{Sym}^{N_- | N_+}(\mathcal{M})}^{\text{unnormalised}} = \frac{\chi_-(id) \chi_P(id) \chi_+(id) g_-^{N_- - P} g_+^{N_+ - P}}{(N_- - P)!(N_+ - P)!P!}, \quad (2.44)$$

where $g_\pm := \langle 0 | a_\pm \rangle$ are the g -factors of the two boundary conditions a_\pm of the seed theory that are imposed along R_\pm^γ . Note that the latter consists of $N_\pm - P$ disconnected components. The expectation value of the seed theory is evaluated in a normalisation in which the sphere partition function of the seed theory \mathcal{M} is set to 1. The same result can alternatively be obtained from the construction in [5], see eq. (C.4).

Torus partition function – statement of the result. Let us now discuss a much richer example of an interface correlator, namely a pair of parallel interfaces inserted on a torus $X = \mathbb{T}^2 = \mathbb{C}/(\mathbb{Z} + \tau\mathbb{Z})$. The interfaces are located along two curves $\gamma_L : s \mapsto \tau s$ and $\gamma_R : s \mapsto \tau s + 1/2$. These cut the torus into two annuli X_\pm . The interface data ϖ^L and ϖ^R can involve two different indices of transmissivity P_L and P_R and two different pairs of boundary conditions a_\pm^L and a_\pm^R . To avoid notational clutter, we shall assume the characters $\chi^{L/R}$ to be trivial, though it would not be difficult to consider the more general case. According to the general definition, the interface correlation function takes the form

$$Z_{N_\pm, P_{L/R}}^{\mathbb{T}^2} = \langle \mathcal{I}^{(P_L)}[\gamma_L] \mathcal{I}^{(P_R)}[\gamma_R] \rangle_{\text{Sym}^{N_- | N_+}(\mathcal{M})}^{\text{unnormalised}} = \sum_{\Gamma \in C[\mathcal{I}^L \mathcal{I}^R]} \frac{1}{|\text{Deck}[\Gamma]|} Z_{\mathcal{M}}^\Sigma, \quad (2.45)$$

where $Z_{\mathcal{M}}^\Sigma$ is the vacuum partition function of \mathcal{M} on Σ with boundary conditions $|a_\pm^{L/R}\rangle$ imposed on $\partial\Sigma$. It was found in [5] that these interface partition functions take a particularly useful shape if we pass to the following grand-canonical partition function

$$Z_{\mu_{L/R}, \nu_{L/R}, \pm}^{\mathbb{T}^2} := \sum_{N_\pm=0}^{\infty} \sum_{P_{L/R}=0}^{\min(N_-, N_+)} Z_{N_\pm, P_{L/R}}^{\mathbb{T}^2} \prod_{A \in \{L, R\}} \mu_A^{P_A} \nu_{A,-}^{N_- - P_A} \nu_{A,+}^{N_+ - P_A} \quad (2.46)$$

where the dependence of the partition function on the integers N_\pm and $P_{L/R}$ is traded for a dependence on the fugacities $\mu_{L/R}$ and $\nu_{L/R, \pm}$. The formula put forward in [5] reads⁸

$$Z_{\mu_{L/R}, \nu_{L/R}, \pm}^{\mathbb{T}^2} = \exp \left(\sum_{w, \ell=1}^{\infty} \sum_{k=1}^w \frac{\mu^{w\ell}}{w\ell} Z\left(\frac{\ell\tau+k}{w}\right) + \sum_{\substack{\omega, \ell \\ A, B}} \frac{1}{\ell} \left(\frac{\mu^\omega \nu_{AB}}{\mu_A \mu_B} \right)^\ell Z_o^{AB}\left(\frac{\ell\tau}{\omega}\right) \right) \quad (2.47)$$

⁸We chose a slightly modified but equivalent way of writing down the result of [5] here.

where the sum in the second terms runs over $A, B \in \{L, R\}$, $\omega \in 2\mathbb{Z}_{>0} - 1 + \delta_A^B$ and $\ell \geq 1$. The variables μ and ν_{AB} are given by $\mu := \mu_L \mu_R$ and

$$\nu_{LL} := \nu_{L,-} \nu_{L,+}, \quad \nu_{LR} := \nu_{L,-} \nu_{R,-}, \quad \nu_{RL} := \nu_{R,+} \nu_{L,+} \quad \text{and} \quad \nu_{RR} := \nu_{R,-} \nu_{R,+}. \quad (2.48)$$

The dependence of the grand-canonical partition function on the seed theory and the choice of boundary conditions $a_{\pm}^{L/R}$ enters through the overlaps

$$Z_{a,b}(t) = \langle a | \hat{x}^{\frac{1}{2}(L_0 + \bar{L}_0 - \frac{c_M}{12})} | b \rangle = \hat{Z}_{a,b}(\hat{t}) \quad \hat{t} := -\frac{1}{t} \quad \hat{x} := e^{2\pi i \hat{t}}, \quad (2.49)$$

between a pair of boundary states $|a\rangle$ and $|b\rangle$ of the seed theory. Through modular transformation, these overlaps are related to annulus partition functions \hat{Z} , as usual. There are four different annulus partition functions that appear in eq. (2.47) which we denoted by

$$Z_o^{LL} = Z_{a_-^L, (a_+^L)^*}, \quad Z_o^{LR} = Z_{a_-^L, a_-^R}, \quad Z_o^{RL} = Z_{a_+^L, a_+^R} \quad \text{and} \quad Z_o^{RR} = Z_{(a_+^R)^*, a_-^R}. \quad (2.50)$$

This concludes our description of the grand-canonical partition function (2.47) for two interfaces $\mathcal{I}[\gamma_L]$ and $\mathcal{I}[\gamma_R]$ on the torus \mathbb{T}^2 , restricted to the case of trivial characters.

Torus partition function – derivation. Let us now derive the formula (2.47) from the general prescription in eq. (2.45). The first ingredient there is the sum over interface covering maps $\Gamma \in C[\mathcal{I}^L \mathcal{I}^R]$. The relevant covering surfaces Σ can be decomposed as

$$\Sigma = \Sigma_c \sqcup \Sigma_o^{LL} \sqcup \Sigma_o^{LR} \sqcup \Sigma_o^{RL} \sqcup \Sigma_o^{RR} \quad (2.51)$$

where the restriction of the covering map Γ to Σ_c is one of the coverings of the torus by tori discussed in Sec. 2.2 and each connected component of the surfaces Σ_o^{AB} is a cylinder

$$\Sigma_{\omega,\ell} := [0, \frac{\omega}{2}] \times [0, \ell|\tau|] / (x, 0) \sim (x, \ell|\tau|). \quad (2.52)$$

The restriction of $\Gamma_o^{AB} : \Sigma_o^{AB} \rightarrow \mathbb{T}^2$ to the connected component $\Sigma_{\omega,\ell}$ is given by

$$\Gamma_{\omega,\ell}^{AB} : \Sigma_{\omega,\ell} \rightarrow \mathbb{T}^2, \quad (x, y) \mapsto \left[\left(x + \frac{1}{2} \delta_A^R, y \frac{\tau}{|\tau|} \right) \right], \quad (2.53)$$

where the value of ω is restricted to $\omega \in 2\mathbb{Z} + 1 - \delta_A^B$. Furthermore, $\text{Deck}[\Gamma_{\omega,\ell}^{AB}] \cong \mathbb{Z}_\ell$ consists of translations $(x, y) \mapsto (x, y + k|\tau|)$. Let us denote by $C_{w,\ell}^k$ the number of copies of the surface $\Sigma_{\omega,\ell}^k$ that appear within Σ_c and similarly denote by $O_{\omega,\ell}^{AB}$ the number of components of type $\Sigma_{\omega,\ell}$ that appear in Σ_o^{AB} . Then the number of Deck transformations is given by

$$|\text{Deck}[\Gamma]| = \prod_{w,\ell,k} C_{w,\ell}^k! (w\ell)^{C_{w,\ell}^k} \prod_{\substack{\omega,\ell \\ A,B}} O_{\omega,\ell}^{AB}! \ell^{O_{\omega,\ell}^{AB}}. \quad (2.54)$$

Inserting this formula into the general definition (2.45) of the interface partition functions on the torus we obtain

$$Z_{N_{\pm}, P_{L/R}}^{\mathbb{T}^2} = \sum_{\text{allowed } C, O^{AB}} \left(\prod_{w,\ell,k} \frac{\left(\frac{1}{w\ell} Z\left(\frac{\ell\tau+k}{w}\right) \right)^{C_{w,\ell}^k}}{C_{w,\ell}^k!} \prod_{\substack{\omega,\ell \\ A,B}} \frac{\left(\frac{1}{\ell} Z_o^{AB}\left(\frac{\ell\tau}{\omega}\right) \right)^{O_{\omega,\ell}^{A,B}}}{O_{\omega,\ell}^{AB}!} \right) \quad (2.55)$$

where the allowed coefficients C and $O^{A,B}$ are exactly those satisfying the constraints

$$N_- - P_L = \sum_{\omega, \ell, B} O_{\omega, \ell}^{LB} \ell, \quad N_+ - P_L = \sum_{\omega, \ell, A} O_{\omega, \ell}^{AL} \ell, \quad N_- - P_R = \sum_{\omega, \ell, A} O_{\omega, \ell}^{AR} \ell, \quad (2.56)$$

$$N_+ - P_R = \sum_{\omega, \ell, B} O_{\omega, \ell}^{RB} \ell, \quad \text{and} \quad P_A = \sum_{w, \ell} \sum_k w \ell C_{w, \ell}^k + \sum_{\omega, \ell} \sum_{A, B} (\omega - \delta_I^A - \delta_J^A) \ell O_{\omega, \ell}^{I, J}. \quad (2.57)$$

For the grand-canonical partition function (2.46), these constraints are lifted and by performing the unconstrained sum over $C_{w, \ell}^k$ and $O_{\omega, \ell}^{AB}$ one immediately obtains eq. (2.47).

Spectrum of interface changing operators. In this paragraph, we rewrite eq. (2.47) in a form that allows us to directly read off the spectrum of interface changing operators. To do so, we start by spelling out the seed partition functions in terms of the bulk and boundary spectra I and I_o^{AB} as well as the multiplicities $d_{h, \bar{h}}$ and d_Δ of the corresponding representations in the Hilbert space, i.e.

$$Z(\tau, \bar{\tau}) = \sum_{(h, \bar{h}) \in I} d_{h, \bar{h}} q^{h - \frac{c\mathcal{M}}{24}} \bar{q}^{\bar{h} - \frac{c\mathcal{M}}{24}} \quad \text{and} \quad Z_o^{AB}(\tau) = \sum_{\Delta \in I_o^{AB}} d_\Delta^{AB} q^{\Delta - \frac{c\mathcal{M}}{24}}. \quad (2.58)$$

Setting $\bar{\tau} = \tau$ for the bulk partition function and using the identities

$$\exp\left(\alpha \sum_{\ell=1}^{\infty} \frac{x^\ell}{\ell}\right) = (1-x)^{-\alpha} \quad \text{and} \quad \frac{1}{w} \sum_{k=1}^w e^{2\pi i \frac{k}{w}(x-\bar{x})} = \begin{cases} 1 & \text{if } x - \bar{x} \equiv 0 \pmod{w} \\ 0 & \text{else} \end{cases} \quad (2.59)$$

then allows us to rewrite eq. (2.47) as

$$Z_{\mu_{L/R}, \nu_{L/R}, \pm}^{\mathbb{T}^2} = \prod_{w>0} \prod_{\substack{(h, \bar{h}) \in I \\ h - \bar{h} \equiv 0 \pmod{w}}} \left(1 - \mu^w q^{\frac{1}{w}(h + \bar{h} - \frac{c\mathcal{M}}{12})}\right)^{-d_{h, \bar{h}}} \prod_{A, B} \prod_{\omega} \prod_{\Delta \in I_o^{AB}} \left(1 - \frac{\mu^\omega \nu_{AB}}{\mu_A \mu_B} q^{\frac{1}{\omega}(\Delta - \frac{c\mathcal{M}}{24})}\right)^{-d_\Delta^{AB}}, \quad (2.60)$$

where ω runs over $2\mathbb{Z}_{>0} - 1 + \delta_A^B$. The scaling dimensions of interface changing operators can be read off from eq. (2.60) by extracting the fixed N_\pm partition functions and adding $\frac{c\mathcal{M}}{24}(N_- + N_+)$ to the exponents of q . From the grand-canonical perspective, this amounts to shifting the exponent of q for the factors of the product over w by $\frac{c\mathcal{M}}{24}2w$ and likewise, shifting the factors of the ω product by $\frac{c\mathcal{M}}{24}\omega$. We conclude that the spectrum of local operators that can be inserted between our interfaces consists of products of single particle fields falling into the five families \mathcal{O}_w and \mathcal{O}_ω^{AB} with $A, B \in \{L, R\}$. The former can simply be interpreted as bulk operators inserted on the transmissive part of the interfaces, while the latter are intrinsically attached to the interface. Quantitatively, the arguments given above tell us that for each $w > 0$ and each seed theory bulk operator \mathcal{O} of dimension $\bar{h} + h$, and spin $\bar{h} - h$ divisible by w , we obtain a single particle interface operator with dimension

$$\Delta_w = \frac{\bar{h} + h}{w} + \frac{c\mathcal{M}}{12} \left(w - \frac{1}{w}\right), \quad (2.61)$$

while each weight $\Delta \in I_o^{AB}$ leads to a family of fields with dimension

$$\Delta_\omega^{AB} = \frac{\Delta}{\omega} + \frac{c\mathcal{M}}{24} \left(\omega + \frac{1}{\omega}\right). \quad (2.62)$$

In the special case where the boundary states that enter the construction of the interfaces are chosen to coincide, i.e. $a_+ = a_-$, the seed theory boundary spectra that are captured by the partition functions (2.50) contain an identity operator, i.e. $0 \in I_o^{AB}$, and thus the spectrum of the symmetric product orbifold contains *interface twist fields* σ_ω^{AB} whose conformal weight is given by eq. (2.62) with $\Delta = 0$. Studying correlation functions of these interface twist fields is the main focus of our work and hence we shall mostly consider interfaces with $|a_+\rangle = |a_-\rangle =: |a\rangle$ (and $\chi_\pm = \chi_P = 1$). The associated interface operators will be denoted by $\mathcal{I}_{|a\rangle}^{(P)}$.

Interface changing correlators. We are finally ready to address the main topic of this work, namely correlation functions including twist field insertions along the interface (and in the bulk). To keep things simple we return to the case in which an interface operator $\mathcal{I}[\gamma]$ is inserted along a single closed curve γ so that we are strictly in the setup we considered previously in Section 2.3. The extension to multiple interface insertions is straightforward. For simplicity we also restrict to the case of trivial characters χ and set $|a_+\rangle = |a_-\rangle =: |a\rangle$, see our discussion at the end of the previous paragraph. This leaves the degree of transmissivity P as the main parameter of the interface, besides the choice of the boundary state $|a\rangle$.

As we explained above, some interface twist fields can only be inserted at points at which the degree of transmissivity changes. To be more precise, the interface twist fields σ_ω^{LL} and σ_ω^{RR} can only be inserted at points along the curve γ at which the degree of transmissivity P jumps by one unit to $P \pm 1$, see also Figure 1. Put differently, if we want to insert these fields we have to break up the curve γ into smaller segments and insert interface operators with different degree of transmissivity along these segments. Since this is notationally a bit cumbersome we shall keep using the interface operator $\mathcal{I}_{|a\rangle}^{(P)}[\gamma]$ where P denotes the degree of transmissivity of $\mathcal{I}[\gamma]$ at the base point $\gamma(0) = \gamma(1)$ of the curve. We shall sometimes refer to this base point as the *reference point* and denote it by t^* in the rest of this paper. It is then understood that this degree jumps whenever γ passes through the insertion point of an interface changing twist field $\sigma_\omega^{LL}(t)$ or $\sigma_\omega^{RR}(t)$.

With this comment on notation in mind let us now spell out the family of observables \mathcal{O} whose expectation values we want to compute. These are given by

$$\mathcal{O} = \mathcal{I}_{|a\rangle}^{(P)}[\gamma] \prod_{i=1}^{n_c} \sigma_{w_i}(x_i) \prod_{i=1}^{n_o} \sigma_{\omega_i}^{A_i B_i}(t_i) \quad (2.63)$$

where we assume that the reference point $t^* = \gamma(0)$ is not the insertion point of a local operator.

As in our previous discussions, the expectation values of the observables \mathcal{O} we consider now can be evaluated by summing certain expectation values on the seed theory over some set of covering maps $\Gamma \in C[\mathcal{O}]$. The insertion of the interface changing operators $\sigma_\omega^{AB}(t_i)$ into the expectation value enforces that covering maps that contribute to the correlator

have a type ω^{AB} interface ramification point that maps to the branch point $t_i \in X$. Thus,

$$C[\mathcal{O}] = \left\{ \begin{array}{l} N_{\pm} \text{ sheeted interface coverings of } X \text{ with deg. of transmissivity } P \\ \text{at } \gamma(0) \text{ and bulk branchpts. } x_i \text{ lifting to ramification pts. with} \\ \text{ramification index } w_i \text{ as well as interface branchpts. } t_i \text{ lifting to} \\ \text{interface ramification pts. with ramification index } \omega_i^{A_i B_i}. \end{array} \right\}. \quad (2.64)$$

Like the bulk vacuum twist fields, the interface vacuum twist fields lift to the identity operator along the covering map, up to some coefficient as in eq. (2.42). Since we assumed that all three characters χ_{\pm} and χ_P are trivial, the factors that depend on the monodromies of the covering map is also trivial and hence we are left with $\alpha[\Gamma]$. In Sec. 3, we determine $C[\mathcal{O}]$ for any correlator with $X = \mathbb{S}^2$ explicitly. The explicit evaluation of the correlators from these data is then addressed in Sec. 4.

3 Generalised Pakman-Rastelli-Razamat diagrammatics

In this section, we introduce diagrammatic rules that provide a systematic classification of the covering maps that contribute to any specific interface correlator. In the first subsection, Sec. 3.1, we review the analogous diagrams for bulk correlators which were introduced by Pakman, Rastelli and Razamat in [11]. The main subsection, 3.2, introduces the interface generalisation. Sec. 3.3 describes how to determine the symmetry group of an interface covering map, i.e. the group $\text{Deck}[\Gamma]$ of its deck transformations, directly from the corresponding diagram. Subsection 3.4 provides an alternative perspective on the same problem and determines the symmetry factors by counting different ways to label faces of diagrams, an approach that more directly connects to the bulk discussion of Reference [11]. The final subsection, 3.5, is devoted to the large- N limit of interface correlators.

3.1 Pakman-Rastelli-Razamat diagrams

This section reviews the Pakman-Rastelli-Razamat (PRR) diagrammatic rules. We first discuss how to construct the associated PRR diagram given a covering map. To do so, we take a slight detour of first constructing auxiliary diagrams with redundant extra vertices and then reducing these to their PRR form. While this makes the discussion of the case without interfaces slightly less efficient than the original description in Reference [11], the approach will pay off in Section 3.2 since it is well aligned with the interface generalisation.

After we have explained how to extract diagrams from covering maps, the second paragraph of the section formulates constructive rules that allow us to generate the set of PRR diagrams without knowledge of the covering maps. Finally, we showcase how to apply the rules in simple examples. Appendix E sketches a proof of the validity of the rules.

Diagrams from covering maps. To construct the PRR diagram $\mathcal{D}[\Gamma]$ of a covering map $\Gamma : \Sigma \rightarrow \mathbb{S}^2$, we perform the following three steps.

1. Draw lines with the same orientation, at distance ε above and below the equator, deformed as in Fig. 2 such that all branch points of Γ are in the strip between them.

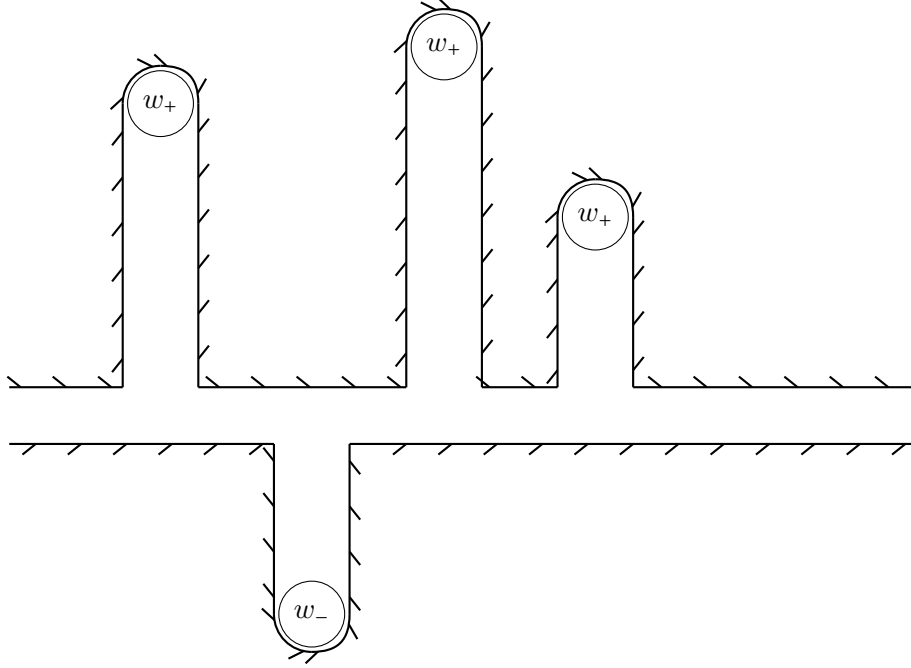


Figure 2: Lines on \mathbb{S}^2 whose preimage w.r.t. a covering map Γ produce $\mathcal{D}_\varepsilon[\Gamma]$. Branch points in the upper and lower hemisphere are denoted by w_+ and w_- . Orientations are represented by half-arrows extending into the disk on whose boundary they are drawn.

2. The preimage $\mathcal{D}_\varepsilon[\Gamma]$ of this configuration with respect to Γ is a network of oriented lines on Σ . Take the limit $\mathcal{D}[\Gamma] := \lim_{\varepsilon \rightarrow 0} \mathcal{D}_\varepsilon[\Gamma]$.
3. Each face of $\mathcal{D}[\Gamma]$ is either the preimage of the upper or the lower hemisphere with respect to Γ . Label the faces with “+” and “-” respectively.

If Γ has degree N then $\mathcal{D}[\Gamma]$ has $2N$ faces, all of them with a consistently oriented boundary and exactly half labelled by +. The diagram has four classes of vertices, two of which are shown in Fig. 3. The other two may be obtained simply by flipping all signs \pm in the faces. In the $\varepsilon \rightarrow 0$ limit, the preimages of the lines on \mathbb{S}^2 , reaching out to branch points from the equator of the sphere, degenerate into double lines which end on the branch points. We shall refer to these double lines as misaligned since the arrows along them point in opposite directions. Each misaligned double line lifts to w copies on Σ , leading to the vertex shown in Fig. 3a.

Note that the faces that touch at a misaligned double line possess the same sign. Furthermore, each region where such a fold leaves the equator becomes a trivalent vertex of the type shown in Fig. 3b. We refer to the latter type of vertices as redundant vertices for reasons that will become clear in a moment. Let us first note, however, that these trivalent vertices involve a single misaligned double line and two aligned double lines for which the arrows on both sides of the double line point in the same direction. Faces joined by aligned double lines carry opposite signs.

As illustrated in Fig. 4a, all edges emanating from a vertex that corresponds to a ramification point end on redundant vertices. We can therefore simplify the diagrams without losing any information by moving the trivalent vertices like a zip toward the ramification vertex until we have entirely eliminated the misaligned double line. For each misaligned double line that was entering the ramification vertex before, this reduction produces two aligned double lines that enter the vertex, with the sign of the faces flipping each time we cross an aligned double line. This fusion of ramification and redundant vertices, leads to diagrams that only have one type of vertices, namely those shown in Fig. 4b. The reduced graphs are the standard PRR diagrams.

Let us close this subsection with further comments on this relation to the diagrams of Pakman, Rastelli and Razamat. The original PRR diagrams use a single type of double lines composed of one dashed and one solid line with no displayed orientation. But in checking consistency of PRR diagrams it becomes important that one goes through the dashed loops in clockwise order and through solid loops in anti-clockwise order. In this sense, the lines of PRR diagrams inherit an orientation from the orientation of Σ . We have decided here to make this orientation manifest in our graphics. The PRR faces that are enclosed by solid loops correspond to the faces we label with $+$, while those surrounded by dashed loops are the ones we label with $-$. The main difference in our approach is that, initially, we have three types of double lines. Our aligned double lines correspond to the PRR double lines. But in addition we have two more double lines, namely the misaligned double lines that run between two faces with label $+$, and the misaligned double lines that run between two faces that carry a $-$ label. Following PRR graphics, one can also picture these as double lines with two solid and two dashed lines, respectively. Our redundant vertex would then be represented as a vertex in which the double line with e.g. two solid lines splits into two double lines of PRR type, i.e. with one dashed and one solid line. As long as there is no interface located at the equator, the misaligned double lines can be removed by the reduction procedure described in the previous paragraph. This leaves us with diagrams that only contain the aligned double lines used by Pakman, Rastelli and Razamat.

Covering maps from diagrams. The PRR diagrams for covering maps Γ of degree N can be constructed by using the vertices in Fig. 4b, as well as those with flipped signs of the faces, choosing an order of the branch points and imposing the following three rules.

1. The boundary of a face contains each ramification point at most once.
2. Traversing the boundary of a face along its orientation, one encounters the ramification points in the order of the corresponding branch points.
3. Each face is simply connected and the number of faces equals the degree N of the covering map.

Clearly, the diagrams that classify equivalence classes of covering maps introduced in the previous paragraph satisfy the three rules above. In Appendix E, we show that vice versa every diagram constructed in this way corresponds to an equivalence class of covering maps.

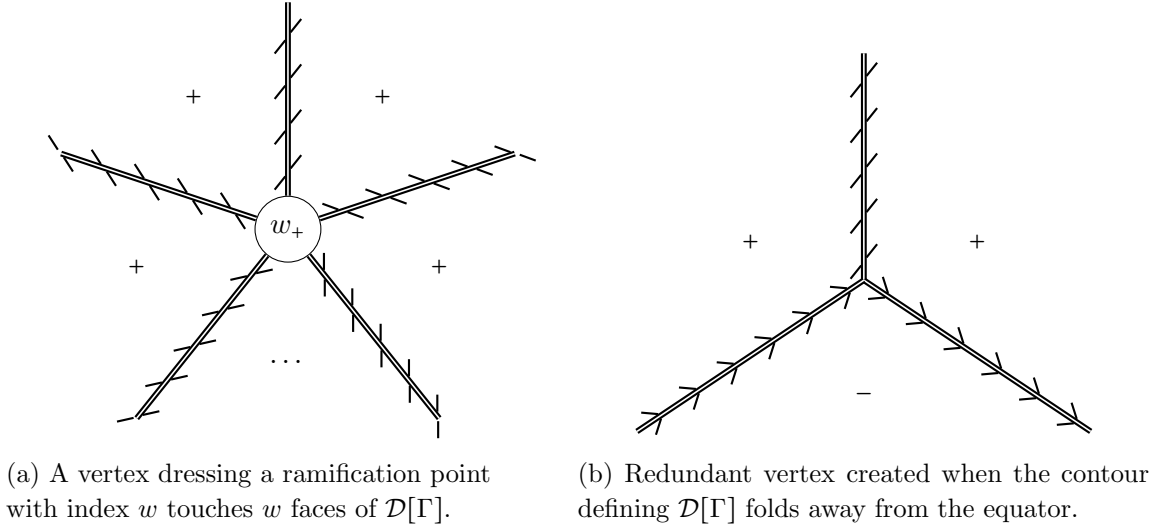


Figure 3: This figure shows half of the vertices of the PRR diagrams. Two more vertices can be generated by turning around all orientations and exchanging $+\leftrightarrow -$.

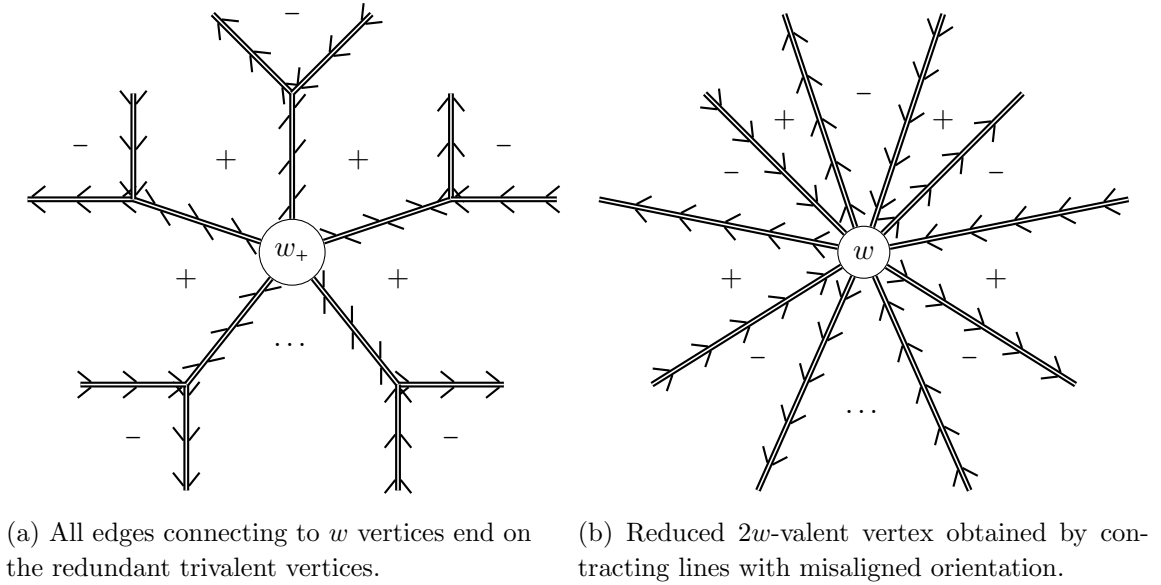
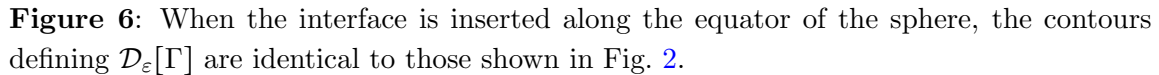


Figure 4: Reduction to standard PRR diagrams.

Example: Two-point correlator. As a simple example, Figure 5 shows the covering map Γ which computes the two-point function $\langle \sigma_w \sigma_w \rangle$ of two twist w operators. This map is a covering of the sphere by the sphere with two ramification points, both of them having ramification index w . Thus, the diagram is a graph embedded in the sphere with two vertices that are connected by double lines of alternating orientation. The graph has $2w$ faces, half of which with a “-” and half with a “+” label.



Following the same strategy as in Section 3.1, we first construct diagrams from interface covering maps. We then present a set of rules that allow us to systematically construct all possible diagrams given a set of prescribed ramification points. Finally, we demonstrate the rules in several examples. A proof for the validity of the rules is sketched in App. E.

Diagrams from interface covering maps. The following three steps construct a diagram⁹ $\mathcal{D}[\Gamma]$ on a Riemann surface Σ given an interface covering map $\Gamma : \Sigma \rightarrow \mathbb{S}^2$.

1. Draw lines with the same orientation, at distance ε above and below the interface, deformed as in Fig. 6 such that all branch points of Γ are in the strip between them.
2. The preimage $\mathcal{D}_\varepsilon[\Gamma]$ of this configuration with respect to Γ is a network of oriented lines on Σ . Take the limit $\mathcal{D}[\Gamma] := \lim_{\varepsilon \rightarrow 0} \mathcal{D}_\varepsilon[\Gamma]$.
3. Each face of $\mathcal{D}[\Gamma]$ is either the preimage of the upper or the lower hemisphere with respect to Γ . Label the faces with “+” and “−” respectively.

In the interface case, the vertices of Fig. 3 are augmented by the vertices of Fig. 7. The first four vertices originate from boundary ramification points of the interface covering map. They involve two oriented (single) lines and $\omega - 1$ aligned double lines. Since all the double lines are aligned, the label on the faces alternates. There are four different assignments of signs in the two faces that involve the single line. These assignments distinguish the four vertices corresponding to the four classes of boundary ramification points. Additionally, there are two vertices in which a misaligned double line splits into a pair of single lines. The two variants of these vertices are distinguished by the sign of the two faces touching the misaligned line, which can be either both + or both −.

The trivalent vertices that we encountered in the absence of the interface were redundant since there was a face with the opposite sign that we could use to split the misaligned double line into a pair of aligned ones. Now, however, the interface can cause the surface to rip open. When this happens, there is no face with opposite sign on the other side. Therefore, these vertices cannot be removed.

As in the case without interface, the two halves of each double line originating in bulk ramification points have opposite orientation, i.e. these double lines are misaligned. Again, we can remove all ‘redundant’ trivalent vertices where misaligned double lines split into a pair of aligned double lines by moving them on top of a bulk ramification point. In this process we can remove some of the misaligned double lines. But if there is a non-trivial interface, it is no longer possible to remove all the misaligned double lines through this process. Hence, the interface diagrams do involve three different types of double lines in general, the aligned ones that also appear in the bulk PRR diagrams and the two types of misaligned ones that run between faces labelled by + and by −.

The bulk vertices involve both aligned and misaligned double lines. Their associated ramification index w fixes the overall number of these double lines but not how they are distributed among the two types. More precisely, $2w$ is the number of aligned double lines plus twice the number of misaligned ones.

Covering maps from diagrams. The interface PRR diagrams of interface covering maps Γ of degrees N_\pm equipped with a consistent choice of order for the branch points are the diagrams built out of the vertices in Figures 3 and 7, satisfying the three rules

⁹In mathematical terms the object that we construct is a combinatorial map i.e. a graph with additional data describing the cyclic configuration of edges at each vertex.

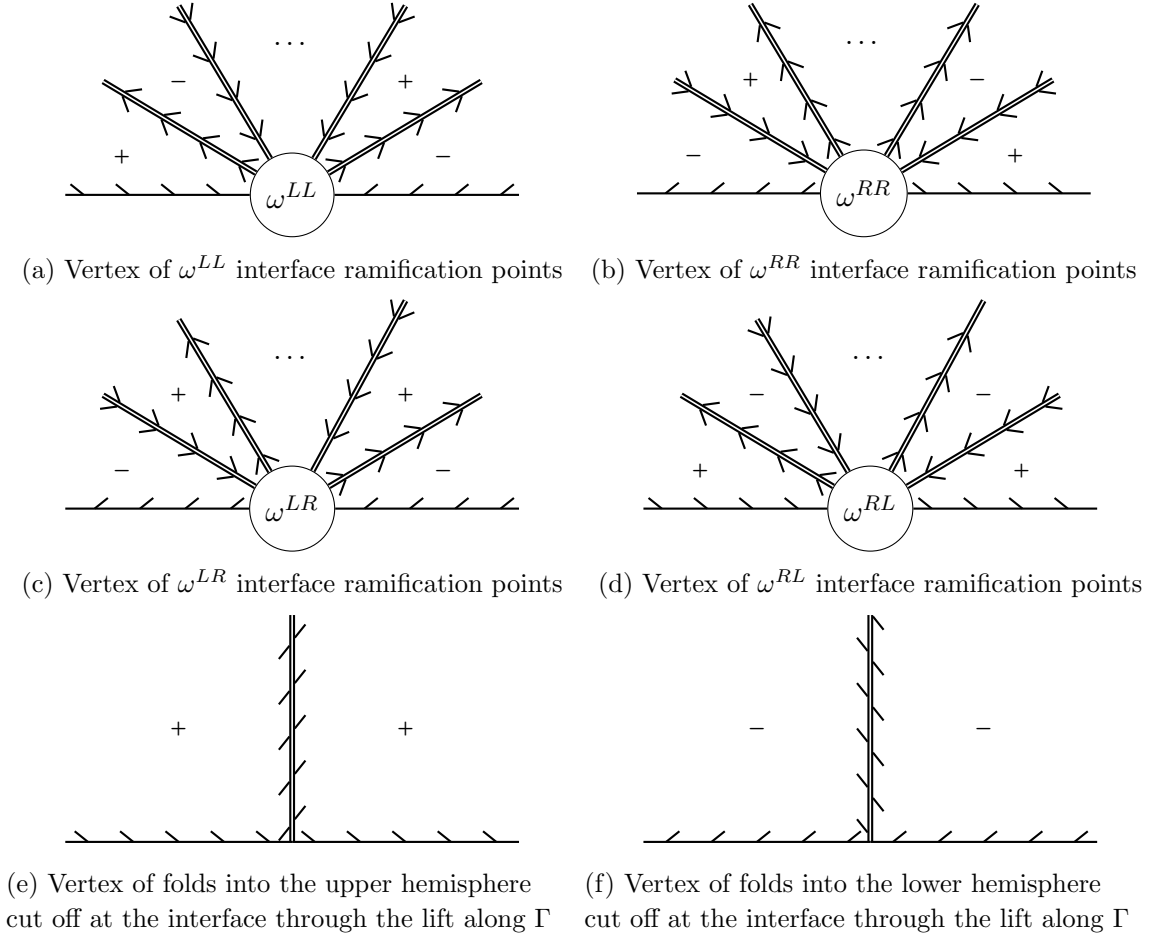


Figure 7: Additional vertices for interface covering maps.

given below. In this context, “consistent choice of order” means that the restriction of the ordering to interface branch points coincides with the order induced by the orientation of the interface.

1. The boundary of a face contains each ramification point at most once.
2. Traversing the boundary of a face along its orientation, one encounters the ramification points in the order of the corresponding branch points.
3. Each face is simply connected and the number of “ \pm ”-faces is N_{\pm} .

Clearly, the diagrams that classify equivalence classes of covering maps introduced in the previous paragraph satisfy the three rules above. In Appendix E we show that, conversely, all interface PRR diagrams actually correspond to interface covering maps.

Example 1. As a first example, let us consider the diagrammatics for the interface covering maps Γ that can contribute to the correlation function

$$\langle \sigma_2^{RR} \sigma_2(z) \sigma_2^{LL} \rangle. \quad (3.1)$$

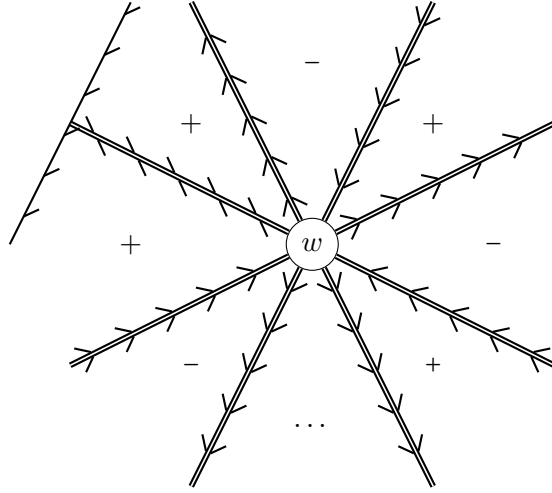


Figure 8: Bulk vertex in a reduced diagram obtained by removing redundant vertices. While this picture shows only a single misaligned line emanating from the bulk vertex to the boundary of Σ , there could in general be up to w such lines attached to the same vertex.

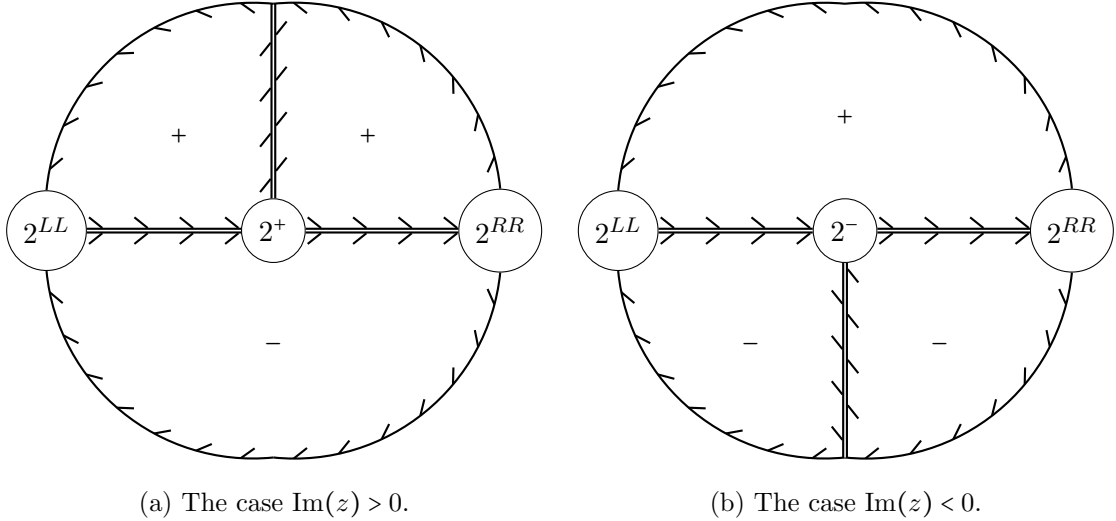


Figure 9: Diagram of $\langle \sigma_2^{RR} \sigma_2(z) \sigma_2^{LL} \rangle$ with order $2^{LL} < 2 < 2^{RR}$.

The only connected covering space contributing to this correlator is a disk. If z is in the upper hemisphere, the corresponding interface covering map has $N_- = 1$ and $N_+ = 2$. The assignment is reversed if z is in the lower hemisphere, i.e. $N_- = 2$ and $N_+ = 1$ in that case. The two corresponding diagrams are shown in Figure 9. The correlator is a good example to highlight the relevance of the order that is assigned to the bulk branch points through the contour in Figure 6. The diagrams shown in Figure 9 correspond to the choice of ordering $2^{LL} < 2 < 2^{RR}$. The other option, i.e. $2^{LL} < 2^{RR} < 2$, is shown in Figure 10. Let us stress that the diagrams arising from different choices of ordering do not correspond to different

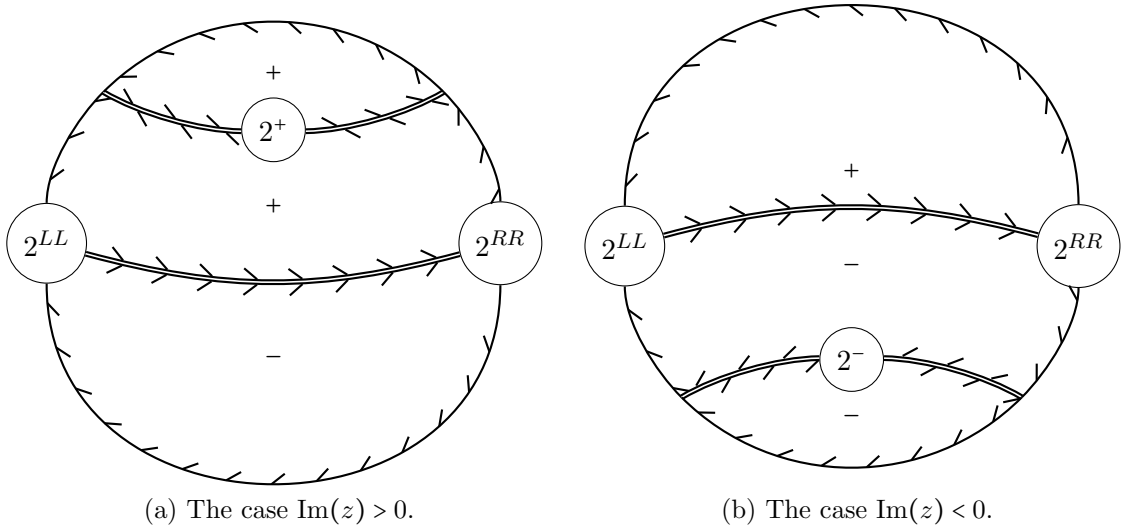


Figure 10: Diagram of $\langle \sigma_2^{RR} \sigma_2(z) \sigma_2^{LL} \rangle$ with order $2^{LL} < 2^{RR} < 2$.

types of covering maps that contribute to the correlator (3.1). Instead they are different graphical representations of the same covering map. Finally, let us also draw the attention of the reader to the subtle feature that performing a reflection of the diagrams along the vertical axis that goes through the vertex corresponding to the bulk field does *not* result in valid diagrams. The vertices of valid diagrams are precisely those listed in Figure 7. In particular, a curve moving around a valid ω^{LL} vertex anticlockwise in a small semi-circle has to start on the boundary of a “-”-face and end on the boundary of a “+”-face. The analogous statement with “+” and “-” exchanged holds for the ω^{RR} vertices.

Example 2. Let us now discuss a less trivial example, where multiple diagrams contribute, namely the four-point correlation function

$$\langle \sigma_5^{RL} \sigma_5^{RL} \sigma_2^{RR} \sigma_2^{LL} \rangle \quad (3.2)$$

of interface operators. Whereas the ordering of bulk operators along the interface is an arbitrary (but necessary) choice that does not have any direct physical meaning, the ordering of interface operators is unambiguous (i.e. different orderings correspond to physically different correlation functions). With the ordering fixed in eq. (3.2), there is a unique disk diagram corresponding to an interface covering map that contributes to the correlator. This diagram is illustrated in Figure 11. Furthermore, there are two distinct cylinder diagrams that contribute to the connected part of the correlator. These are shown in Figure 12.

Example 3. As the complexity of correlators increases, the number of diagrams that contributes for each covering surface also grows. Figure 13 shows only one of many diagrams that contribute at disk level to the four-point function

$$\langle \sigma_7^{RL} \sigma_2(z_2^+) \sigma_3(z_3^+) \sigma_2(z_2^-) \rangle. \quad (3.3)$$

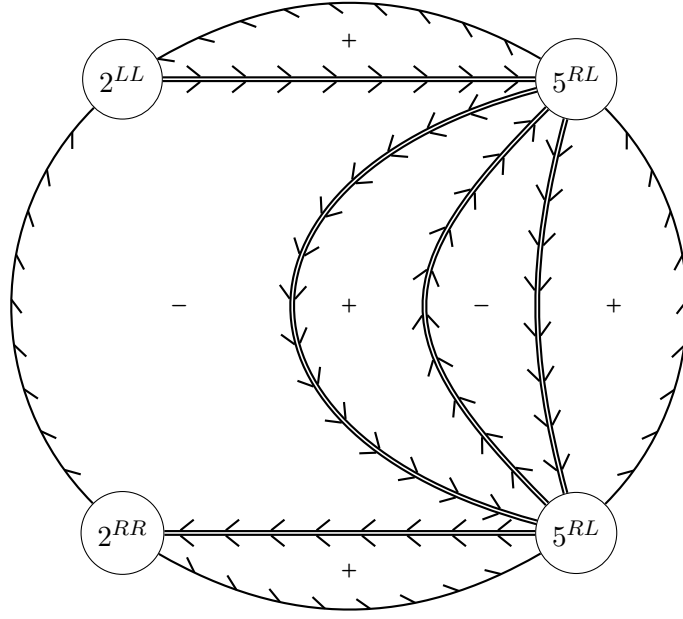
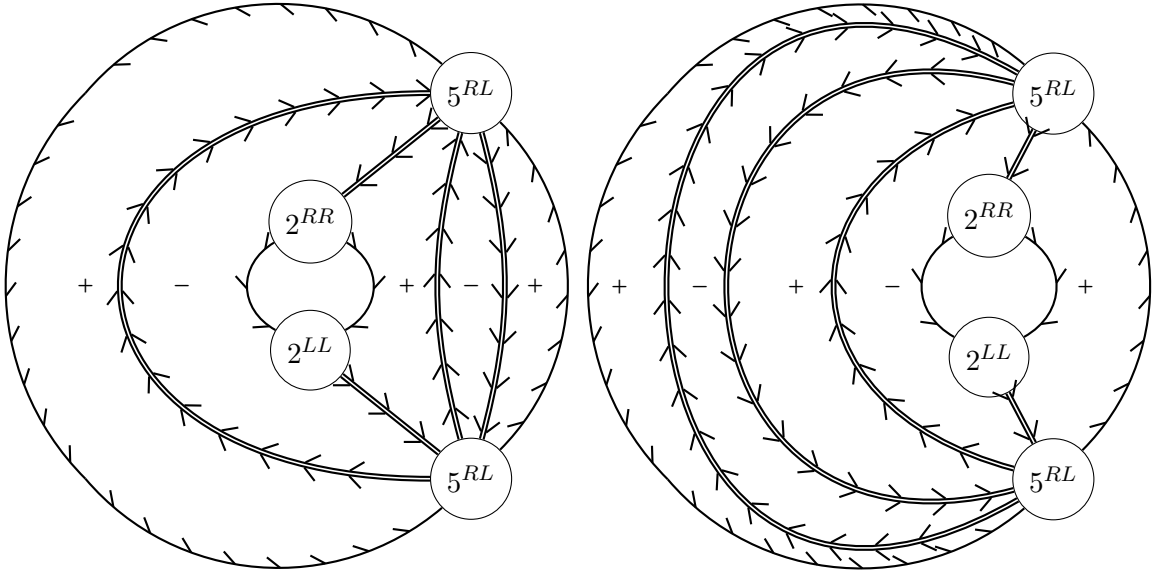


Figure 11: Disk contribution to the correlator (3.2) at $N_- = 2$ and $N_+ = 4$.



(a) Diagram with separated boundaries.

(b) Diagram with adjacent boundaries.

Figure 12: Cylinder contributions to the correlator (3.2) at $N_- = 2$ and $N_+ = 3$.

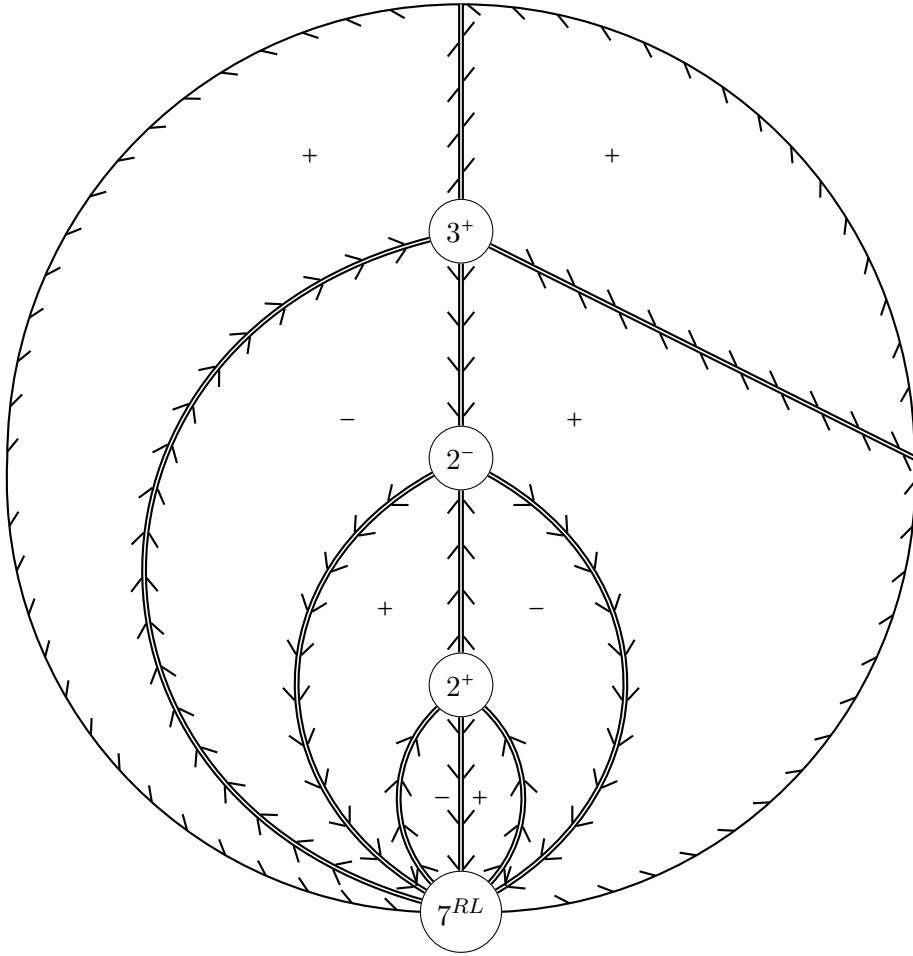


Figure 13: Diagram for one of the disk covering maps contributing to (3.3).

We hope that these three examples suffice to illustrate the diagrammatic rules that we have introduced in order to describe interface covering maps.

Diagrams with reference point. By construction, we can read off N_{\pm} from a diagram by counting the faces labelled by $+$ and $-$. We now explain how one can read off the degree of transmissivity P . Recall that, when moving along the interface, P changes by one unit whenever we cross an interface branch point of type LL or RR , see Section 2. Thus, the integer P is not a global property of the covering map, but a local property associated to a reference point t^* on the interface, as also discussed below eq. (2.63). Given a choice of t^* , we decorate our diagrams with the elements of the preimage $\Gamma^{-1}(t^*)$ under the covering map. The degree of transmissivity P at t^* is then given by the number of these preimages occurring in the interior of the covering space, i.e. on double lines. The relevant data encoded in the choice of t^* is its position in the ordering of interface and bulk branch points. Using this data, the reference points have to be distributed on the diagrams according to the following three rules

1. The boundary of each face includes exactly one reference point.

2. Moving along the boundary of a face along its orientation, one encounters not only the ramification points but also the reference point in the correct order.
3. Reference points cannot occur on misaligned double lines.

As an example, Fig. 14 shows a t^* dressed version of the diagram shown in Fig. 11. The decoration shown here amounts to the ordering $t^* < 5^{RL} < 5^{RL} < 2^{RR} < 2^{LL}$ for which we read off that $P = 2$ since two of the black dots are placed on double lines. The reader is invited to draw the diagram that is associated with the order $5^{RL} < 5^{RL} < 2^{RR} < t^* < 2^{LL}$ and to verify that this returns $P = 1$.

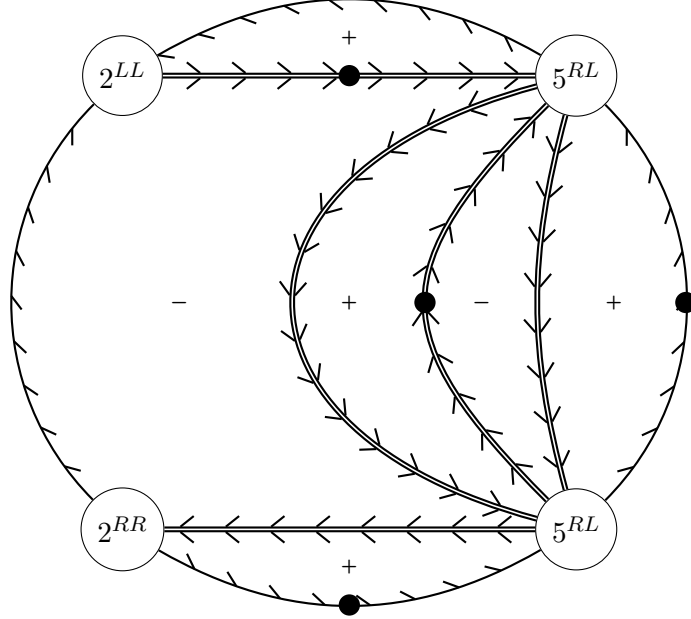


Figure 14: Dressed version of Fig. 11. Preimages $\Gamma^{-1}(t^*)$ of the reference point t^* under the covering map are depicted by black dots.

3.3 Symmetry group of interface PRR diagrams

In this short subsection, we discuss how to determine the symmetry group of an (interface) covering map from the corresponding diagram. To do so, we first define the automorphism group of (interface) PRR diagrams. From the definition, it will directly be clear that the automorphism group of a diagram is isomorphic to the group of deck transformations of the covering map. We end the section by applying this isomorphism in two examples.

Definition of the symmetry group. As already mentioned above, an interface PRR diagram is not a just graph but comes with some additional structure. To begin with it is a fat graph – the edges and faces that meet at any vertex come with a cyclic order. In addition, the vertices of the diagram are labelled by the associated branch points of the covering map. For covering maps that arise from single-cycle twist fields, this labelling is

injective, i.e. no two vertices possess the same label. However, in case of multi-cycle twist fields, vertices that carry the same label can arise.

Now that we understand the relevant structure of the interface PRR diagram, we can define its symmetry group: It is the group of all permutations of (vertices), edges and faces of the diagram that respect the labelling of vertices, the cyclic ordering at each vertex and of course the structure of the underlying graph. In terms of an explicit embedding representing a PRR diagram in Σ , the symmetries of the diagram are exactly the permutations of (vertices), edges and faces that descend from automorphisms of Σ which preserve the embedded labelled graph. Let us also note that the symmetry group of an interface PRR diagram is much smaller than the symmetry group of an associated graph which one obtains from the diagram by dropping the additional structure.

Identification with deck transformations. We now argue that the symmetry group of an interface PRR diagram is isomorphic to the group of deck transformations of the corresponding covering maps. Given a diagram, we pick a representative Γ of the equivalence class of covering maps that the diagram corresponds to. Clearly, each deck transformation gives a symmetry of the associated interface PRR diagram. Vice versa, if ϕ is an automorphism of Σ that descends to an symmetry of the diagram, then Γ and $\Gamma \circ \phi$ are two holomorphic maps that by construction coincide on the vertices and edges of the embedded interface PRR diagram. But since both Γ and $\Gamma \circ \phi$ are holomorphic (and the faces of diagrams are simply connected), this means that they also need to coincide on the faces, which implies that ϕ is a deck transformation of Γ .

Examples. The only diagram with a non trivial symmetry group discussed so far in this section is the one shown in Fig. 5. The symmetry group of this diagram is the \mathbb{Z}_w sub-group of the rotations of the sphere that fix the two ramification points and cyclically permute the edges of the graph. On higher genus covering spaces the symmetry groups can be more general transformations than rotations. For instance, the cylinder diagram contributing to the two-point function $\langle \sigma_2 \sigma_2 \rangle$ of bulk twist 2 operators shown in Fig. 15 has a \mathbb{Z}_2 symmetry group that is generated by a modular S -transformation of the cylinder which flips the two boundaries but leaves the ramification points fixed.

3.4 Gauge fixing of interface PRR diagrams

In equation (2.22), we identified the coefficient $\alpha[\Gamma]$ that weighs the contribution of the covering map Γ to a connected sphere correlator, see eq. (2.18), with the size of a particular orbit under an S_N action. This subsection provides an analogous interpretation for the interface coefficient $\alpha[\Gamma]$, see eqs. (2.42) and (2.43), as the size of an orbit of some $S_{N_-} \times S_{N_+}$ action. It is straight forward to obtain such an interpretation from a generalisation of the monodromy based arguments that led to eq. (2.22). However, now that we have developed the PRR diagrammatics of interface covering maps we can do better and provide a more transparent description in terms of graphs.

Gauge fixed PRR diagrams. Consider an interface covering map Γ with $\deg[\Gamma_{\pm}] = N_{\pm}$. As in the case of bulk covering maps, we refer to a bijective assignment of integers in

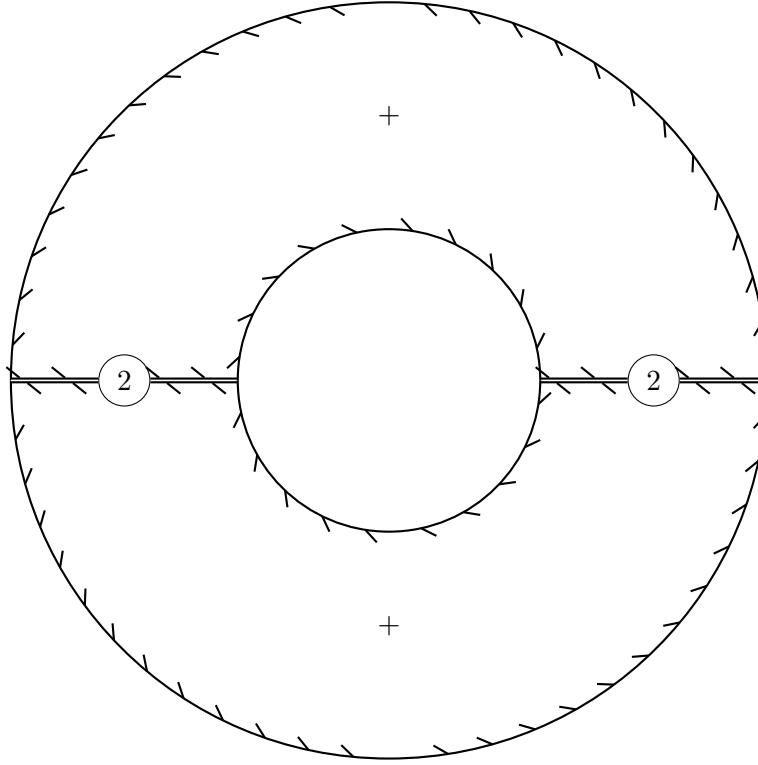


Figure 15: Cylinder contribution to $\langle \sigma_2 \sigma_2 \rangle$ at $N_+ = 2, N_- = 0$.

$\underline{N}_\pm := \{1, \dots, N_\pm\}$ to sheets of the covering as a gauge choice. In terms of interface PRR diagrams, such a gauge choice assigns integers to the \pm -faces. We call a PRR diagram whose faces are labelled in such a way *gauge fixed*.

Gauge fixed ramification indices. Gauge fixed PRR diagrams associate ramification points of Γ with cyclic permutations of $\underline{N}_- \sqcup \underline{N}_+$. These permutations are determined by circumnavigating the associated vertices of the diagram anti-clockwise and reading off the encountered \underline{N}_\pm labels of the traversed faces. We refer to these permutations as *gauge fixed ramification indices*. To give a more detailed description it is useful to introduce different variables j and a to denote elements of \underline{N}_- and \underline{N}_+ , respectively.

With this convention, every ramification point of Γ with ramification index w whose branch point is in the upper half plane, is associated with a permutation $\mathbf{g} = (a_1 j_1 a_2 a_3 \dots a_w)$ of length $|\mathbf{g}|$. The length is constrained by $w \leq |\mathbf{g}| \leq 2w$. There must be exactly w a -labels. In addition one may have up to w j -labels which, however, must always be separated by a -labels in the permutation. The labels of interior ramification points whose branch point is in the lower half plane are defined analogously with a and j labels interchanged. The labels corresponding to branch points on the interface are also defined in the same manner. In this case, however, the associated permutation necessarily alternates between a - and j -labels and has length $|\mathbf{g}| = 2w$.

Finally, every type ω^{AB} boundary ramification point is associated with a sequence

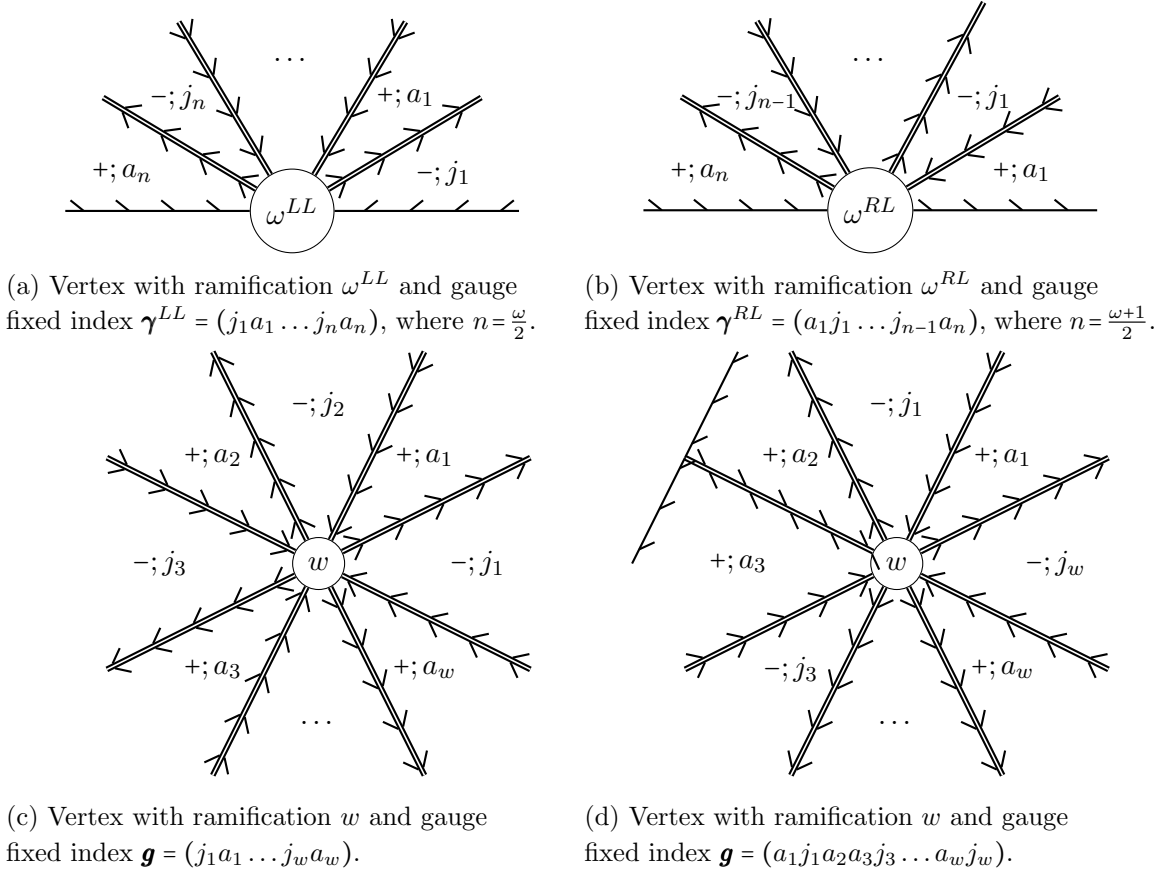


Figure 16: Examples of vertices and corresponding sequences.

γ^{AB} of length ω , whose entries alternate between a - and j -labels. We choose sequences instead of permutations to describe gauge fixed boundary ramification since the boundary case involves more data than just the cyclic ordering: Boundary ramification points also distinguish a particular first and last element of the associated sequence of \underline{N}_\pm labelled faces. At these end-point the sequence stops since the boundary of the covering space is reached.

Examples of various types of gauge fixed ramification indices are illustrated in Fig. 16.

Gauge fixed twist fields. Gauge fixed ramification indices allow us to define gauge-fixed twist fields labelled by such indices. These are non-local operators whose correlators are computed by a restriction of the sum over covering maps of local twist fields to gauge fixed PRR diagrams compatible with the gauge fixed ramification indices. Clearly, the constraint can be lifted by taking a linear combination of all possible ways to fix the gauge. Thus, local twist fields can be expressed as linear combinations of their gauge fixed counterpart. In fact, this is how we initially defined the interface changing operators in [5].

Gauge fixed interfaces. The gauge fixed PRR diagram also allows us to associate a permutation to the interface itself. For a covering map with degree of transmissivity P ,

the permutation ι that describes the gauge fixed glueing condition of the interface at the reference point t^* is a product $\iota = (j_1 a_1)(j_2 a_2) \dots (j_P a_P)$ of P commuting transpositions $(j_i a_i)$. Recall from our discussion at the end of Section 3.2 that the preimage $\Gamma^{-1}(t^*)$ can be represented by placing black dots on the edges of the PRR diagram according to some rules we spelled out before. For an interface covering with the degree of transmissivity P at t^* , there will be exactly P black dots on aligned double lines. Hence we can associate P pairs $(j_i a_i)$ to the choice of t^* . Note that the permutations that would describe the analogous data for any other choices of the reference point is fixed by the gauge fixed ramification indices along with the ι of one specific choice t^* of the reference point.

Symmetry factors from gauge fixed diagrams. Now we are actually ready to determine the weight factor $\alpha(\Gamma)$ we are after. Consider an arbitrary gauge fixed PRR diagram for Γ and read off the corresponding gauge fixed interior ramification indices $\mathbf{g}_1, \dots, \mathbf{g}_{n_c}$ and gauge fixed boundary ramification indices $\gamma_1^{A_1 B_1}, \dots, \gamma_{n_o}^{A_{n_o} B_{n_o}}$ as well as the permutation ι describing the glueing data at the reference point t^* . Given all this data, the weight is given by

$$\alpha[\Gamma] = \frac{\deg[\Gamma_-]! \deg[\Gamma_+]!}{|\text{Deck}[\Gamma]|} = |[\mathbf{g}_1, \dots, \mathbf{g}_{n_c}, \iota, \gamma_1^{A_1 B_1}, \dots, \gamma_{n_o}^{A_{n_o} B_{n_o}}]|. \quad (3.4)$$

The number on the r.h.s. is the size of the orbit

$$[\mathbf{g}_1, \dots, \iota, \gamma_1^{A_1 B_1}, \dots] := \{(g \mathbf{g}_1 g^{-1}, \dots, g \iota g^{-1}, g \gamma_1^{A_1 B_1}, \dots) | g \in S_{N_-} \times S_{N_+}\}. \quad (3.5)$$

that is obtained from the gauged fixed ramification indices and ι by simultaneous action with elements g in the product $S_{N_-} \times S_{N_+}$ of the permutation groups. On the interior ramification indices \mathbf{g} and on ι elements g act through the adjoint action. Recall that \mathbf{g}_i and ι are themselves elements of $S_{N_-} \times S_{N_+}$ so that the adjoint action is well defined. The action of g on the gauged fixed boundary ramification indices γ_i is through the defining action of $S_{N_-} \times S_{N_+}$ on the entries of the $\gamma_i^{A_i B_i}$ sequences.

Diagrammatically, this group action just corresponds to the relabelling of faces in the gauge fixed PRR diagram. The action of a deck transformation on the covering space amounts to a permutation of faces of the diagram. Therefore, a gauge choice for the diagram allows us to identify $\text{Deck}[\Gamma]$ with a subgroup of $S_{N_-} \times S_{N_+}$. Since deck transformations leave the structure of the covering map invariant, this subgroup of $S_{N_-} \times S_{N_+}$ is exactly the stabiliser of the orbit (3.5) under the permutation action. Hence, equation (3.4) directly follows from the orbit-stabiliser theorem.

3.5 The large N expansion

In this section, we discuss a particular limit in which the computation of our interface correlation functions simplifies and non-planar diagrams are suppressed. Concretely, we study connected correlators on the sphere $X = \mathbb{S}^2$ with an interface $\mathcal{I}_{|a}^{(P)}$ inserted along the equator and the parameters N_{\pm} and P scaling as

$$N_{\pm} \sim N, \quad P \sim N \quad \text{and} \quad N_{\pm} - P \sim N^{\frac{1}{2}} \quad (3.6)$$

with an expansion parameter N that we will take to be large. Our main finding is that contributions of genus g covering spaces with b boundaries to connected correlators of n_c bulk and n_o interface twist fields scale, to leading order in N , as

$$N^{1-g-\frac{b}{2}-\frac{n_c}{2}-\frac{n_o}{4}} \quad (3.7)$$

if the two point-functions of the operators are normalised to 1. Equation (3.7) is suggestive of an identification $N \sim g_s^{-2}$ of the parameter N with the string coupling of a potential holographic dual. As in the bulk case, the true relationship between the parameters of the symmetric orbifold and the string coupling is however slightly more subtle. In Section 5.3, we will show that the resemblance of eq. (3.7) to a string genus expansion can be traced back to the fact that eq. (3.6) with $N \sim g_s^{-2}$ describes the expectation values of N_\pm and P in the truly holographic grand-canonical ensemble of interfaces to leading order in small g_s .

Connected sphere correlators. Towards the end of Section 2.2, we defined connected sphere correlators for bulk twist fields in symmetric product orbifolds. Connected correlation functions in the presence of the interface $\mathcal{I}_{|a}^{(P)}$ are defined analogously, i.e.

$$\langle \mathcal{I}_{|a}^{(P)} \mathcal{O} \rangle_{\text{Sym}^{N_-|N_+}(\mathcal{M})}^{\text{conn, unnormalised}} := \frac{1}{N_-!N_+!} \sum_{\substack{n_\pm=0 \\ n_-+n_+ \neq 0}}^{N_\pm} \sum_{p=0}^{\min(n_\pm, P)} \sum_{\Gamma \in C_{n_\pm, p}^{\text{conn}}[\mathcal{I}_{|a}^{(P)} \mathcal{O}]} \langle \mathcal{O}^\Gamma \rangle_{\mathcal{M}}, \quad (3.8)$$

where the third sum runs over the subset of connected interface coverings maps Γ . By definition, these are interface covering maps

$$\Gamma : \overline{\mathbb{C}}^{\sqcup(P-p)} \sqcup \mathbb{D}_-^{\sqcup(N_- - P - b_-)} \sqcup \mathbb{D}_+^{\sqcup(N_+ - P - b_+)} \sqcup \Sigma \rightarrow \overline{\mathbb{C}}, \quad (3.9)$$

with $b_\pm = n_\pm - p$ that satisfy three conditions: First of all, they restrict to the identity map on the $P - p$ spheres $\overline{\mathbb{C}}$. Furthermore they are also required to restrict to the identity embedding of the upper and lower hemispheres on the $N_\pm - P - b_\pm$ disconnected discs \mathbb{D}_\pm . Finally, we impose that Σ should be connected. The parameters n_\pm and p correspond to the degrees and transmissivity of the restriction $\Gamma|_\Sigma$. For $\Gamma \in C_{n_\pm, p}^{\text{conn}}[\mathcal{I}_{|a}^{(P)} \mathcal{O}]$, we have

$$|\text{Deck}[\Gamma]| = (N_- - P - b_-)!(N_+ - P - b_+)!(P - p)! |\text{Deck}[\Gamma|_\Sigma]| \quad (3.10)$$

which we can use to partially evaluate the correlator $\langle \mathcal{O}^\Gamma \rangle_{\mathcal{M}}$ on the r.h.s. of eq. (3.8) as

$$\langle \mathcal{O}^\Gamma \rangle_{\mathcal{M}} = \frac{N_-!N_+! g^{N_-+N_+-2P-(b_-+b_+)}}{(N_- - P - b_-)!(N_+ - P - b_+)!(P - p)!} \frac{\langle \mathcal{O}^{\Gamma|_\Sigma} \rangle_{\mathcal{M}}}{n_-!n_+!}. \quad (3.11)$$

The factors in front of the remaining expectation value $\langle \mathcal{O}^{\Gamma|_\Sigma} \rangle_{\mathcal{M}}$ account for the contribution of the trivial connected components of the covering space. When inserted into eq. (3.8), the formula (3.11) leads to

$$\langle \mathcal{I}_{|a}^{(P)} \mathcal{O} \rangle_{\text{Sym}^{N_-|N_+}(\mathcal{M})}^{\text{conn}} = \sum_{\substack{n_\pm=0 \\ n_-+n_+ \neq 0}}^{N_\pm} \sum_{p=0}^{\min(n_\pm, P)} \sum_{\Gamma \in C_{n_\pm, p}^{\text{conn}}[\mathcal{I}_{|a}^{(P)} \mathcal{O}]} C_\Gamma(N_\pm, P) \frac{g^{-(b_-+b_+)}}{n_-!n_+!} \langle \mathcal{O}^{\Gamma|_\Sigma} \rangle_{\mathcal{M}} \quad (3.12)$$

for normalised connected correlators, where

$$C_\Gamma(N_\pm, P) := \frac{(N_- - P)!(N_+ - P)!P!}{(N_- - P - b_-)!(N_+ - P - b_+)!(P - p)!} \quad (3.13)$$

Normalisation of twist fields. Eq. (3.12) makes the N_{\pm} and P dependence and hence, with the scaling (3.6), the N dependence of correlators fully manifest, since $\langle \mathcal{O}^{\Gamma|\Sigma} \rangle_{\mathcal{M}}$ is independent of the parameter N . To have a well behaved large N expansion, we would like to replace bulk and interface twist fields by normalised versions

$$\hat{\sigma}_{\omega}^{AB} = \mathcal{N}_{\omega}^{AB} \sigma_{\omega}^{AB} \quad \text{and} \quad \hat{\sigma}_w(x) = \mathcal{N}_w^s \sigma_w(x) \quad (3.14)$$

whose two-point functions are of order 1 in the large N limit. The superscript s we placed on the normalization constants \mathcal{N}_w^s is the sign of the imaginary part of the insertion point x . It can take one of the three values $-$, 0 and $+$, depending on whether x is in the lower half-plane, on the real line or in the upper half-plane. The correlators defining the normalizations $\mathcal{N}_{\omega}^{AB}$ of the interface operators are

$$\langle \sigma_{\omega}^{RR}(0) \sigma_{\omega}^{LL}(1) \rangle, \quad \langle \sigma_{\omega}^{LR}(0) \sigma_{\omega}^{LR}(1) \rangle \quad \text{and} \quad \langle \sigma_{\omega}^{RL}(0) \sigma_{\omega}^{RL}(1) \rangle, \quad (3.15)$$

each of which is computed by a single covering map. Let us refer to the three covering maps as $\Gamma_{\omega}^{RR} = \Gamma_{\omega}^{LL}$, Γ_{ω}^{LR} and Γ_{ω}^{RL} . With this notation, we have

$$\mathcal{N}_{\omega}^{AB} := C_{\Gamma^{AB}}(N_{\pm}, P)^{-\frac{1}{2}} \quad (3.16)$$

with C as defined in eq. (3.13). For $A \neq B$, the index ω is odd and our formula for C_{Γ} evaluates to

$$\mathcal{N}_{\omega}^{LR} = \sqrt{\frac{(P - \frac{\omega-1}{2})!}{(N_- - P)P!}} \quad \text{and} \quad \mathcal{N}_{\omega}^{RL} = \sqrt{\frac{(P - \frac{\omega-1}{2})!}{(N_+ - P)P!}}, \quad (3.17)$$

independently of the choice of reference point defining P and p . In the first case with $AB = LR$, for example, the degrees n_{\pm} of Γ^{AB} are given by $n_- = \omega/2 + 1/2$ and $n_+ = \omega/2 - 1/2$ while the transmissivity is $p = \omega/2 - 1/2$. Hence, the parameters b_{\pm} take the values $b_- = 1$ and $b_+ = 0$. Insertion into eq. (3.13) gives the first formula in eq. (3.17). The second formula is obtained in the same way with the role of \pm exchanged. If $A = B$, on the other hand, the label ω must be even and the resulting normalizations

$$\mathcal{N}_{\omega}^{AA} = \begin{cases} \sqrt{\frac{(P - \frac{\omega-2}{2})!}{(N_- - P)(N_+ - P)P!}} & \text{if } t^* \in]0, 1[\\ \sqrt{\frac{(P - \frac{\omega}{2})!}{P!}} & \text{else} \end{cases} \quad (3.18)$$

explicitly depend on the choice of the reference point t^* . The derivation is similar to the previous one but now the degrees n_{\pm} coincide, i.e. $n_- = n_+ = \omega/2$. The two possible decorations of the corresponding interface PRR diagrams with black dots lead to a degree of transmissivity $p = n_{\pm} + 1$ and $p = n_{\pm}$, respectively. This gives the two possible values of the normalization constant.

For bulk fields $\hat{\sigma}_w$ the normalization is determined along the same lines. The resulting normalization constants are given by

$$\mathcal{N}_w^{\pm} = \sqrt{\frac{w(N_{\pm} - w)!}{N_{\pm}!}} \quad \text{and} \quad \mathcal{N}_w^0 = \sqrt{\frac{w(P - w)!}{P!}}. \quad (3.19)$$

Large N expansion. If we let N_{\pm} and P scale with a large parameter N as in eq. (3.6), then, to leading order in N ,

$$\mathcal{N}_{\omega}^{AB} = N^{-\frac{\omega}{4}}, \quad \mathcal{N}_w^s = N^{-\frac{w}{2}} \quad \text{and} \quad C_{\Gamma}(N_{\pm}, P) \sim N^{\frac{n_- + n_+}{2}}, \quad (3.20)$$

independently of the choice of the reference point, as one can directly read off from eqs. (3.13), (3.17), (3.18) and (3.19). Thus, we find that the contribution of elements $\Gamma \in C_{n_{\pm}, p}^{\text{conn}}$ to the correlator

$$\langle \mathcal{I}_{|a}^{(P)} \prod_{i=1}^{n_o} \hat{\sigma}_{\omega_i}^{A_i B_i} \prod_{i=1}^{n_c} \hat{\sigma}_{w_i} \rangle_{\text{Sym}^{N-|N_+}(\mathcal{M})}^{\text{conn}} \quad (3.21)$$

scales, to leading order in N , as

$$N^{-\sum_{i=1}^{n_o} \frac{\omega_i}{4} - \sum_{i=1}^{n_c} \frac{w_i}{2} + \frac{n_- + n_+}{2}} = N^{1-g-\frac{b}{2}-\frac{n_c}{2}-\frac{n_o}{4}}, \quad (3.22)$$

where g and b are the genus and number of boundaries of the non-trivial connected component Σ of the covering space associated with Γ . The equality between the l.h.s. and r.h.s. of eq. (3.22) follows directly from the interface Riemann-Hurwitz formula (2.28). As advertised in the beginning of this section, higher genus and multi-boundary covering spaces are hence systematically suppressed in the large N limit.

4 Generalised Lunin-Mathur construction

In this short section, we present an interface version of the Lunin-Mathur construction to compute correlation functions of the seed theory on the covering surface Σ or rather partition functions which are relevant for pure twist field insertions in the symmetric product orbifold. Its first half, i.e. Subsection 4.1, is devoted to a review of the bulk method. In the second half, i.e. Subsection 4.2, we introduce the interface generalisation and then illustrate its usage in several examples. Appendix D contains detailed computations supporting the main text. Throughout this section, whenever we write c without any further specifications, we mean the central charge $c_{\mathcal{M}}$ of the seed theory.

4.1 Review of the bulk method

As reviewed in Section 2, correlation functions in symmetric orbifolds are defined in terms of the data of associated covering maps. More specifically, correlators of (single cycle) twist fields on a Riemann surface X can, through the definitions (2.17) and (2.18), be expressed as a sum

$$\langle \sigma_{w_1}(x_1) \dots \sigma_{w_n}(x_n) \rangle_{\text{Sym}^N(\mathcal{M})}^{\text{unnormalised}} = \sum_{\Gamma} Z[\Gamma] \quad \text{with} \quad Z[\Gamma] := \frac{Z_1^{\Sigma}}{\text{Deck}[\Gamma]} \quad (4.1)$$

where Z_1^{Σ} denotes the partition function Z_1^{Σ} of the seed theory on the covering space Σ . As before, the sum runs over coverings $\Gamma : \Sigma \rightarrow X$ of X whose branch points are exactly x_1, \dots, x_n with indices w_1, \dots, w_n . In this subsection, we review the Lunin-Mathur method [8] for the evaluation of Z_1^{Σ} .

General setup. We assume that for each conformal equivalence class of Riemannian structures ds_Σ^2 on the covering surface Σ , there is a representative ds_Σ^2 for which the value of the vacuum partition function of the seed theory is known. The problem whose solution we describe in the paragraphs below is how to express Z_1^Σ in terms of $Z_1^{\hat{\Sigma}}$. Two steps need to be performed to achieve this goal. First, we need to compute the conformal factor ϕ in

$$ds_\Sigma^2 = e^\phi ds_\Sigma^2, \quad (4.2)$$

relating the metric $ds_\Sigma^2 = \Gamma^* ds_X^2$ to the reference metric ds_Σ^2 . Once ϕ has been computed, we need to calculate the value of the Liouville action on ϕ in a second step,

$$S_L[\phi] = \frac{c}{96\pi} \int_\Sigma d^2t \sqrt{g_\Sigma} \left(\partial_\mu \phi \partial_\nu \phi g_\Sigma^{\mu\nu} + 2R^{\hat{\Sigma}} \phi \right). \quad (4.3)$$

The partition function Z_1^Σ that appears on the right hand side of eq. (4.1) is then given by

$$Z_1^\Sigma = e^{S_L[\phi]} Z_1^{\hat{\Sigma}}. \quad (4.4)$$

It is thus reduced to the reference partition function $Z_1^{\hat{\Sigma}}$ which we assumed to be known.

The sphere. For concreteness, we focus on the case where both X and Σ are spheres. Following [8], we introduce a family of metrics ds_δ^2 on the Riemann sphere $\bar{\mathbb{C}}$ which are parametrised by some $\delta > 0$. On \mathbb{C} , these metrics are given by

$$ds_\delta^2 = \begin{cases} dz d\bar{z} & \text{if } |\delta z| < 1 \\ \frac{dz d\bar{z}}{|z\delta|^4} & \text{else} \end{cases}. \quad (4.5)$$

They extend continuously to the Riemann sphere. Given a seed conformal field theory with central charge c , its partition function on $\bar{\mathbb{C}}$ equipped with ds_δ^2 is

$$Z_1^{\bar{\mathbb{C}}_\delta} = Q \delta^{-\frac{c}{3}}, \quad (4.6)$$

where Q is an arbitrary normalisation constant [8]. We take ds_δ^2 as the reference metric on $\hat{\Sigma} = \bar{\mathbb{C}}_\delta$. When dealing with the sphere X that is covered by Σ we shall use the same metric, but denote the parameter by η instead of δ , i.e.

$$X = \bar{\mathbb{C}}_\eta \quad \text{for some small } \eta > 0. \quad (4.7)$$

We fix the normalization constant to $Q = \eta^{\frac{c}{3}}$ such that the sphere partition function of the seed theory is trivial, $Z_1^X = 1$. Without loss of generality, we assume that all twist fields of the correlator that we would like to compute are inserted in the region $|\eta z| < 1$. Since we are only interested in covering maps up to the action of automorphisms of Σ , we can fix

$$\Gamma(\infty) = \infty. \quad (4.8)$$

As explained above, we compute Z_1^Σ by relating it to the partition function $Z_1^{\hat{\Sigma}}$ with $\hat{\Sigma} = \bar{\mathbb{C}}_\delta$ for an appropriately chosen δ .

Regulating the Liouville action. Consider the subset $B_{\delta^{-1}} \subseteq \mathbb{C}$ that consists of all points $z \in X$ with $|z\delta| < 1$. We denote the preimage of this ball with respect to Γ by $\Sigma_0 := \Gamma^{-1}(B_{\delta^{-1}})$. On the subset $\Sigma_0 \subseteq \Sigma$, the metric is given by

$$ds_{\Sigma}^2|_{\Sigma_0} = \Gamma^* ds_X^2|_{|z\delta|<1} = d\Gamma(t)d\bar{\Gamma}(t) = \left|\frac{d\Gamma}{dt}\right|^2 dt d\bar{t} \quad (4.9)$$

and therefore

$$\phi = \log\left(\frac{d\Gamma}{dt}\right) + \text{h.c.}, \quad (4.10)$$

which diverges if the derivative Γ' vanishes and the metric of Σ degenerates. Thus, at the ramification points $R[\Gamma]$ of Γ , it is necessary to regulate the Liouville action. We explain the details of this regularisation in App. D.1 following [8]. It involves cutting out small neighbourhoods of each ramification point from Σ . The result of the detailed computation performed in that appendix is

$$Z_1^{\Sigma} = \eta^{-\frac{c}{3}(\text{Deg}[\Gamma]-1)} \prod_{r \in R[\Gamma]} w^{-\frac{c}{12}(w-1)} |a_r|^{-\frac{c}{12}(1-\frac{1}{w})} \prod_{p \in P[\Gamma]} |b_p|^{-\frac{c}{6}}, \quad (4.11)$$

where η parametrises the metric of X (see eq. (4.7)), $R[\Gamma]$ is the set of ramification points of Γ , $P[\Gamma]$ is the set of poles of Γ in $\Sigma \setminus \{\infty\}$ and the complex numbers a_r and b_p are defined via the local behaviour

$$\Gamma(r+t) = \Gamma(r) + a_r t^w + O(t^{w+1}) \quad \text{and} \quad \Gamma(p+t) = \frac{b_p}{t} + O(1) \quad (4.12)$$

of the covering map Γ near the ramification points and poles. While formula (4.11) was derived in a few examples in the original work [8] an explicit, fully detailed derivation was only recently published in [12]. While the latter uses somewhat different methods, the derivation we spell out in Appendix D.1 follows exactly the route of [8]. It will also turn out to directly extend to the interface case. Before we go there, let us illustrate the Lunin-Mathur construction through an example.

Example: Two-point functions. As an application of eq. (4.11), let us compute the two-point functions of two bulk fields σ_w with identical index $w_1 = w = w_2$ in the symmetric product orbifold. Without loss of generality, we can insert the first field at $z_1 = 0$ and then denote the insertion point of the second twist field by $z_2 = z$. In this setup, only a single class of coverings contributes. We choose the representative

$$\Gamma(t) = z \frac{t^w}{t^w - (t-1)^w}. \quad (4.13)$$

This covering map has two ramification points $R[\Gamma] = \{0, 1\}$, around which it expands as

$$\Gamma(t) = 0 + z(-1)^{w+1}t^w + O(t^{w+1}) \quad \text{and} \quad \Gamma(1+t) = z + zt^w + O(t^{w+1}). \quad (4.14)$$

Moreover, Γ has $w-1$ finite poles which are located at the zeroes of the denominator,

$$t_k := \left(1 - e^{2\pi i \frac{k}{w}}\right)^{-1} \quad (4.15)$$

where k runs from $k = 1$ to $k = w - 1$, i.e. $P[\Gamma] = \{t_1, \dots, t_{w-1}\}$. The residues at these poles are easy to determine,

$$b_k = \frac{z}{4w \sin^2\left(\frac{k\pi}{w}\right)}. \quad (4.16)$$

Now we have assembled all the data we need in order to evaluate the formula (4.11). The result is given by

$$Z_1^\Sigma = |z|^{-2\Delta^{(w)}} w^{\frac{c}{3}} \eta^{-\frac{c}{3}(w-1)} \quad (4.17)$$

with

$$\Delta^{(w)} = \frac{c}{12} \left(w - \frac{1}{w} \right). \quad (4.18)$$

The last ingredient we need in order to evaluate the unnormalised correlator (4.1) is the number of Deck transformations, which is given by

$$|\text{Deck}[\Gamma]| = w(N - w)! . \quad (4.19)$$

Hence, the the unnormalised two-point function is given by

$$\langle \sigma_w(0) \sigma_w(z) \rangle_{\text{Sym}^N(\mathcal{M})}^{\text{unnormalised}} = \frac{w^{\frac{c}{3}} \eta^{-\frac{c}{3}(w-1)}}{w(N - w)!} |z|^{-2\Delta^{(w)}}. \quad (4.20)$$

We use the term “unnormalised” in the sense of definition (2.9). In particular, the normalised two-point function is

$$\langle \sigma_w(0) \sigma_w(z) \rangle_{\text{Sym}^N(\mathcal{M})} = N! \langle \sigma_w(0) \sigma_w(z) \rangle_{\text{Sym}^N(\mathcal{M})}^{\text{unnormalised}} \quad (4.21)$$

and not just $|z|^{-2\Delta^{(w)}}$.

4.2 The interface generalisation

Let us now turn to the interface generalisation of the Lunin-Mathur construction. The interface generalisation introduces two modifications to the evaluation of correlators which we detail in the next two paragraphs. The first modification arises from the fact that we now need to evaluate the Liouville action on surfaces with boundaries which requires in particular to add an additional boundary term, see eq. (4.22). The second modification is that bulk covering maps are replaced by interface covering maps. This can be dealt with by applying the method of images. After generally discussing disk correlators in the third paragraph of the section, we conclude by computing several example correlation functions.

Boundary Liouville action. As in Section 4.1, we assume that there is a reference geometry $\hat{\Sigma}$ such that the partition function $Z_1^{\hat{\Sigma}}$ on $\hat{\Sigma}$ is known. As before, the partition function Z_1^Σ on Σ with the induced metric (4.2) is then given by eq. (4.4). The difference to the bulk case is that the Liouville action now also has a boundary contribution. Concretely,

$$S_L[\phi] = \frac{c}{96\pi} \int_{\Sigma} d^2t \sqrt{g_{\hat{\Sigma}}} \left(\partial_\mu \phi \partial_\nu \phi g_{\hat{\Sigma}}^{\mu\nu} + 2R^{\hat{\Sigma}} \phi \right) + \frac{c}{24\pi} \int_{\partial\Sigma} \sqrt{\gamma_{\hat{\Sigma}}} K^{\hat{\Sigma}} \phi, \quad (4.22)$$

where γ is the induced metric on the boundary $\partial\Sigma$ of the covering surface and $K^{\hat{\Sigma}}$ is the extrinsic curvature of the boundary.

The method of images. In the case where X is a disk, we can use the method of images in order to reduce the discussion of interface covering maps $\Gamma : \Sigma \rightarrow X$ to that of coverings Γ' of the sphere by the Schottky¹⁰ double $\Sigma \# \bar{\Sigma}$. The restriction of the doubled map to Σ coincides with Γ . On $\bar{\Sigma}$, the covering Γ' is given by $\Gamma'(\bar{z}) := \overline{\Gamma(z)}$. The doubled map Γ' has two copies of each interior ramification point of Γ . Additionally, each boundary ramification point with index ω leads to a single ramification point with index $w = \omega$ for Γ' . Below, we use the method of images for two purposes. First, it allows us to construct interface covering maps as restrictions of bulk covering maps. Second, it allows us to evaluate the bulk part of the Liouville action (4.22) by applying eq. (4.11) to Γ' .

The hemisphere. In the case of coverings of the upper hemisphere in $\bar{\mathbb{C}}_\eta$ by another hemisphere, where we take the reference metric to again be of the type ds_δ^2 , the extrinsic curvature vanishes along the entire boundary of the covering space. Thus, only the bulk part contributes to the Liouville action. In Appendix D.2, we evaluate this bulk part using the method of images. This leads to the interface generalisation

$$Z_1^\Sigma = \eta^{-\frac{c}{6}(N_- + N_+ - 1)} \left(\prod_{r \in R_B[\Gamma]} w^{w-1} a_r^{1-\frac{1}{w}} \prod_{p \in P_B[\Gamma]} b_p^2 \right)^{-\frac{c}{12}} \left(\prod_{r \in R_I[\Gamma]} \omega^{w-1} a_r^{1-\frac{1}{w}} \prod_{p \in P_I[\Gamma]} b_p^2 \right)^{-\frac{c}{24}} \quad (4.23)$$

of eq. (4.11) for interface coverings of the upper half plane by itself. Here, N_+ and N_- are the degrees of the covering map Γ on the upper and lower half plane. The sets $R_B[\Gamma]$ and $R_I[\Gamma]$ contain the bulk and interface ramification points of Γ . Likewise, the sets $P_B[\Gamma]$ and $P_I[\Gamma]$ contain all complex and real poles, except for ∞ (which we however continue to w.l.o.g. assume to be a pole). The coefficients a_r and b_p for interface ramification points and poles are defined as we defined the analogous bulk coefficients in eq. (4.12).

Example: Bulk one-point functions. Let us consider the one-point function

$$\langle \mathcal{I}_{|a_\pm}^{(P)} \sigma_w(z) \rangle_{\text{Sym}^{N_-|N_+}(\mathcal{M})}^{\text{unnormalised}} \quad (4.24)$$

of a bulk twist field $\sigma_w(z)$ inserted on the upper half plane, with the interface $\mathcal{I}_{|a_\pm}^{(P)}$ inserted along the real line. The correlation function can be non-trivial only if $N_+ - P \geq w$. In that case, it evaluates to

$$\langle \mathcal{I}_{|a_\pm}^{(P)} \sigma_w(z) \rangle_{\text{Sym}^{N_-|N_+}(\mathcal{M})}^{\text{unnormalised}} = \frac{g_-^{N_- - P} g_+^{N_+ - P - w} Z_{|a_+}^{(w)}}{P!(N_- - P)!(N_+ - P - w)!w}, \quad (4.25)$$

where g_\pm are the g -functions of $|a_\pm\rangle$ and $Z_{|a_\pm}^{(w)}$ captures the contribution of a w -fold cover of the upper half plane by itself with a ramification point at z . To compute $Z_{|a_\pm}^{(w)}$, we choose the explicit covering map

$$\Gamma(t) := z \frac{(it-1)^w}{(it-1)^w - (it+1)^w} + \bar{z} \frac{(-it-1)^w}{(-it-1)^w - (-it+1)^w}. \quad (4.26)$$

¹⁰The Schottky double is a closed Riemann surface obtained by taking two copies Σ and $\bar{\Sigma}$ of the Riemann surface Σ and glueing them along the boundary.

The way Γ is written above makes manifest two important properties, namely

$$\Gamma(\bar{t}) = \overline{\Gamma(t)} \quad \text{and} \quad \Gamma(i) = z. \quad (4.27)$$

A more economical way of writing Γ is

$$\Gamma(t) = \frac{z(it-1)^w - \bar{z}(it+1)^w}{(it-1)^w - (it+1)^w}. \quad (4.28)$$

The coefficient associated with the ramification point i is

$$a_i = \frac{z - \bar{z}}{(2i)^w}. \quad (4.29)$$

The poles and residues are

$$P[\Gamma] = \{\cot(\frac{k\pi}{w})\}_{k=1}^{w-1} \quad \text{and} \quad b_k = \frac{i(z - \bar{z})}{2w \sin^2(\frac{k\pi}{w})}. \quad (4.30)$$

Plugging this into eq. (4.23) gives

$$Z_{|a_+}^{(w)} = g_+ \eta^{-\frac{c}{6}(w-1)} |z - \bar{z}|^{-\Delta^{(w)}} w^{\frac{c}{6}} \quad (4.31)$$

and therefore,

$$\langle \mathcal{I}_{|a_+}^{(P)} \sigma_w(z) \rangle_{\text{Sym}^{N_-|N_+}(\mathcal{M})}^{\text{unnormalised}} = \frac{g_-^{N_- - P} g_+^{N_+ - P - (w-1)} \eta^{-\frac{c}{6}(w-1)} w^{\frac{c}{6}}}{P!(N_- - P)!(N_+ - P - w)!w} |z - \bar{z}|^{-\Delta^{(w)}}. \quad (4.32)$$

Example: Interface two-point functions. The evaluation of the two-point functions

$$\langle \mathcal{I}_{|a}^{(P)} \sigma_\omega^{RR}(0) \sigma_\omega^{LL}(x) \rangle_{\text{Sym}^{N_-|N_+}(\mathcal{M})}^{\text{unnormalised}} \quad \text{and} \quad \langle \mathcal{I}_{|a}^{(P)} \sigma_\omega^{RL}(0) \sigma_\omega^{RL}(x) \rangle_{\text{Sym}^{N_-|N_+}(\mathcal{M})}^{\text{unnormalised}} \quad (4.33)$$

directly reduces to that of the bulk two-point function (4.20) for even and odd $w = \omega$ respectively via the method of images. We thus deduce that the two correlators above are given by¹¹

$$\langle \mathcal{I}_{|a}^{(P)} \sigma_\omega^{RR}(0) \sigma_\omega^{LL}(x) \rangle_{\text{Sym}^{N_-|N_+}(\mathcal{M})}^{\text{unnormalised}} = \frac{g^{N_- + N_+ - 2P + 1} \omega^{\frac{c}{6}} \eta^{-\frac{c}{6}(\omega-1)}}{(N_- - P)!(N_+ - P)!(P - \frac{\omega}{2})!} |x|^{-2\Delta_\omega^{AB}}, \quad (4.34)$$

where the reference point for the interface is -1 and, with the same reference point,

$$\langle \mathcal{I}_{|a}^{(P)} \sigma_\omega^{RL}(0) \sigma_\omega^{RL}(x) \rangle_{\text{Sym}^{N_-|N_+}(\mathcal{M})}^{\text{unnormalised}} = \frac{g^{N_- + N_+ - 2P} \omega^{\frac{c}{6}} \eta^{-\frac{c}{6}(\omega-1)}}{(N_- - P)!(N_+ - P - 1)!(P - \frac{\omega-1}{2})!} |x|^{-2\Delta_\omega^{AB}}. \quad (4.35)$$

These results follow from applying (4.23) to the covering map (4.13) with real $z = x$. Here,

$$\Delta_\omega^{AB} = \frac{c}{24} \left(\omega - \frac{1}{\omega} \right), \quad (4.36)$$

which agrees with the special case $\Delta = 0$ of eq. (2.62). For $\omega = 2$, the interface two-point function was essentially already computed in [13], see Section 5.3 of that reference.

¹¹ Assuming of course a sufficiently large number of sheets N_- and N_+ on the upper/lower hemisphere as well as a sufficient number of reflecting and transmitting boundary conditions to ensure that the correlator is non vanishing.

Example: Interface four-point functions. The disk contribution to general interface four-point functions

$$\langle \mathcal{I}_{|a\rangle}^{(P)} \sigma_{\omega_1}^{A_1, B_1}(x_1) \sigma_{\omega_2}^{A_2, B_2}(x_2) \sigma_{\omega_3}^{A_3, B_3}(x_3) \sigma_{\omega_4}^{A_4, B_4}(x_4) \rangle_{\text{Sym}^{N_-|N_+}(\mathcal{M})}^{\text{unnormalised}} \quad (4.37)$$

can be evaluated using section 2 of the notebook `CoveringMaps.nb` provided in the ancillary files of this publication. The corresponding covering maps, via the method of images, reduce to covering maps of the sphere in the absence of an interface, which satisfy the extra constraint $\Gamma(s) = \overline{\Gamma(\bar{s})}$. The latter can be computed by first using the approach described in Appendix D.3 to compute generic covering maps and then restricting to the subset that satisfies the additional reality constraint. By applying $SL(2; \mathbb{R})$ transformations of the upper hemisphere, we can w.l.o.g. ensure that $x_1 = 0$, $x_3 = 1$ and $x_4 = -1$ with corresponding ramification points $s_i = x_i$ for $i \neq 2$. The value of s_2 on the other hand is a non trivial function of the parameter x_2 . Sections 2.2 and 2.3 of the notebook automatically generate plots from the covering maps, which resemble the diagrams discussed in Section 3. Using eq. (4.23) it is straight forward to evaluate correlation functions by simply determining the poles as well as the local expansions around ramification points of the explicitly computed covering maps. For eq. (4.23) to be applicable, one has to, however, ensure that $\Gamma(\infty) = \infty$ i.e. pick an arbitrary pole and conformally map it to ∞ . This operation is performed in Section 2.4. of the notebook.

Example: Interface-Interface-Bulk three-point functions. To study interface-interface-bulk three-point functions, we fix the $SL(2, \mathbb{R})$ symmetry of the disk by mapping the two interface operators to 0 and 1 and the real part of the bulk operator to $\frac{1}{2}$. The remaining kinematical freedom consists then of a single positive real number χ , the imaginary part of the position of the bulk twist field. Hence, the correlators take the form

$$\langle \mathcal{I}_{|a\rangle}^{(P)} \sigma_{\omega_1}^{A_1, B_1}(0) \sigma_w(\frac{1}{2} + i\chi) \sigma_{\omega_2}^{A_2, B_2}(1) \rangle_{\text{Sym}^{N_-|N_+}(\mathcal{M})}^{\text{unnormalised}} \quad (4.38)$$

and are computable by determining the bulk covering maps of the sphere with ramification points 0 and 1 of index ω_1 and ω_2 that are mapped to 0 and 1, as well as ramification points at $\frac{1}{2} \pm is$ for some real number s , which map to $\frac{1}{2} \pm i\chi$ with ramification index w . The maps that contribute non-trivially to the correlator are again those that satisfy $\Gamma(z) = \overline{\Gamma(\bar{z})}$. They are computed and visualised in Section 3 of the `CoveringMaps.nb` notebook.

Example: Bulk two-point functions. The last type of correlators whose evaluation reduces to the computation of sphere coverings with four ramification points are bulk two-point functions. Again, the kinematical freedom reduces to a single real number, which we choose to be the imaginary part of the insertion points of the two bulk fields after using the $SL(2, \mathbb{R})$ symmetry to fix the real parts to -1 and 1 and sending the intersection of the line through the two insertion points with $\text{Im}(z) = 0$ to ∞ . The resulting correlator

$$\langle \mathcal{I}_{|a\rangle}^{(P)} \sigma_{w_1}(-1 + i\chi) \sigma_{w_2}(1 + i\chi) \rangle_{\text{Sym}^{N_-|N_+}(\mathcal{M})}^{\text{unnormalised}} \quad (4.39)$$

can be computed from covering maps with ramification points at $-1 \pm is$ and $1 \pm is$ for some $s > 0$, which are mapped to $-1 \pm i\chi$ and $1 \pm i\chi$ with ramification index w_1 and w_2 . Section 4 of the `CoveringMaps.nb` notebook computes and visualises the relevant $\Gamma(z) = \overline{\Gamma(\bar{z})}$ maps.

5 String theory and the interface grand-canonical ensemble

So far, we have described correlation functions at fixed N_{\pm} and P . The purpose of this section is to discuss a grand-canonical ensemble in which the parameters N_{\pm} and P are averaged with a fixed chemical potential. As reviewed in Subsection 5.1, studying such an ensemble is strongly motivated by holography. In fact, super string theory on $\text{AdS}_3 \times S^3 \times \mathbb{T}^4$ at minimal pure NS-NS flux $k = 1$ is known to be precisely dual to a grand-canonical ensemble of symmetric product orbifolds whose construction we review in Subsection 5.2. The key result of this section is a novel grand-canonical ensemble of interfaces introduced in Subsection 5.3. Using this new construction, we show that the grand-canonical ensemble of correlation functions studied in this paper structurally matches the genus expansion of string scattering amplitudes. We discuss the expectation values of N_{\pm} and P at the end of Subsection 5.3, and show the leading-order agreement to the canonical ensemble result shown in Sec. 3.5.

5.1 Holographic motivation

Pure NSNS $\text{AdS}_3 \times S^3 \times \mathbb{T}^4$ can be obtained from $\mathbb{R}^6 \times \mathbb{T}^4$ as the near horizon limit of Q_1 fundamental strings and Q_5 NS5 branes, with four directions of the latter wrapping \mathbb{T}^4 . String perturbation theory around this pure NSNS background is described in the hybrid formalism by a world sheet theory based on the $\text{PSU}(1,1|2)_k$ WZNW model. The level k of the model can be directly identified with the number Q_5 of the brane construction. However, the naive expectation that the string coupling g_s is fixed in terms of Q_1 is not realised. Instead of being determined by the expectation values of fields in the target space, the string coupling is a continuous parameter of the world sheet theory¹². This parameter can be interpreted as a chemical potential controlling the averaging over different values of Q_1 in a grand-canonical ensemble.

Since string perturbation theory therefore does not compute scattering amplitudes in a fixed Q_1 background, but in the grand-canonical ensemble, one should expect the space time CFT description of these amplitudes to analogously be given in terms of correlation functions in a grand-canonical ensemble. For minimal NSNS flux $k = 1$, this expectation has been confirmed in great detail. Concretely, it was established [3, 18, 20–22] that string theory on $\text{AdS}_3 \times S^3 \times \mathbb{T}^4$ at $k = 1$ is dual to a grand-canonical ensemble of free symmetric orbifold theories $\text{Sym}^{Q_1}(\mathbb{T}^4)$. Section 3 of Reference [23] provides a detailed description of this grand-canonical ensemble, which we partially review in the next subsection, as well as a broader discussion of the string theoretic context that we have sketched above.

Reference [5] provided evidence strongly suggesting that AdS_2 branes in the $k = 1$ background are similarly not dual to a single interface, but rather an ensemble of the interfaces $\mathcal{I}^{(P)}$. We conjecture this to be true not only in the sense that N_{\pm} need to be averaged over since the bulk theory is not a fixed N symmetric product orbifold, but also in the sense that P is averaged over all its possible values for each fixed N_{\pm} .

¹²For more details consult e.g. [14–17] on pure NSNS AdS_3 strings in the RNS formalism for $Q_5 \geq 2$ and [18, 19] on the special case $Q_5 = 1$ in the hybrid formalism.

To qualitatively motivate this expectation, consider that, in string theory, the AdS_2 branes are realised by the insertion of a probe string on which the fundamental strings which create the $\text{AdS}_3 \times S^3 \times \mathbb{T}^4$ background can end [24]. The fixed P interface $\mathcal{I}^{(P)}$ corresponds to a setup where P parallel fundamental strings go through the probe string and another $Q_1^- - P$ and $Q_1^+ - P$ end on it extending into either of the two directions parallel to the other fundamental strings and orthogonal to the probe. As recalled above, the issue that the $\text{PSU}(1,1|2)_1$ world sheet theory at a first glance cannot account for the parameter Q_1 , or for that matter Q_1^\pm , is resolved by understanding that it describes a grand-canonical ensemble. Since the AdS_2 boundary states of the world sheet theory do not have a parameter describing the value of P , it is natural to also expect this parameter to be controlled by a chemical potential, which is set by to the only available world sheet parameter – the string coupling. While the result for the torus partition function obtained in Reference [5] is consistent with this expectation, it is not possible to directly infer the precise relation between the chemical potential controlling P and the string coupling from it. The purpose of this section is to go beyond these prior results by fixing the interface chemical potentials in terms of the string coupling, and showing that the ensemble defined in this way produces correlators that structurally reproduce the string genus expansion.

5.2 The bulk grand-canonical ensemble

Among the first attempts to connect symmetric product orbifolds to potentially dual string theories it was common to consider correlators of twist fields $\tilde{\sigma}_w$ with the normalisation

$$\tilde{\sigma}_w = \sqrt{\frac{(N-w)!w}{N!}} \sigma_w \quad (5.1)$$

at fixed N . Here, σ_w is the twist field with the canonical normalisation used in Sec. 2.2. At leading order in $N \gg 1$, the connected part of these correlation functions indeed shares some features of scattering amplitudes in string perturbation theory. As observed in [1, 8], for instance, the contribution of genus g covering spaces to a connected correlation function of bulk twist fields scales as

$$\left\langle \prod_{i=1}^{n_c} \tilde{\sigma}_{w_i} \right\rangle_{\text{conn}}^{N,g} \sim N^{1-g-\frac{n_c}{2}} \quad (5.2)$$

with N . Upon the identification $g_s^2 \sim N^{-1}$, this matches the scaling of genus g contributions to string scattering amplitudes with g_s . However, this proposal breaks down as soon as subleading N corrections or disconnected contributions are considered.

These issues can be fixed by working in the grand-canonical ensemble, as argued in Sec. 3.3 of [23]. To arrive at this conclusion, consider the partition function

$$Z_N^X[J] := \left\langle \exp \left(\sum_{w=1}^{\infty} \int d^2z g_s^w J_w(z) \sigma_w(z) \right) \right\rangle_{\text{Sym}^N(\mathcal{M})}^{\text{unnormalised}} \quad (5.3)$$

of $\text{Sym}^N(\mathcal{M})$ with sources J_1, \dots, J_w on a Riemann surface X of genus G defined using the unnormalised symmetric orbifold correlators of eq. (2.9). Here, g_s is the parameter that

turns out to control the genus expansion of symmetric orbifold correlators. It does not only multiply the sources in the definition (5.3) but, more importantly, also parametrises the chemical potential μ which controls N in the grand-canonical ensemble. More concretely, the grand-canonical partition function on X is defined as

$$Z_{g_s}^X[J] := \sum_{N=0}^{\infty} \mu^N Z_N^X[J] \quad \text{where} \quad \mu := g_s^{2G-2}. \quad (5.4)$$

The key feature of this ensemble is that grand-canonical correlation functions

$$\left\langle \prod_{i=1}^{n_c} \sigma_{w_i}(z_i) \right\rangle_{g_s}^X := \left[\prod_{i=1}^{n_c} \frac{\delta}{\delta J_{w_i}(z_i)} \right] \frac{Z_{g_s}^X[J]}{Z_{g_s}^X[0]} \Big|_{J=0} \quad (5.5)$$

have a genus expansion that, to all orders in g_s and for both connected and disconnected contributions, structurally matches the genus expansion of string perturbation theory with string coupling g_s . This can be shown in three simple steps.

First, we expand the exponential in eq. (5.3) and express the resulting correlation functions in terms of covering maps, which leads to

$$Z_N^X[J] = \sum_{n=0}^{\infty} \frac{1}{n!} \left(\sum_{w=1}^{\infty} \int d^2 z J_w(z) \right)^n \sum_{\Gamma} Z_{g_s}[\Gamma]. \quad (5.6)$$

The sum runs over all coverings Γ of X with the appropriate¹³ ramification points and

$$Z_{g_s}[\Gamma] := \frac{g_s^{w[\Gamma]}}{\text{Deck}[\Gamma]} \langle \mathbb{1} \rangle_{\mathcal{M}}, \quad (5.7)$$

where $w[\Gamma]$ is the total ramification index of Γ i.e. the sum of the indices of all ramification points. Each covering space that is involved has

$$c_{\Gamma} = \sum_{i=1}^k n_i \quad (5.8)$$

connected components falling into k isomorphism classes of sizes n_1, \dots, n_k . The restriction Γ_i of Γ to any element of the i^{th} isomorphism class has some degree N_i and is associated with the contribution $Z_{g_s}[\Gamma_i]$ to the correlation function. In terms of this decomposition,

$$\text{Deck}[\Gamma] = \prod_{i=1}^k S_{n_i} \times \text{Deck}[\Gamma_i]^{n_i} \quad (5.9)$$

and thus $Z_{g_s}[\Gamma]$ can be expressed as

$$Z_{g_s}[\Gamma] = \prod_{i=1}^k \frac{1}{n_i!} (Z_{g_s}[\Gamma_i])^{n_i}. \quad (5.10)$$

¹³There is some slight abuse of notation in eq. (5.6). In a more literal formulation, we should have expanded the n^{th} power of sums over source terms, into a sum of product of sources, corresponding to twist fields whose order and insertion location determines the ramification points.

Therefore,

$$Z_N^X[J] = \sum_{n=0}^{\infty} \frac{1}{n!} \left(\sum_{w=1}^{\infty} \int d^2 z J_w(z) \right)^n \sum_{\Gamma} \prod_{i=1}^k \frac{1}{n_i!} (Z_{g_s}[\Gamma_i])^{n_i}. \quad (5.11)$$

Note that, since the overall degree of Γ is N , n_i and N_i are constrained by

$$N = \sum_{i=1}^k n_i N_i. \quad (5.12)$$

Next, observe that since N is no longer fixed in the grand-canonical ensemble, the sum over n_i and N_i becomes unconstrained for $Z_{g_s}^X$. Upon inserting eq. (5.11) into the definition of Z_{g_s} , one therefore finds that the grand-canonical partition function is an exponential

$$Z_{g_s}^X[J] = \exp \left(\sum_{n=0}^{\infty} \frac{1}{n!} \left(\sum_{w=1}^{\infty} \int d^2 z J_w(z) \right)^n \sum_{\Gamma \text{ conn.}} \mu^N Z_{g_s}[\Gamma] \right) \quad (5.13)$$

of a sum over connected coverings with covering maps Γ of arbitrary degree N .

Finally, we infer from Definition (5.7) that

$$Z_{g_s}[\Gamma] = g_s^{w[\Gamma]} Z[\Gamma] \quad \text{with} \quad w[\Gamma] = \sum_{i=1}^{n_c} w_i \quad \text{and} \quad Z[\Gamma] := Z_1[\Gamma]. \quad (5.14)$$

Thus, the power of g_s weighing the contribution of Γ to Z_{g_s} can be expressed using the Riemann-Hurwitz formula (2.6) as

$$N(2G - 2) + \sum_{i=1}^{n_c} w_i = -2 + 2g + n_c, \quad (5.15)$$

where G is the genus of X . Putting all this together we obtain the following formula for the grand-canonical partition function

$$Z_{g_s}^X[J] = \exp \left(\sum_{n=0}^{\infty} \frac{1}{n!} \left(\sum_{w=1}^{\infty} \int d^2 z J_w(z) \right)^n \sum_{\Gamma \text{ conn.}} g_s^{-2+2g+n_c} Z[\Gamma] \right). \quad (5.16)$$

We hence conclude that the logarithm of the grand-canonical partition function is the sum over all connected coverings, or equivalently, connected PRR diagrams. The individual contributions to this sum are weighted with the parameter g_s taken to the power of (minus) the Euler characteristic of the surface Σ on which the PRR diagram is drawn. In the equation, we have expressed the Euler characteristic in terms of number n_c of bulk vertices of the diagram or punctures of the surface Σ and the genus g of Σ . Correlation functions in the grand-canonical ensemble therefore possess a topological expansion which structurally resembles the 't Hooft large N expansion and, crucially, string perturbation theory. This the result that we aimed to establish.

5.3 The grand-canonical ensemble for interfaces

As we have shown in Section 3.5, it is possible to fix the normalisation of the interface changing operators of our interfaces in such a way that the corresponding connected correlation functions, to leading order in a $1/N$ expansion, match the structure of string perturbation theory. However, this approach leads to the same issues as the bulk fixed N genus expansion, i.e. the match is restricted to the leading large N contribution. In the three paragraphs of this section, we first introduce the interface grand-canonical ensemble, then show that our definition remedies this deficiency, leading to a fully consistent topological expansion, and finally reinterpret the results of Section 3.5 as a saddle-point approximation of the full ensemble.

Definition of the interface grand-canonical partition function. This paragraph constructs an interface analogue of the grand-canonical ensemble reviewed in Sec. 5.2. In Sec. 2.4, we defined the interface $\mathcal{I}_{|a)}^{(P)}$ as interpolating between $\text{Sym}^{N_-}(\mathcal{M})$ and $\text{Sym}^{N_+}(\mathcal{M})$ on Riemann surfaces X_{\pm} of genus G_{\pm} that are glued along their boundaries to form a closed Riemann surface X of genus G . In order to study correlators with a single interface insertion, let us restrict to X_{\pm} with boundaries

$$\partial X_- \cong \partial X_+ \cong \mathbb{S}^1. \quad (5.17)$$

In this setup, we use the notation introduced in Section 2.4 to define

$$Z_{N_{\pm}, P}^{X_-, X_+}[J] := \left\langle \mathcal{I}_{|a)}^{(P)} \exp \left(\oint g_s^w J_w \sigma_w + \oint \sqrt{g_s^w} J_{\omega}^{AB} \sigma_{\omega}^{AB} \right) \right\rangle_{\text{Sym}^{N_- | N_+}(\mathcal{M})}^{\text{unnormalised}} \quad (5.18)$$

with

$$\oint g_s^w J_w \sigma_w := \sum_{w=1}^{\infty} \int_X d^2 z g_s^w J_w(z) \sigma_w(z) \quad (5.19)$$

and

$$\oint \sqrt{g_s^w} J_{\omega}^{AB} \sigma_{\omega}^{AB} := \sum_{A, B \in \{L, R\}} \sum_{\omega} \int_{\partial X_{\pm}} dx \sqrt{g_s^w} J_{\omega}^{AB}(x) \sigma_{\omega}^{AB}(x) \quad (5.20)$$

where ω runs over $2\mathbb{Z}_{>0} - 1 + \delta_A^B$. Given this definition (5.18) of the interface partition functions we now introduce its grand-canonical counterpart which we define as

$$Z_{g_s}^{X_-, X_+}[J] := \sum_{N_{\pm}=0}^{\infty} \sum_{P=0}^{\min(N_-, N_+)} \mu^P \nu_-^{N_- - P} \nu_+^{N_+ - P} Z_{N_{\pm}, P}^{X_-, X_+}[J]. \quad (5.21)$$

It involves three fugacities μ, ν_{\pm} which are associated to the integers N_{\pm} that determine the symmetric product orbifolds on both sides of the interface and on the degree of transmissivity P that characterizes the interface itself. We suggest to control these three fugacities through a single loop counting parameter g_s as

$$\mu := g_s^{2G-2}, \quad \nu_{\pm} := g_s^{2G_{\pm}-1} \quad (5.22)$$

where G and G_{\pm} denote the genus of the surface $X = X_+ \cup_{\mathbb{S}^1} X_-$ and of the two components X_{\pm} that X is glued from.

The string genus expansion. We now show that the g_s expansion of correlation functions in the grand-canonical ensemble (5.21) has the structure of a string genus expansion describing the scattering of open and closed strings in the presence of a D -brane.

As in the bulk case, our first step is to expand the exponential in the fixed N_\pm partition function (5.18) and to express the result in terms of covering maps. This leads to

$$Z_{N_\pm, P}^{X_-, X_+}[J] = \sum_{n_o, n_c=0}^{\infty} \frac{(\oint J_w)^{n_c} (\oint J_\omega^{AB})^{n_o}}{n_o! n_c!} \sum_{\Gamma} Z_{g_s}[\Gamma]. \quad (5.23)$$

Here, the sum runs over all coverings Γ of X with the appropriate ramification points and

$$Z_{g_s}[\Gamma] := \frac{g_s^{w[\Gamma] + \omega[\Gamma]}}{\text{Deck}[\Gamma]} \langle \mathbf{1} \rangle_{\mathcal{M}}^{\Sigma}, \quad (5.24)$$

where $w[\Gamma]$ is the sum of bulk ramification indices and $\omega[\Gamma]$ is half the sum of boundary ramification indices of Γ .

As in the bulk case, the covering maps generically have several connected components, which fall into k isomorphism classes n_1, \dots, n_k . Let us denote by N_i^\pm the order of the covering maps Γ_i in the i^{th} isomorphism class restricted to the preimage of X^\pm . Analogously, let p_i be the degree of transmissivity of Γ_i at a reference point t_* . Then,

$$\mu^P \nu_-^{N_- - P} \nu_+^{N_+ - P} Z_{g_s}[\Gamma] = \sum_{i=1}^k \frac{1}{n_i!} \left(\mu^{p_i} \nu_-^{N_i^- - p_i} \nu_+^{N_i^+ - p_i} Z_{g_s}[\Gamma_i] \right)^{n_i}. \quad (5.25)$$

From the powers of μ and ν_\pm we can read off the constraints

$$\sum_{i=1}^k n_i (N_i^\pm - p_i) = N_\pm - P \quad \text{and} \quad \sum_{i=1}^k n_i p_i = P \quad (5.26)$$

on n_i , N_i^\pm and p_i . The sum over P and N_\pm in the grand-canonical ensemble lifts these constraints such that the grand-canonical partition function becomes the exponential

$$Z_{g_s}^{X_-, X_+}[J] = \exp \left(\sum_{n_o, n_c=0}^{\infty} \frac{(\oint J_w)^{n_c} (\oint J_\omega^{AB})^{n_o}}{n_o! n_c!} \sum_{\Gamma \text{ conn.}} \mu^P \nu_-^{N_- - P} \nu_+^{N_+ - P} Z_{g_s}[\Gamma] \right) \quad (5.27)$$

of a sum of connected covering maps with orders N_\pm on the preimage of X_\pm and the degree of transmissivity P at t^* .

Applied to this setup, the interface Riemann-Hurwitz formula (2.28) gives

$$N_-(2G_- - 1) + N_+(2G_+ - 1) + \sum_{i=1}^{n_c} w_i + \frac{1}{2} \sum_{i=1}^{n_o} \omega_i = -2 + 2g + b + n_c + \frac{1}{2} n_o, \quad (5.28)$$

where g is the genus of the covering space b and is the number of its boundaries. With

$$Z_{g_s}[\Gamma] = g_s^{w[\Gamma] + \omega[\Gamma]} Z[\Gamma], \quad \text{where} \quad w[\Gamma] = \sum_{i=1}^{n_c} w_i, \quad \omega[\Gamma] = \frac{1}{2} \sum_{i=1}^{n_o} \omega_i \quad (5.29)$$

and $Z[\Gamma] := Z_1[\Gamma]$ carries no more dependence on the coupling g_s . Using the definitions (5.22) of the fugacities in terms of g_s we conclude that

$$Z_{g_s}^{X_-, X_+}[J] = \exp \left(\sum_{n_o, n_c=0}^{\infty} \frac{(\oint J_w)^{n_c} (\oint J_w^{AB})^{n_o}}{n_o! n_c!} \sum_{\Gamma \text{ conn.}} g_s^{-2+2g+b+n_c+\frac{n_o}{2}} Z[\Gamma] \right), \quad (5.30)$$

which is the result that we wanted to derive. Once again it contains a sum over connected covering maps, or interface PRR diagrams, in the exponent. Each contribution is weighted by a specific power of the parameter g_s that can be read off from the diagram. It involves the number n_c and n_o of bulk and interface operator insertions, respectively, as well as the genus g and number b of boundary components for the surface Σ the interface PRR diagram is drawn on. As we have anticipated, the exponent mimics precisely that of a string genus expansion for scattering of open strings in the presence of a D -brane.

Expectation value and saddle point approximation. Before we conclude this section we would like to make contact with our analysis in Section 3.5. To this end we compute the expectation values of N_{\pm} and P in the grand-canonical ensemble through saddle-point approximation of the interface partition function at small g_s . We will see that the leading contribution to this saddle point approximation agrees with the results of Section 3.5.

For the rest of this section, we focus on the sphere case $X = \mathbb{S}^2$, $X_{\pm} = \mathbb{D}_{\pm}$. Let us first consider the vacuum grand-canonical partition function

$$Z_{g_s}^{\mathbb{D}_{\pm}}[0] = \exp [\mu z + \nu_- g_- + \nu_+ g_+], \quad (5.31)$$

where z is the sphere partition function of the seed theory, and $g_{\pm} = \langle 0|a_{\pm} \rangle$ are the boundary g -functions of two boundary states $|a_{\pm} \rangle$ therein. The expectation value of P (the number of seed spheres) and $N_{\pm} - P$ (the number of disks \mathbb{D}_{\pm}) can directly be evaluated as

$$\overline{P} = \mu \partial_{\mu} \log(Z_{g_s}^{\mathbb{D}_{\pm}}[0]) = \mu z, \quad \overline{N_{\pm} - P} = \nu_{\pm} \partial_{\nu_{\pm}} \log(Z_{g_s}^{\mathbb{D}_{\pm}}[0]) = \nu_{\pm} g_{\pm}. \quad (5.32)$$

After setting $\mu = \nu_{\pm}^2 = g_s^{-2}$ and $z = 1$, we find that $\overline{N_{\pm} - P}$ is proportional to $(\overline{P})^{1/2}$ with a constant of proportionality controlled by the boundary conditions a_{\pm} . Hence, the scaling behaviour for the averages agrees with the one we used for the symbols N_{\pm}, P and $N_{\pm} - P$ in eq. (3.6) with $N \sim g_s^{-2}$. Let us also note that the ratio

$$\frac{\overline{N_+ - P}}{\overline{N_- - P}} = \frac{\langle 0|a_+ \rangle}{\langle 0|a_- \rangle}. \quad (5.33)$$

is controlled by the ratio of boundary entropies in the seed theory. To leading order in g_s , the normalised correlation functions

$$\left\langle \prod_{i=1}^{n_o} \sigma_{\omega_i}^{A_i B_i}(t_i) \prod_{i=1}^{n_c} \sigma_{w_i}(z_i) \right\rangle_{g_s}^{\mathbb{D}_{\pm}} = \left[\prod_{i=1}^{n_o} \frac{\delta}{\delta J_{\omega_i}^{A_i B_i}(t_i)} \prod_{i=1}^{n_c} \frac{\delta}{\delta J_{w_i}(z_i)} \right] \frac{Z_{g_s}^{\mathbb{D}_{\pm}}[J]}{Z_{g_s}^{\mathbb{D}_{\pm}}[0]} \Big|_{J=0} \quad (5.34)$$

of the grand-canonical theory can be approximated by fixing N_{\pm} and P to their expectation values. If we saddle-point approximate¹⁴ the numerator $\delta_J Z_{g_s}^{\mathbb{D}_{\pm}}[J]|_{J=0}$ and the denominator

¹⁴Approximating the sum

$$Z_{g_s}^{\mathbb{D}_{\pm}}[0] = \sum_{P=0}^{\infty} \sum_{N_{\pm}-P=0}^{\infty} \frac{(\mu z)^P (\nu_- g_-)^{N_- - P} (\nu_+ g_+)^{N_+ - P}}{P!(N_- - P)!(N_+ - P)!} \quad (5.35)$$

$Z_{g_s}^{\mathbb{D}^\pm}[0]$, correlators of twist fields in the normalisation of (5.19) and (5.20) reproduce the results of Sec. 3.5 to leading order in $g_s \sim 1/\sqrt{N}$.

6 Conclusion

In this work, we have developed the necessary covering map machinery to efficiently analyse interface correlation functions of symmetric product orbifolds on arbitrary Riemann surfaces. These methods open up the possibility to answer several interesting questions about the nature of interfaces in symmetric product orbifolds and the holography of AdS₂ branes in pure NSNS AdS₃ string backgrounds. We would like to conclude by briefly sketching some of the potential directions to pursue in future research.

Deriving AdS₃/CFT₂ for open strings. In Section 5, we established a structural match between the genus expansion of interface correlators in the symmetric product orbifold and string perturbation theory. To complete the derivation of the duality between our interfaces and AdS₂ branes in minimal pure NSNS AdS₃, it is necessary to furthermore show that open string scattering amplitudes also quantitatively match the proposed dual correlators at each order in the string genus expansion. The analogous derivation of the duality for closed string scattering amplitudes provided in the seminal paper [3] was based on a localisation of the string world sheet to ramified coverings of the holographic boundary. It was already conjectured in [25] that this localisation property should extend to the open string case. Now that we identified the class of interface covering maps to which the world sheet is expected to localise in that case, this conjecture can be fully established.

A derivation of the bulk correspondence that directly matches CFT correlations functions with string scattering amplitudes, without the need to compute either of them was proposed in [22]. It passes through a deformation of the string background that involves AdS₃ backgrounds with NSNS flux $k > 1$. The dual CFT is a non-rational symmetric product orbifold that involves a Liouville-like direction [26]. In [22], the H₃⁺-Liouville correspondence of [27, 28] was run backwards to reconstruct string theory on AdS₃ from the non-rational symmetric product orbifold, see also [29] for related work based on path integral representations. In the limit $k \rightarrow 1$, a $\mathcal{N} = 4$ supersymmetric Liouville field theory decouples from the CFT₂, leaving a rational symmetric product orbifold for the supersymmetric 4-torus behind and hence one recovers the holographic relation of [3]. It would be interesting to extend this approach to interfaces and open strings using previous work on a boundary version of the H₃⁺-Liouville relation, see [30, 31].

by the largest summand, which occurs at $P \sim \mu z, N_\pm - P \sim \nu_\pm g_\pm$, produces

$$Z_{g_s}^{\mathbb{D}^\pm}[0] \sim \prod_{\Lambda \in \{\mu z, \nu_- g_-, \nu_+ g_+\}} \frac{e^\Lambda}{\sqrt{2\pi\Lambda}}, \quad (5.36)$$

which underestimates the full sum by the Gaussian fluctuation prefactor $\sqrt{2\pi\Lambda}$. However, this does not affect our leading-order estimation since the numerator and denominator have the same width and the prefactor cancels in the normalised ratio.

Thermal correlators and superficial holography. Reference [32] reports universal behaviour of thermal correlation functions in symmetric product orbifolds, compatible with a BTZ black hole as semi-classical gravity dual. The result implies that conditions on the analysed thermal correlators of local operators cannot be sufficient criteria to determine whether a given CFT has a geometric bulk dual. It would be interesting to investigate how the inclusion of extended operators such as $\mathcal{I}_{|a\pm}^{(P)}$ fits into this picture – presumably leading to the construction of a superficial semi-classical gravity dual of our interfaces.

SUSY interface covering maps. Recently, a supersymmetric extension of the covering map approach to symmetric product orbifolds was formulated [33]. We expect that our construction of interface covering maps naturally extends to coverings of super Riemann surface, using the formalism that Reference [33] developed for the bulk case.

Interface deformations of symmetric product orbifolds. Reference [34] provides a detailed description of a broad class of generalised symmetries in symmetric product orbifolds, especially emphasizing constraints on deformations by operators from twisted sectors of the theory. It would be interesting to generalise these results to our interface setup and systematically analyse deformations by interface twist fields. Another direction that is now accessible would be to study the effect of marginal bulk deformations on the spectrum of interface operators. Of particular relevance in this context is the deformation that drives the system towards the geometric regime in which the interacting CFT_2 possesses a dual supergravity description. The effect of such deformations on the bulk spectrum has been addressed e.g. in [35? , 36]. The interfaces we have studied here seem to be ideal new probes for this deformation.

Partial permutations and the interface grand-canonical ensemble. From the definition of grand-canonical correlations function (Section 5.2), neither the existence of a state operator correspondence nor the consistency of the operator product expansion are manifest. Reference [37] solves these problems by working with an enlarged Hilbert space graded by conjugacy classes of partial permutations. The construction should straightforwardly generalise to the interface grand-canonical ensemble proposed in Sec. 5.3, providing a more complete picture of the interface spectrum and OPE. In the context of gauge gravity dualities for topological symmetric product orbifolds [38], such a boundary generalisation was recently investigated in Reference [39].

Acknowledgments

We thank Lior Benizri, Andrea Dei, Gaston Giribet, Michael Gutperle, Yasuaki Hikida, Emil Martinec, Sylvain Ribault and Yifan Wang for useful comments and discussions. This project received funding from the German Research Foundation DFG under Germany’s Excellence Strategy - EXC 2121 Quantum Universe - 390833306 and the Collaborative Research Center - SFB 1624 “Higher structures, moduli spaces and integrability” - 506632645. SH is further supported by the Studienstiftung des Deutschen Volkes. TT is supported by JSPS KAKENHI Grant Number JP24KJ1374.

A Symmetric product orbifolds as discrete gauge theories

Symmetric product orbifolds are discrete gauge theories and therefore we often use gauge theory language in the main text to describe objects in these theories. At a first glance, the formulation in terms of covering maps provided in Section 2.2 however might seem very different from the usual construction of a gauge theory. The purpose of this appendix is to bridge this gap. We first formulate symmetric product orbifolds in the usual language of gauge theory i.e. using sections of associated bundles of principal bundles. We then discuss how to recover the covering map description for vacuum partition functions. Finally, we extend the match to also include twist fields. The overall dictionary that we end up with is summarised in the box below.

N sheeted covering maps $\Gamma \leftrightarrow S_N$ principal bundles P Group of Deck transformations $\text{Deck}[\Gamma] \leftrightarrow$ Gauge group $\mathcal{G}(P)$ Measure monodromy of coverings \leftrightarrow Insert Wilson lines Change covering via cutting and glueing \leftrightarrow Insert 't Hooft lines S_N twist fields $\leftrightarrow S_N$ monopoles

Symmetric product orbifolds and S_N principal bundles. For simplicity, let us assume that the seed theory can be formulated in terms of some real scalar field ϕ with Lagrangian density $\mathcal{L}[\phi]$ (consider for instance \mathcal{M} to be the free boson). For every S_N principal bundle $\pi : P \rightarrow X$, we can define an associated fibre bundle

$$\Gamma_P : \Sigma_P \rightarrow X \quad \text{with} \quad \Sigma_P := (P \times \underline{N})/S_N \quad (\text{A.1})$$

whose fibres are sets of N discrete points,

$$\underline{N} = \{1, 2, \dots, N\}. \quad (\text{A.2})$$

In the construction, we let S_N act on \underline{N} in the canonical way by permutations. By considering the elements of \underline{N} as basis vectors of an \mathbb{R} vector-space, we can also define an \mathbb{R}^N vector-bundle \mathbb{R}_P^N over X . In local trivialisations, sections of \mathbb{R}_P^N are maps

$$\Phi : U \subseteq X \rightarrow U \times \mathbb{R}^N, \quad z \mapsto (z, \Phi^{(1)}(z), \Phi^{(2)}(z), \dots, \Phi^{(N)}(z)). \quad (\text{A.3})$$

The action of $\text{Sym}^N(\mathcal{M})$ is a functional on the space of such sections, which we define in local coordinates by using the Lagrangian \mathcal{L} of \mathcal{M} :

$$S_X[\Phi] = \int_X d^2z \sum_{i=1}^N \mathcal{L}[\Phi^{(i)}]. \quad (\text{A.4})$$

Note that the action is well defined, and in particular not dependent on the choice of trivialisation, since the coordinate changes by construction act as permutations on the components of ϕ and the sum $\sum_{i=1}^N \mathcal{L}[\phi^{(i)}]$ is permutation invariant.

Vacuum partition functions. As usual in gauge theory, the vacuum partition function is a sum over all gauge bundles P weighted by the volumes of their gauge groups $\mathcal{G}(P)$. For the symmetric orbifold on a space time X , it is defined as the path integral

$$Z_N^X := \sum_P \frac{1}{|\mathcal{G}(P)|} \int_{\text{Sections of } \mathbb{R}_P^N} D\Phi e^{-S_X[\Phi]}. \quad (\text{A.5})$$

To translate this into the formulation in terms of covering maps, note that there is a natural identification of sections Φ of \mathbb{R}_P^N with functions $\phi : \Sigma_P \rightarrow \mathbb{R}$, namely

$$\Phi(z) = (z, \Phi^{(1)}(z), \dots, \Phi^{(n)}(z)) \quad \leftrightarrow \quad \phi(z, i) = \Phi^{(i)}(z). \quad (\text{A.6})$$

Defining this map does not require a choice of trivialisation. Instead we are using that, by construction, there is a natural basis of the fibre $(\mathbb{R}_P^N)_z$ of \mathbb{R}_P^N over z given by the fibre $(\Sigma_P)_z$ of Σ_P over z . Through this identification, we can rewrite eq. (A.5) as

$$Z_X^N = \sum_P \frac{1}{|\mathcal{G}(P)|} \int_{\phi : \Sigma_P \rightarrow \mathbb{R}} D\phi e^{-S_{\Sigma_P}[\phi]}, \quad (\text{A.7})$$

where S_{Σ_P} is just the action of the seed theory \mathcal{M} on Σ_P . This already almost looks like the sum over covering spaces in e.g. equation (2.14). To complete the match, we need to replace the sum over S_N principal bundles by a sum over unramified covering maps. For later convenience, let us directly write down an extended version of this correspondence that also holds for branched covering maps.

Singular S_N principal bundles and branched covering maps. There is a natural one-to-one correspondence between the N sheeted branched coverings of X whose set of branch points is contained in a finite subset B of X and singular S_N principal bundles $\pi : P \rightarrow X$ over X whose singular locus¹⁵ is a subset of B .

To show this, let us first construct a covering map from the principal bundle P . By construction, the projection map Γ_P of the associated fibre bundle $(P \times \underline{N})/S_N$ to the base space $X \setminus B$ is a N sheeted covering map. We can induce a complex structure of P by pulling back the complex structure on X along Γ_P . Then, Γ_P is trivially holomorphic. There is a unique analytic continuation of Γ_P to a ramified covering map of X , whose branch points are a subset of B .

Clearly, this construction is reversible. Starting with a branched covering map Γ , we can remove the ramification points from its domain to obtain a \underline{N} bundle over $X \setminus B$. The structure group of this fibre bundle is S_N and the associated S_N principal bundle is the bundle P_Γ we are after.

Since furthermore $\text{Deck}[\Gamma_P]$ is identical to the group of bundle automorphisms of Σ_P which is isomorphic to $\mathcal{G}(P)$, we can use the above bijection to rewrite eq. (A.6) as a sum

$$Z_X^N = \sum_P \frac{1}{|\mathcal{G}(P)|} \int_{\phi : \Sigma_P \rightarrow \mathbb{R}} D\phi e^{-S_{\Sigma_P}[\phi]} = \sum_\Gamma \frac{\langle \mathbb{1} \rangle_{\mathcal{M}}^\Sigma}{|\text{Deck}[\Gamma]|}, \quad (\text{A.8})$$

over N sheeted covering maps Γ and thus reproduce the prescription of Section 2.2.

¹⁵For our purposes, a singular principal bundle over X is a principle bundle over $X \setminus S$, where S is a finite subset of X , which we call the singular locus of the bundle.

Gauge transformations. In gauge theory, the name “gauge transformation” is used for several types of operations, which are distinguished in the language of principal bundles as

1. **Small gauge transformations** i.e. the action of isomorphisms of the gauge bundle that are homotopic to the identity map.
2. **Large gauge transformation** i.e. the action of topologically non trivial isomorphisms of the gauge bundle.
3. **Coordinate changes** of a trivialisation of the bundles, which are sometimes also considered as “small gauge transformations”.
4. **Changes of the global structure of the bundles**, which are sometimes also considered “large gauge transformations”.

Since the gauge group S_N is discrete, the only small gauge transformation is the identity. Relatedly, discreteness of the fibre implies that every automorphism of the gauge bundle is already fixed over each connected component of X by the action on a single fibre. Thus, if X has n connected components, then the group of large gauge transformations $\mathcal{G}(P)$ is isomorphic to a subgroup of S_N^n .

If $(U_i, s_i)_{i \in I}$ is a trivialisation of P (i.e. a collection of local sections) then the coordinate changes are described by transition functions

$$t_{ij} : U_i \cap U_j \rightarrow S_N, \quad (\text{A.9})$$

such that $s_j(z) = s_i(z)t_{ij}(z)$. The transition functions satisfy the cocycle condition

$$t_{ik}(z) = t_{ij}(z)t_{jk}(z) \quad \text{for all} \quad z \in U_i \cap U_j \cap U_k \quad (\text{A.10})$$

and fully encode the structure of the bundle P .

We can change the global structure of the gauge bundle by altering the trivialisation through a cut and glue procedure that allows us to act with oriented closed curves on X labelled by permutations $g \in S_N$ on the set of S_N principal bundles. Physically, this corresponds to the insertion of a ’t Hooft line of the product theory. The procedure consists of the following three steps.

1. **Setup.** Given an oriented non-self-intersecting closed curve γ on X , a permutation $g \in S_N$ and an S_N principal bundle $\pi : P \rightarrow X$, we define a new bundle P_g^γ .
2. **Trivialisation of P .** Since $\gamma([0, 1]) \cong \mathbb{S}^1$, we can pick a trivialisation of P such that only two charts U and V have a non trivial intersection with $\gamma([0, 1])$. Also, we can ensure that U, V are simply connected, the intersection of U and V with $\gamma([0, 1])$ is connected and that $U \cap V$ has exactly two connected components UV and \widetilde{UV} . The transition function t_{UV} is specified by two permutations: Its values on UV and \widetilde{UV} respectively. W.l.o.g. let the value on \widetilde{UV} be 1 and denote the value on UV by h .

3. **Trivialisation of P_g^γ .** The curve γ splits both U and V in two connected components U'_\pm and V'_\pm such that $U'_\pm \cap V'_\mp = \emptyset$. Thicken U'_\pm and V'_\pm slightly to obtain open sets U_\pm and V_\pm that cover γ but whose intersection $U_\pm \cap V_\mp$ is still disjoint from all charts of P except for U and V . If g commutes with h , then replacing (U, t_U) and (V, t_V) by the four local sections

$$(U_-, s_U|_{U_-}) \quad (V_-, s_V|_{V_-}) \quad (U_+, (s_U|_{U_+}) \cdot g) \quad \text{and} \quad (V_+, (s_V|_{V_+}) \cdot g), \quad (\text{A.11})$$

leads to

$$t_{U_+V_+} = g^{-1} \cdot (t_{UV}|_{U_+ \cap V_+}) \cdot g = t_{UV}|_{U_+ \cap V_+} \quad \text{and} \quad t_{U_-V_-} = t_{UV}|_{U_- \cap V_-}. \quad (\text{A.12})$$

Therefore, we can use the transition functions of P to consistently construct local sections over the entire connected component of X containing γ from the four new local sections defined in eq. (A.11). Complementing this with the local sections of P over the rest of X yields the bundle P_g^γ .

Note that, with the choice of trivialisation of P made above, the permutation h is exactly the monodromy of P along γ . The condition that h and g need to commute can therefore be phrased as the statement that we can only act with g along γ on P if the S_N monodromy of P along γ commutes with g .

Monopoles. The field Φ whose action we defined in eq. (A.4) is the lift of ϕ to the untwisted sector of the symmetric orbifold. In addition, the spectrum of local excitations also includes monopoles i.e. operators whose insertion in the path integral restricts the sum over gauge bundles by fixing a certain monodromy around their insertion point. Under the identification between S_N gauge bundles and degree N covering maps, this translates to the statements that the insertion of monopoles creates ramification points with a fixed index. Thus, the S_N monopoles are exactly the twist fields as introduced in Sec. 2.2.

B Wilson and 't Hooft lines in symmetric orbifolds

In this appendix, we first use Wilson loops to obtain an alternative definition of gauge fixed twist fields. We then discuss the 't Hooft lines that implement an S_N action on the global structure of covering maps. These provide us with a different perspective on gauge choices and gauge invariance in symmetric orbifolds and also allow us to quite conveniently describe other permutation orbifolds.

Wilson lines. The data defining a Wilson line $\mathcal{W}[\gamma]$ is a curve $\gamma : [0, 1] \rightarrow X$. The insertion of such a line does not affect the set of covering maps associated with an operator $\mathcal{O} \in \mathcal{A}_X[\text{Sym}^N(\mathcal{M})]$, that is

$$C[\mathcal{O}\mathcal{W}[\gamma]] = C[\mathcal{O}] \quad \text{for all } \mathcal{O} \in \mathcal{A}_X[\text{Sym}^N(\mathcal{M})]. \quad (\text{B.1})$$

It only acts through its lift, which is a bijection from $\Gamma^{-1}(\gamma(0))$ to $\Gamma^{-1}(\gamma(1))$, i.e.

$$\mathcal{W}[\gamma]^\Gamma \in \text{Bij}[\Gamma^{-1}(\gamma(0)), \Gamma^{-1}(\gamma(1))]. \quad (\text{B.2})$$

Concretely, the value of $\mathcal{W}[\gamma]^\Gamma$ is the map defined by parallel transport along $\Gamma^*\gamma$. Through local gauge choices of $C[\mathcal{O}]$ at $\gamma(0)$ and $\gamma(1)$, we can identify $\mathcal{W}[\gamma]^\Gamma$ with an element $\mathcal{W}[\gamma]_{\text{gf}}^\Gamma$ of S_N . If we change the local gauge at $\gamma(0)$ by acting with a permutation g_0 and that at $\gamma(1)$ by acting with a permutation g_1 , then $\mathcal{W}[\gamma]_{\text{gf}}^\Gamma$ transforms as

$$\mathcal{W}[\gamma]_{\text{gf}}^\Gamma \rightarrow g_1 \mathcal{W}[\gamma]_{\text{gf}}^\Gamma g_0^{-1}. \quad (\text{B.3})$$

Wilson loops. For closed Wilson lines i.e. Wilson loops, $\gamma(0) = \gamma(1)$ and we only make a single local gauge choice. Thus, Wilson loops transform by conjugation under a change of the gauge. We can hence define a \mathbb{C} valued operator

$$\mathcal{W}_R[\gamma] := \chi_R(\mathcal{W}[\gamma]) \quad (\text{B.4})$$

for every closed loop γ and every representation R of S_N with character χ_R by making an arbitrary gauge choice to evaluate $\chi_R(\mathcal{W}[\gamma]^\Gamma)$. As usual in gauge theory, these topological loops are not the only gauge invariant extended objects that can be built from $\mathcal{W}[\gamma]_{\text{gf}}^\Gamma$. Another option is to consider Wilson lines whose end-points are dressed with operators charged under S_N .

Gauge fixed twist fields. Using Wilson lines, we can define gauge fixed versions σ_g of the twist fields $\sigma_{[g]}$:

$$\sigma_g(z) := \lim_{\epsilon \rightarrow 0} \delta_{\mathcal{W}[\gamma_\epsilon]_{\text{gf}}, g} \sigma_{[g]}(z), \quad (\text{B.5})$$

where γ_ϵ is a small loop winding once around z clockwise at distance ϵ . The gauge dependence of σ_g comes from the choice of how to identify $\mathcal{W}[\gamma_\epsilon]$ with an element of S_N . In particular, the transformation behaviour (B.3) of the Wilson loop implies that under a change h of the local gauge choice, σ_g transforms as

$$\sigma_g \mapsto \lim_{\epsilon \rightarrow 0} \delta_h \mathcal{W}[\gamma_\epsilon]_{\text{gf}} h^{-1}, g \sigma_{[g]} = \lim_{\epsilon \rightarrow 0} \delta_{\mathcal{W}[\gamma_\epsilon]_{\text{gf}}, h^{-1}gh} \sigma_{[g]} = \sigma_{h^{-1}gh}. \quad (\text{B.6})$$

Note that the linear combination

$$\hat{\sigma}_{[g]} = \sum_{\tilde{g} \in [g]} \sigma_{\tilde{g}} \quad (\text{B.7})$$

is gauge invariant. But of course, $\hat{\sigma}_{[g]}$ is simply $\sigma_{[g]}$

$$\hat{\sigma}_{[g]} = \sum_{\tilde{g} \in [g]} \lim_{\epsilon \rightarrow 0} \delta_{\mathcal{W}[\gamma_\epsilon], \tilde{g}} \sigma_{[g]} = \sigma_{[g]}. \quad (\text{B.8})$$

't Hooft lines. The insertion of Wilson lines does not affect the set of covering maps associated with a correlation function and only acts through the lift of the lines along the covering maps. Let us now construct a dual set of lines that only act by changing the structure of covering maps but lift to the trivial defect in the seed theory. These oriented topological lines $\mathcal{L}_g[\gamma]$ are labeled by a permutation $g \in S_N$ and a non-self intersecting curve γ . They depend on a local gauge choice at $\gamma(0)$ only.

The set $C[\mathcal{OL}_g[\gamma]]$ of covering maps computing correlators in the presence of $\mathcal{L}_g[\gamma]$ is given by applying a cutting and glueing procedure that maps each $\Gamma \in C[\mathcal{O}]$ to a new covering which we shall denote by $\mathcal{L}_g[\gamma] \cdot \Gamma$. To construct $\mathcal{L}_g[\gamma] \cdot \Gamma$, first cut out the pre-image $\Gamma^{-1}(\gamma([0, 1]))$ of the image of γ under Γ from the covering space Σ to obtain

$$\tilde{\Sigma} := \Sigma \setminus \Gamma^{-1}(\gamma([0, 1])). \quad (\text{B.9})$$

By parallel transport of the local gauge choice at $\gamma(0)$ along γ , every point on $\Gamma^{-1}(\gamma([0, 1]))$ has a label $i \in \{1, \dots, N\}$. We now glue $\tilde{\Sigma}$ back together along its cut by identifying the i^{th} sheet with the gi^{th} sheet upon travelling along the cut from below (w.r.t. the orientation of γ). In particular, this identifies several of the N points in $\Gamma^{-1}(\gamma(0))$ (and $\Gamma^{-1}(\gamma(1))$) among each other, namely all those that are elements of the same g orbit. Let the Riemann surface constructed in this manner be denoted by $\mathcal{L}_g[\gamma] \cdot \Sigma$. We define $\mathcal{L}_g[\gamma] \cdot \Gamma$ as the analytic extension of Γ from $\tilde{\Sigma}$ to $\mathcal{L}_g[\gamma] \cdot \Sigma$.

Changing the local gauge at $\gamma(0)$ by acting with a permutation h transforms $\mathcal{L}_g[\gamma]$ as

$$\mathcal{L}_g[\gamma] \rightarrow \mathcal{L}_{hgh^{-1}}[\gamma] \quad (\text{B.10})$$

since glueing the i^{th} sheet to that labelled by gi is the same as first relabelling $i \rightarrow i' = hi$ and then glueing the sheet with the new label i' to that carrying the new label $h(gi) = hgh^{-1}i'$.

Thus, a simple way to construct gauge invariant lines from $\mathcal{L}_g[\gamma]$ is to average over characters χ_R of S_N . This leads to the lines

$$\mathcal{L}_R[\gamma] := \sum_{g \in S_N} \chi_R(g) \mathcal{L}_g[\gamma]. \quad (\text{B.11})$$

Note that if we average over a particular conjugacy class,

$$\mathcal{L}_{[g]}[\gamma] := \sum_{\tilde{g} \in [g]} \mathcal{L}_{\tilde{g}}[\gamma], \quad (\text{B.12})$$

the resulting non-local operators are in effect pairs of $[g]$ -twist fields inserted at $\gamma(0)$ and $\gamma(1)$ that are coupled to each other in a non-local fashion.

There is an obstruction to inserting \mathcal{L}_g along a closed curve γ . The operator $\mathcal{L}_g[\gamma]$ is only well defined for closed γ if the monodromy along γ as measured by $\mathcal{W}[\gamma]$ commutes with g . Thus, we define $\mathcal{L}_g[\gamma] \cdot \Gamma$ for closed curves γ as

$$\mathcal{L}_g[\gamma] \cdot \Gamma = \begin{cases} \text{as in the } \gamma(0) \neq \gamma(1) \text{ case} & \text{if } \mathcal{W}[\gamma]^\Gamma \in \mathcal{C}_g \\ \Gamma & \text{else.} \end{cases} \quad (\text{B.13})$$

Global gauge choices and gauge invariance. As made precise in Appendix A, the sums over covering maps in symmetric product orbifolds are sums over gauge bundles of S_N gauge theories. The closed permutation lines introduced at the end of the previous paragraphs can in this sense be thought of as implementing large gauge transformations. Gauge invariance of the symmetric product orbifold is the statement that for every closed curve γ , every $g \in S_N$ and every $\mathcal{O} \in \mathcal{A}_X[\text{Sym}^N(\mathcal{M})]$,

$$C[\mathcal{O}] = C[\mathcal{OL}_g[\gamma]]. \quad (\text{B.14})$$

As an example, let us verify that the vacuum of the symmetric product orbifold as defined in eq. (2.10) is gauge invariant. Given any holomorphic covering map $\Gamma : \Sigma \rightarrow X$ and a closed curve γ on X , there are two cases to consider. The first case is that the monodromy of Γ along γ does not commute with g . In this case, we have defined the permutation line as acting trivially. In the second case $\mathcal{L}_g[\gamma]$ maps Γ into another holomorphic covering map without changing the monodromy along γ . Thus, $\mathcal{L}_g[\gamma]$ simply permutes the different holomorphic covering maps among each other, leaving the set $C[1]$ invariant.

Other permutation orbifolds. As a side comment, let us briefly note that it is also possible to consider a variation of the above procedure where one only imposes invariance under a certain subset of the operators \mathcal{L}_g . This, together with an appropriate analogue of eq. (2.10), leads to more general permutation orbifolds.

For example, we could choose to impose no invariance at all. Together with

$$C_{\mathcal{M}^{\otimes N}}[1] := \{\text{trivial covering of } X \text{ by } X^N\}, \quad (\text{B.15})$$

this leads to the product theory. While the lines $\mathcal{L}_R[\gamma]$ defined in eq. (B.11) are trivial in the symmetric product orbifold if γ is closed, they do have interesting correlation functions in the product theory.

C Comments on the normalisation of the interfaces

The purpose of this appendix is to compare the normalisation of the interfaces as defined in eq. (2.33) to the normalisation fixed through the explicit expressions for boundary states of the folded theory given in Reference [5].

In [5], the normalisation of the boundary states $|p^{L/R}\rangle'$ was fixed by demanding that

$$Z_{N_{\pm}, p_{L/R}}^{\text{torus}} := \langle p^L |' \exp(\pi i \hat{t}(L_0 + \bar{L}_0 - \frac{c}{12}) | p^R \rangle' \quad (\text{C.1})$$

leads to formula (2.47) for the grand-canonical torus partition function (2.45). Since we derived the very same formula using the normalisation of interfaces fixed by eq. (2.33), the approach presented in this paper clearly agrees with the approach of [5] for the two interface torus partition function.

However, to obtain a fully consistent picture, the boundary states should be rescaled

$$|p\rangle := \sqrt{N_-!} \sqrt{N_+!} |p\rangle' \quad (\text{C.2})$$

and the overlap should be divided by $N_-!N_+!$, so that the torus partition function

$$Z_{N_{\pm}, p_{L/R}}^{\text{torus}} := \frac{1}{N_-!N_+!} \langle p^L | \exp(2\pi i \hat{t}(L_0 + \bar{L}_0 - \frac{c}{12}) | p^R \rangle \quad \text{with} \quad c = (N_- + N_+)c_{\mathcal{M}} \quad (\text{C.3})$$

remains unchanged. As long as we are only interested in $Z_{N_{\pm}, p_{L/R}}^{\text{torus}}$, the question of whether we work with $|p\rangle'$ or $|p\rangle$ is of course irrelevant and purely a matter of taste. But once we move on to other partition functions, we should work with $|p\rangle$. Let us for instance consider

the sphere partition function with a single interface insertion, splitting the sphere into the two disks \mathbb{D}_\pm . The fixed N_\pm, p partition function in terms of $|p\rangle$ is

$$Z_{N_\pm, p}^{\mathbb{D}_-, \mathbb{D}_+} = \frac{\langle p|0\rangle}{N_-!N_+!} = \frac{g_-^{N_- - p} g_+^{N_+ - p}}{(N_- - p)!(N_+ - p)!p!}, \quad (\text{C.4})$$

where we obtained the r.h.s. from an expression for $\langle 0|p\rangle'$ given in eq. (2.40) of [5]. This result agrees with the expression derived from the interface covering map perspective in the main text, see eq. (2.44). As another indication towards the fact that (C.4) is the correct prescription, observe that the grand-canonical partition function

$$Z_{g_s}^{\mathbb{D}_-, \mathbb{D}_+} := \sum_{N_\pm=0}^{\infty} \sum_{p=0}^{\min(N_-, N_+)} \mu^p \nu^{N_- + N_+ - 2p} Z_{N_\pm, p}^{\mathbb{D}_-, \mathbb{D}_+} \quad (\text{C.5})$$

with $\mu := g_s^{-2}$ and $\nu := g_s^{-1}$ exponentiates as¹⁶

$$Z_{g_s}^{\mathbb{D}_-, \mathbb{D}_+} = \exp(\mu + \nu g_- + \nu g_+) \quad (\text{C.6})$$

only if we work with $|p\rangle$ and not $|p'\rangle$.

D Generalised Lunin-Mathur construction – computational details

This appendix contains detailed derivations and computations underlying the results discussed in Section 4.

D.1 Details on the regularisation procedure

In this appendix, we derive eq. (4.11). In the first short paragraph, we briefly describe the setup of the derivation to make the appendix self-contained. We then begin with the derivation by dividing the covering space Σ into three regions. One of the three regions contains a pathological subregion, which we cut out in order to define the regularised Liouville action (D.10). The next three paragraphs evaluate the Liouville action on each individual region. After this, we add the three contributions to obtain the regularised vacuum partition function (D.21). The regularised partition function still depends on an unphysical regulator, which we remove in the final paragraph of the section by rescaling the twist fields. This final step directly produces the result (4.11) that we want to show.

The setup. In Section 4.1, we introduced the family

$$ds_\delta^2 = \begin{cases} dzd\bar{z} & \text{if } |\delta z| < 1 \\ \frac{dzd\bar{z}}{|z\delta|^4} & \text{else} \end{cases} \quad (\text{D.1})$$

of continuous metrics on the Riemann sphere parametrised by $\delta > 0$. While ds_δ^2 is continuous, it is not smooth. In particular, its scalar curvature is the distribution

$$R_\delta = 4\delta \left(|z| - \frac{1}{\delta} \right) \quad (\text{D.2})$$

¹⁶As a consistency check, note that setting $\nu = 0$ reproduces $Z_{g_s}^{\text{sphere}}[0]$ in a normalisation where the sphere partition function of the seed theory is set to 1.

whose support is the circle $|z\delta| = 1$. We noted in the main text that the partition function of a CFT with central charge c on $\overline{\mathbb{C}}$ equipped with ds_δ^2 is

$$Z_1^{\overline{\mathbb{C}}_\delta} = Q\delta^{-\frac{c}{3}}, \quad (\text{D.3})$$

where Q is an arbitrary constant, which we fixed to $Q = \eta^{\frac{c}{3}}$ so that $X = \overline{\mathbb{C}}_\eta$ has $Z_1^X = 1$. In this appendix, we show in detail how to evaluate Z_1^Σ for a sphere Σ with metric induced via a covering map $\Gamma : \Sigma \rightarrow X$, which is unramified at $\Gamma^{-1}(\infty)$ and satisfies $\Gamma(\infty) = \infty$. As explained in the main text, we can do so (for an appropriate $\delta > 0$ specified in the next paragraph) via the relation

$$Z_1^\Sigma = e^{S_L[\phi]} Z_1^{\overline{\mathbb{C}}_\delta} \quad \text{with} \quad S_L[\phi] = \frac{c}{96\pi} \int_\Sigma d^2t \sqrt{g_\delta} (\partial_\mu \phi \partial_\nu \phi g_\delta^{\mu\nu} + 2R_\delta \phi), \quad (\text{D.4})$$

where ϕ is the Weyl factor relating Σ to $\overline{\mathbb{C}}_\delta$.

Divide and cover. To organise the computation, we divide Σ into three disjoint regions and evaluate the Liouville action separately on each of these. The first of the regions is

$$\mathcal{B} = \{t \in \mathbb{C} : |\eta\Gamma(t)| < 1\} \subseteq \Sigma. \quad (\text{D.5})$$

We pick δ sufficiently small to ensure that

$$\mathcal{B} \subseteq \Sigma^0 := \{t \in \mathbb{C} : |t\delta| < 1\}. \quad (\text{D.6})$$

Furthermore, we denote the complement of Σ^0 by Σ^∞ . Our decomposition of Σ is

$$\Sigma = \mathcal{B} \sqcup (\Sigma^0 \setminus \mathcal{B}) \sqcup \Sigma^\infty. \quad (\text{D.7})$$

We use this decomposition to evaluate the Liouville action

$$S_L[\phi] = S_L^\mathcal{B}[\phi] + S_L^{\Sigma^0 \setminus \mathcal{B}}[\phi] + S_L^{\Sigma^\infty}[\phi] \quad (\text{D.8})$$

for the Weyl factor ϕ relating metric ds^2 , induced on Σ via Γ , to the metric ds_δ^2 .

Regularisation of $S_L[\phi]$. The region \mathcal{B} contains all ramification points of Γ . At the ramification points, the induced metric degenerates, the Weyl factor diverges and the Liouville action needs to be regularised. To do so, we introduce a regulator $\varepsilon > 0$ that is sufficiently small to ensure that

$$R_\varepsilon := \bigcup_{r \in R[\Gamma]} \{t : |\Gamma(t) - \Gamma(r)| < \varepsilon\} \subseteq \mathcal{B}. \quad (\text{D.9})$$

We regularise the Liouville action by removing R_ε from \mathcal{B} . That is, we define $\mathcal{B}_\varepsilon := \mathcal{B} \setminus R_\varepsilon$ and use $S_L^{\mathcal{B}_\varepsilon}[\phi]$ as a regularised version of $S_L^\mathcal{B}[\phi]$, leading to

$$S_L^\varepsilon[\phi] := S_L^{\mathcal{B}_\varepsilon}[\phi] + S_L^{\Sigma^0 \setminus \mathcal{B}}[\phi] + S_L^{\Sigma^\infty}[\phi] \quad (\text{D.10})$$

as a regularised version of (D.8).

Evaluation of $S_L^{\mathcal{B}_\epsilon}[\phi]$ On \mathcal{B}_ϵ the metric $ds_\delta^2 = dt d\bar{t}$ is flat. Thus, only the kinetic term of the Liouville action contributes. The latter evaluates to

$$S_L^{\mathcal{B}_\epsilon}[\phi] = \frac{c}{96\pi} \int_{\mathcal{B}_\epsilon} d^2t 4\partial\phi\bar{\partial}\phi = \frac{c}{96\pi} \int_{\mathcal{B}_\epsilon} d^2t 4\partial(\phi\bar{\partial}\phi) = \frac{c}{96\pi} \int_{\partial\mathcal{B}_\epsilon} ds \phi \partial_n \phi. \quad (\text{D.11})$$

via Stokes theorem, where n is the normal vector of $\partial\mathcal{B}_\epsilon$. In the second step, we used that

$$\phi = \log(\partial\Gamma) + \log(\bar{\partial}\bar{\Gamma}) \quad \text{and hence} \quad \partial\bar{\partial}\phi = 0. \quad (\text{D.12})$$

To further evaluate the integral, note that each connected component of $\partial\mathcal{B}$ either belongs to a pole $p \in P[\Gamma]$ of Γ in the complex plane, the point ∞ , or to a ramification point $r \in R[\Gamma]$. Around these three different types of point, Γ behaves as

$$-\Gamma(p+t) = \frac{b_p}{t} + O(1), \quad \Gamma(t) = b_\infty t + O(1) \quad \text{and} \quad \Gamma(r+t) = \Gamma(r) + a_r t^w + O(t^{w+1}). \quad (\text{D.13})$$

Thus, a pole p in the complex plane contributes

$$-\int_0^{2\pi} ds b_p \eta (-2\log(b_p \eta^2)) (-4b_p^{-1} \eta^{-1}) = -16\pi \log(b_p \eta^2) \quad (\text{D.14})$$

to (D.11), the point ∞ contributes nothing and a ramification point r contributes

$$-\int_0^{2\pi} ds \varepsilon_r (-2\log(w a_r \varepsilon_r^{w-1})) (-2(w-1)\varepsilon_r^{-1}) = -8\pi(w-1)\log(w a_r \varepsilon_r^{w-1}) \quad (\text{D.15})$$

to leading order in ε and η . Here, $\varepsilon_r := \left(\frac{\varepsilon}{a_r}\right)^{\frac{1}{w}}$. In total, we conclude

$$S_L^{\mathcal{B}_\epsilon}[\phi] = -\frac{c}{12} \sum_{r \in R[\Gamma]} (w-1) \log\left(w\varepsilon \left(\frac{a_r}{\varepsilon}\right)^{\frac{1}{w}}\right) - \frac{c}{6} \sum_{p \in P[\Gamma]} \log(b_p \eta^2) \quad (\text{D.16})$$

Evaluation of $S_L^{\Sigma^0 \setminus \mathcal{B}}[\phi]$. On $\Sigma^0 \setminus \mathcal{B}$ the metric $ds_\delta^2 = \frac{dt d\bar{t}}{|\delta t|^4}$ is flat. Thus, only the kinetic term is non-vanishing. Two regions contribute to the corresponding integral. The first consists of disks around the poles of Γ . Their contribution is suppressed by δ^2 . To leading order, $S_L^{\Sigma^0 \setminus \mathcal{B}}[\phi]$ is thus fully determined by the integral over the second region: The annulus around ∞ . There, $\phi = -\log(b_\infty^2 |\delta t|^4)$ and we get

$$S_L^{\Sigma^0 \setminus \mathcal{B}}[\phi] = \frac{c}{96\pi} \int_{(\Sigma^0 \setminus \mathcal{B})_\infty} d^2t 4\partial\phi\bar{\partial}\phi = \frac{c}{24\pi} \int_{\frac{1}{b_\infty\eta}}^{\frac{1}{\delta}} dr \int_0^{2\pi} d\theta r b_\infty \frac{4}{r^2} = -\frac{c}{3} \log\left(\frac{\delta}{b_\infty\eta}\right) \quad (\text{D.17})$$

Evaluation of $S_L^{\Sigma^\infty}[\phi]$. On Σ^∞ the Weyl factor $\phi = \log(\frac{\delta^4}{b_\infty^2 \eta^4})$ is constant. Thus, the kinetic term vanishes and $S_L^{\Sigma^\infty}[\phi]$ is fully determined by the curvature term, which yields

$$S_L^{\Sigma^\infty}[\phi] = \frac{c}{96\pi} 16\pi\phi = \frac{c}{3} \log \delta^2 - \frac{c}{3} \log(b_\infty \eta^2) \quad (\text{D.18})$$

Putting everything together. Combining eqs. (D.16), (D.17) and (D.18), we conclude

$$S_L^\varepsilon[\phi] = -\frac{c}{12} \sum_{r \in R[\Gamma]} (w-1) \log \left(w \varepsilon \left(\frac{a_r}{\varepsilon} \right)^{\frac{1}{w}} \right) - \frac{c}{6} \sum_{p \in P[\Gamma]} \log(b_p \eta^2). \quad (\text{D.19})$$

Therefore, the regularised version of Z_1^Σ is

$$Z_{1;\varepsilon}^\Sigma := e^{S_L^\varepsilon[\phi]} Z_1^{\bar{C}_\delta} = \left(\prod_{r \in R[\Gamma]} w^{w-1} \varepsilon^{\frac{(1-w)^2}{w}} a_r^{1-\frac{1}{w}} \prod_{p \in P[\Gamma]} b_p^2 \eta^4 \right)^{-\frac{c}{12}}. \quad (\text{D.20})$$

Since ∞ is not a branch point of Γ , we have $|P[\Gamma]| = \text{Deg}[\Gamma] - 1$. Thus,

$$Z_{1;\varepsilon}^\Sigma = \eta^{-\frac{c}{3}(\text{Deg}[\Gamma]-1)} \left(\prod_{r \in R[\Gamma]} w^{w-1} \varepsilon^{\frac{(1-w)^2}{w}} a_r^{1-\frac{1}{w}} \prod_{p \in P[\Gamma]} b_p^2 \right)^{-\frac{c}{12}}. \quad (\text{D.21})$$

Rescaling the twist fields. The regularisation scheme introduced an explicit dependence of $Z_{1;\varepsilon}^\Sigma$ on the unphysical parameter ε . To remove the regulator dependence, we need to rescale the twist fields i.e. replace σ_w by $\mathcal{N}_w \sigma_w$. We make the minimal choice

$$\mathcal{N}_w = \varepsilon^{\frac{c}{12} \frac{(1-w)^2}{w}} \quad (\text{D.22})$$

so that, after rescaling, $Z_{1;\varepsilon}^\Sigma$ becomes the physical quantity

$$Z_1^\Sigma = \eta^{-\frac{c}{3}(\text{Deg}[\Gamma]-1)} \prod_{r \in R[\Gamma]} w^{-\frac{c}{12}(w-1)} a_r^{-\frac{c}{12}(1-\frac{1}{w})} \prod_{p \in P[\Gamma]} b_p^{-\frac{c}{6}} \quad (\text{D.23})$$

which is independent of ε .

D.2 Regularisation for the upper half plane

In this appendix, we regulate the Liouville action for interface coverings of the upper half complex plane by the upper half complex plane.

The setup. The setup treated in this appendix is almost identical to that described in the beginning of Appendix D.1. In particular, the reference metric that we consider is the restriction of the metric ds_δ^2 defined in eq. (D.1) to the upper half plane. Generically, we would have to evaluate the extrinsic curvature contribution in addition to the bulk Liouville action in the interface case. For the upper half plane equipped with ds_δ^2 , the derivative of the normal vector w.r.t. the tangent vector of the boundary is however always proportional to the normal vector and hence the extrinsic curvature vanishes. Accordingly, only the bulk Liouville action is relevant. As we argue in the next paragraph, the latter can be evaluated using the method of images.

Method of images. Given an interface covering map Γ that covers the upper half complex plane by itself, we can readily construct a covering map

$$\Gamma' : \mathbb{C} \rightarrow \mathbb{C}, \quad z \mapsto \begin{cases} \Gamma(z) & \text{if } \text{Im}(z) > 0 \\ \overline{\Gamma(\bar{z})} & \text{else.} \end{cases} \quad (\text{D.24})$$

For each bulk ramification point of Γ , the doubled map Γ' has two ramification points with the same index. For each interface ramification point of index ω , it has a bulk ramification point with index $w = \omega$ on the real line. The bulk part of the regulated Liouville action for the conformal factor ϕ relating the upper half plane with metric induced by Γ' to the upper half plane with metric ds_δ^2 is given by

$$S_L^\varepsilon[\phi]_{\text{Bulk}} = \frac{1}{2} S_L^\varepsilon[\phi'] \quad (\text{D.25})$$

in terms of the Liouville action for the conformal factor ϕ' of the doubled covering map. We can therefore directly generalise eq. (D.21) to

$$Z_{1;\varepsilon}^\Sigma = \Omega(\eta) \left(\prod_{r \in R_B[\Gamma]} w^{w-1} \varepsilon^{\frac{(1-w)^2}{w}} a_r^{1-\frac{1}{w}} \prod_{p \in P_B[\Gamma]} b_p^2 \right)^{-\frac{c}{12}} \left(\prod_{r \in R_I[\Gamma]} \omega^{\omega-1} \varepsilon^{\frac{(1-\omega)^2}{\omega}} a_r^{1-\frac{1}{\omega}} \prod_{p \in P_I[\Gamma]} b_p^2 \right)^{-\frac{c}{24}}, \quad (\text{D.26})$$

where $\Omega(\eta) := \eta^{-\frac{c}{6}(N_- + N_+ - 1)}$ and $N_\pm = \text{Deg}_\pm[\Gamma]$. Furthermore, $R_B[\Gamma]$ and $R_I[\Gamma]$ are the sets of bulk and interface ramification points of Γ respectively. Likewise, $P_B[\Gamma]$ and $P_I[\Gamma]$ are the sets of poles in the bulk and on the interface, not including ∞ .

Rescaling the twist fields. The result (D.26) is consistent with the bulk twist field normalisation found in eq. (D.22). To fully remove the regulator dependence, we need to also redefine the normalisation of the interface twist fields. We work with the minimal bulk and interface normalisations

$$\mathcal{N}_w^B = \varepsilon^{\frac{c}{12} \frac{(1-w)^2}{w}} \quad \text{and} \quad \mathcal{N}_\omega^I = \varepsilon^{\frac{c}{24} \frac{(1-\omega)^2}{\omega}}. \quad (\text{D.27})$$

In this normalisation, we obtain the physical partition function

$$Z_1^\Sigma = \eta^{-\frac{c}{6}(N_- + N_+ - 1)} \left(\prod_{r \in R_B[\Gamma]} w^{w-1} a_r^{1-\frac{1}{w}} \prod_{p \in P_B[\Gamma]} b_p^2 \right)^{-\frac{c}{12}} \left(\prod_{r \in R_I[\Gamma]} \omega^{\omega-1} a_r^{1-\frac{1}{\omega}} \prod_{p \in P_I[\Gamma]} b_p^2 \right)^{-\frac{c}{24}}. \quad (\text{D.28})$$

D.3 Computing covering maps

This appendix discusses how covering maps are computed in the first section of the mathematica notebook `CoveringMaps.nb` uploaded in the ancillary files associated with the arXiv page of this publication. We focus on coverings $\Gamma : \mathbb{C} \rightarrow \mathbb{C}$ that have branch points

$$x_1 = 0, \quad x_2, \quad x_3 = 1, \quad \text{and} \quad x_4 = \infty \quad (\text{D.29})$$

which correspond to ramification points

$$s_1 = 0, \quad s_2, \quad s_3 = 1, \quad \text{and} \quad s_4 = \infty \quad (\text{D.30})$$

with ramification indices w_1, \dots, w_4 . The covering map Γ satisfies

$$\Gamma(s_i + s) = x_i + a_i s^{w_i}. \quad (\text{D.31})$$

The choices $s_1 = x_1 = 0$ and $x_4 = s_4 = \infty$ ensure that we can directly satisfy two of these conditions by making the Ansatz

$$\Gamma(s) = \frac{q(s)}{p(s)} \quad (\text{D.32})$$

with polynomials q and p that satisfy

$$q(s) = a_1 s^{w_1} + O(s^{w_1+1}), \quad p(s) = 1 + O(s) \quad \text{and} \quad \deg(p) - \deg(q) = w_4. \quad (\text{D.33})$$

Since the degree of the covering map coincides with the degree of the polynomial p , we can fix it through the Riemann-Hurwitz formula. This leads to

$$\deg(p) = \frac{1}{2}(w_1 + w_2 + w_3 + w_4) - 1 \quad \text{and} \quad \deg(q) = \frac{1}{2}(w_1 + w_2 + w_3 - w_4) - 1. \quad (\text{D.34})$$

Fixing the polynomials p and q hence amounts to computing $w_2 + w_3 - 1$ coefficients and the additional unknown s_2 . This is achieved in the notebook by solving the $w_2 + w_3$ equations

$$\partial_s^n (\Gamma(s) - x_i)|_{s=s_i} = 0 \quad \text{for} \quad i \in \{2, 3\} \quad \text{and} \quad n = 0, 1, \dots, w_i - 1. \quad (\text{D.35})$$

E Proving the diagrammatic rules

In this appendix, we sketch a proof for the validity of interface PRR diagrammatics. In the first paragraph, we introduce sharpened terminology that allows us to distinguish between embeddings of the diagrams and the intrinsic data of the diagrams more clearly than in the main text. With this preparation, we then show that the map from equivalence classes of covering maps to abstract PRR diagrams is injective i.e. that two covering maps producing the same diagram are equivalent. Next, we show that the map is also surjective i.e. that every abstract PRR diagram indeed arises from a covering map. Together, these two steps imply that there is indeed a one-to-one correspondence between PRR diagrams and equivalence classes of covering maps.

Embedded and abstract PRR diagrams.

Definition. *Embedded (interface) PRR diagrams* are the graphs embedded in Riemann surfaces that can be constructed from the vertices in Sec. 3.1 and Sec. 3.2 with the constraints outlined in those sections. Consider two embedded diagrams \mathcal{D} and \mathcal{D}' on Riemann surfaces Σ and Σ' whose vertices are labelled by the same branch points. We say that the diagrams are isomorphic if there is an isomorphism between Σ and Σ' that restrict to an isomorphism of graphs for the diagrams \mathcal{D} and \mathcal{D}' preserving the labels of the vertices.

Definition. *Abstract (interface) PRR diagrams* are equivalence classes of embedded diagrams w.r.t. the notion of isomorphism introduced in the previous paragraph.

Injectivity of PRR diagrammatics.

Claim. *If taking the preimage of the contour 6 for two covering maps Γ and Γ' with the same branch points produces the same abstract PRR diagram, then Γ and Γ' are equivalent i.e. identical up to an isomorphism of the covering space.*

Proof. If the two embedded PRR diagrams \mathcal{D} and \mathcal{D}' are isomorphic, then there is an isomorphism $\phi: \Sigma \rightarrow \Sigma'$ such that $\phi(\mathcal{D}) = \mathcal{D}'$. We now show that ϕ is also an isomorphism of the associated covering maps i.e. $\Gamma = \tilde{\Gamma} := \Gamma' \circ \phi$. By definition, ϕ identifies ramification points that are labelled by the same branch-point. Thus, $\Gamma(r) = \tilde{\Gamma}(r)$ for every ramification point $r \in \Sigma$ of Γ . Furthermore, $\Gamma(x) = \tilde{\Gamma}(x)$ for every point x on an edge of \mathcal{D} , since the value at the vertices and the fact that Γ and $\tilde{\Gamma}$ have to be both length and orientation preserving already uniquely characterises these functions on the edges. Finally, the restrictions of Γ and $\tilde{\Gamma}$ to a face of \mathcal{D} are restrictions of two holomorphic maps between disks that coincide on the boundary of the disk. Therefore, Γ and $\tilde{\Gamma}$ also coincide on the faces of \mathcal{D} .

Surjectivity of PRR diagrammatics.

Claim. *Every abstract PRR diagram that can be constructed using the rules of Section 3 has a representative that is the preimage of the contour 6 w.r.t. an interface covering map.*

Proof. Take an arbitrary realisation of the PRR diagram on a surface Σ . We now define a map Γ by first setting its value at each ramification-point to the branch-point by which it is labelled and then picking an arbitrary continuous, bijective, orientation preserving identification between each edge of the diagram and the interval of the contour on the sphere that connects the branch-points corresponding to the ramification points at the ends of the edge. The PRR rules enforce that the restriction of the map Γ constructed in this way to any face of the diagram is a homeomorphism that identifies that face with the boundary of a disk on the sphere. For each face, extend Γ to the interior such that it becomes a homeomorphism between the face and a disk on the sphere. Away from the ramification points, Γ is a local homeomorphism and therefore, we can use it to induce a metric and complex structure on Σ , which makes the restriction of Γ to the complement of the ramification points a holomorphic local isometry by construction. Clearly, the PRR diagram corresponding to Γ is the diagram that we used to construct Γ .

References

- [1] A. Pakman, L. Rastelli and S.S. Razamat, *Diagrams for symmetric product orbifolds*, *JHEP* **10** (2009) 034 [[0905.3448](#)].
- [2] L. Eberhardt, M.R. Gaberdiel and R. Gopakumar, *The worldsheet dual of the symmetric product CFT*, *JHEP* **04** (2019) 103 [[1812.01007](#)].
- [3] L. Eberhardt, M.R. Gaberdiel and R. Gopakumar, *Deriving the AdS_3/CFT_2 correspondence*, *JHEP* **02** (2020) 136 [[1911.00378](#)].
- [4] N. Berkovits, *Topological A-Model for $AdS_5 \times S^5$ Superstring and the Maldacena Conjecture*, [2506.10907](#).
- [5] S. Harris, Y. Hikida, V. Schomerus and T. Tsuda, *Holographic Interfaces in Symmetric Product Orbifolds*, [2504.00078](#).
- [6] G. Belleri and M.R. Gaberdiel, *D-branes in $AdS_3 \times S^3 \times S^3 \times S^1$* , *JHEP* **10** (2025) 065 [[2506.15776](#)].
- [7] A. Karch and L. Randall, *Open and closed string interpretation of SUSY CFT's on branes with boundaries*, *JHEP* **06** (2001) 063 [[hep-th/0105132](#)].

- [8] O. Lunin and S.D. Mathur, *Correlation functions for M^N/S_N orbifolds*, *Commun. Math. Phys.* **219** (2001) 399 [[hep-th/0006196](#)].
- [9] M. Gutperle, Y.-Y. Li, D. Rathore and K. Roumpedakis, *Non-invertible symmetries in S_N orbifold CFTs and holography*, *JHEP* **09** (2024) 110 [[2405.15693](#)].
- [10] A. Belin, S. Biswas and J. Sully, *The spectrum of boundary states in symmetric orbifolds*, *JHEP* **01** (2022) 123 [[2110.05491](#)].
- [11] A. Pakman, L. Rastelli and S.S. Razamat, *Extremal correlators and Hurwitz numbers in symmetric product orbifolds*, *Phys. Rev. D* **80** (2009) 086009 [[0905.3451](#)].
- [12] Y. Hikida and T. Liu, *Correlation functions of symmetric orbifold from AdS_3 string theory*, *JHEP* **09** (2020) 157 [[2005.12511](#)].
- [13] E.J. Martinec, *A defect in AdS_3/CFT_2 duality*, *JHEP* **06** (2022) 024 [[2201.04218](#)].
- [14] A. Giveon, D. Kutasov and N. Seiberg, *Comments on string theory on AdS_3* , *Adv. Theor. Math. Phys.* **2** (1998) 733 [[hep-th/9806194](#)].
- [15] D. Kutasov and N. Seiberg, *More comments on string theory on AdS_3* , *JHEP* **04** (1999) 008 [[hep-th/9903219](#)].
- [16] A. Giveon and D. Kutasov, *Notes on $AdS(3)$* , *Nucl. Phys. B* **621** (2002) 303 [[hep-th/0106004](#)].
- [17] J. Kim and M. Porrati, *On the central charge of spacetime current algebras and correlators in string theory on AdS_3* , *JHEP* **05** (2015) 076 [[1503.07186](#)].
- [18] L. Eberhardt, *Partition functions of the tensionless string*, *JHEP* **03** (2021) 176 [[2008.07533](#)].
- [19] L. Eberhardt, *Summing over Geometries in String Theory*, *JHEP* **05** (2021) 233 [[2102.12355](#)].
- [20] M.R. Gaberdiel and R. Gopakumar, *Tensionless string spectra on AdS_3* , *JHEP* **05** (2018) 085 [[1803.04423](#)].
- [21] L. Eberhardt and M.R. Gaberdiel, *String theory on AdS_3 and the symmetric orbifold of Liouville theory*, *Nucl. Phys. B* **948** (2019) 114774 [[1903.00421](#)].
- [22] Y. Hikida and V. Schomerus, *Engineering perturbative string duals for symmetric product orbifold CFTs*, *JHEP* **06** (2024) 071 [[2312.05317](#)].
- [23] O. Aharony and E.Y. Urbach, *Type II string theory on $AdS_3 \times S^3 \times \mathbb{T}^4$ and symmetric orbifolds*, *Phys. Rev. D* **110** (2024) 046028 [[2406.14605](#)].
- [24] C. Bachas, J. de Boer, R. Dijkgraaf and H. Ooguri, *Permeable conformal walls and holography*, *JHEP* **06** (2002) 027 [[hep-th/0111210](#)].
- [25] M.R. Gaberdiel, B. Knighton and J. Vošmera, *D-branes in $AdS_3 \times S^3 \times \mathbb{T}^4$ at $k = 1$ and their holographic duals*, *JHEP* **12** (2021) 149 [[2110.05509](#)].
- [26] L. Eberhardt, *A perturbative CFT dual for pure NS-NS AdS_3 strings*, *J. Phys. A* **55** (2022) 064001 [[2110.07535](#)].
- [27] S. Ribault and J. Teschner, *H_3^+ -WZNW correlators from Liouville theory*, *JHEP* **06** (2005) 014 [[hep-th/0502048](#)].
- [28] Y. Hikida and V. Schomerus, *H_3^+ WZNW model from Liouville field theory*, *JHEP* **10** (2007) 064 [[0706.1030](#)].

- [29] B. Knighton and V. Sriprachyakul, *Unravelling AdS_3/CFT_2 near the boundary*, [2404.07296](#).
- [30] V. Fateev and S. Ribault, *Boundary action of the H_3^+ model*, *JHEP* **02** (2008) 024 [[0710.2093](#)].
- [31] T. Creutzig, Y. Hikida and P.B. Rønne, *The FZZ duality with boundary*, *JHEP* **09** (2011) 004 [[1012.4731](#)].
- [32] A. Belin, S. Bintanja, A. Castro and W. Knop, *Symmetric Product Orbifold Universality and the Mirage of an Emergent Spacetime*, [2502.01734](#).
- [33] B. Nairz, *Super Covering Maps*, [2509.12302](#).
- [34] N. Benjamin, S. Bintanja, Y.-J. Chen, M. Gutperle, C. Luo and D. Rathore, *Generalized Symmetries and Deformations of Symmetric Product Orbifolds*, [2509.12180](#).
- [35] A. Pakman, L. Rastelli and S.S. Razamat, *A spin chain for the symmetric product CFT_2* , *JHEP* **05** (2010) 099 [[0912.0959](#)].
- [36] M.R. Gaberdiel, R. Gopakumar and B. Nairz, *Beyond the tensionless limit: Integrability in the symmetric orbifold*, *JHEP* **06** (2024) 030 [[2312.13288](#)].
- [37] L. Benizri, *Grand-Canonical Symmetric Orbifold Theories*, [2510.03132](#).
- [38] L. Benizri and J. Troost, *Symmetric group gauge theories and simple gauge/string dualities*, *J. Phys. A* **57** (2024) 505401 [[2404.12543](#)].
- [39] J. Troost, *Inverse Monoid Topological Quantum Field Theories and Open-Closed Grand Canonical Symmetric Orbifolds*, [2510.02782](#).